NASA Reference Publication 1347

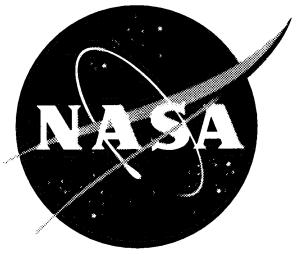

A Shadowgraph Study of the National Launch System's 1 1/2 Stage Vehicle Configuration and Heavy Lift Launch Vehicle Configuration

Darlene C. Pokora and Anthony M. Springer
Marshall Space Flight Center • MSFC, Alabama

National Aeronautics and Space Administration
Marshall Space Flight Center • MSFC, Alabama 35812

August 1994

ACKNOWLEDGMENTS

The authors would like to acknowledge the wind tunnel test team of the George C. Marshall Space Flight Center. They were instrumental in running the wind tunnel test and installation of the shadowgraph process. A sincere thanks to H. Brewster, S. Epsey, A. Frost, and C. Dill.

TABLE OF CONTENTS

LIST OF ILLUSTRATIONS

LIST OF ILLUSTRATIONS (Continued)

LIST OF ILLUSTRATIONS (Continued)

LIST OF ILLUSTRATIONS (Continued)

REFERENCE PUBLICATION

A SHADOWGRAPH STUDY OF THE NATIONAL LAUNCH SYSTEM'S 1 1/2 STAGE VEHICLE CONFIGURATION AND HEAVY LIFT LAUNCH VEHICLE CONFIGURATION

I. INTRODUCTION

This is the third in a series of shadowgraph studies[1] [2] of various launch vehicle configurations. This report presents shadowgraphs for the National Launch System's (NLS's) 1 1/2 stage vehicle configuration and heavy lift launch vehicle (HLLV) configurations. The shadowgraphs are for the trisonic Mach range of 0.6 to 5.0. Shadowgraphs at angles-of-attack of 0° and –4° and also for a role angle of 90° for the HLLV configuration are shown for the Mach range. The 1 1/2 stage configuration is symmetric except for the feedlines, so no shadowgraphs of any roll angle were taken. These shadowgraphs present a pictorial view of the flow fields over the NLS 1 1/2 stage configuration and HLLV configuration. These configurations were tested in the Marshall Space Flight Center's (MSFC's) 14-Inch Trisonic Wind Tunnel (TWT) over the period of January 1992 to November 1992.[3]

This report presents shadowgraphs for the NLS 1 1/2 stage and HLLV configurations in a concise format, is a means of easy transfer of the data to interested parties, and also documents the results for future study.

II. MODEL AND FACILITY DESCRIPTION

A. Facility Description

The MSFC 14- by 14-Inch Trisonic Wind Tunnel is an intermittent blowdown tunnel which operates by high-pressure air flowing from storage to either vacuum or atmosphere conditions. The transonic test section provides a Mach number range from 0.2 to 2.0. A solid-wall supersonic test section provides the entire range from 2.74 to 5.0 with one set of automatically actuated contour blocks. Downstream of the test section is a hydraulically controlled pitch sector that provides the capability of testing up to 20 angles-of-attack from –10° to +10° during each run. Sting offsets are available for obtaining various maximum angels-of-attack up to 90°. This is further detailed in reference 4. The MSFC 14- by 14-Inch TWT facility is shown in figure 1.

B. Model Description

The 1 1/2 stage vehicle 0.004 scale model consists of a cylindrical payload section 2.88 inches in length and 0.800 inches in diameter with a biconic nose cone (15°/25°). The interstage section (0.838 inches in length) connects the payload section to the space transportation system (STS) external tank (ET) section which has been modified to include an additional 5 ft in length, full scale (ET section including the propulsion module is 7.647 inches in length and 1.324 inches in diameter). The additional 5-ft length was added to the aft end of the ET hydrogen tank. Figure 2 depicts the 1 1/2 stage configuration. The model is built in two pieces. The forward section contains the nose, the payload section, the interstage section, and a small section of the ET for a total length of 4.771 inches. The aft body includes

the ET and the propulsion module for a total length of 7.547 inches. The reference configuration engine shrouds are made to be removable and are 0.692 inches in length and have a 0.252 inch radius. The model utilizes removable feedlines. Due to the complexity of fabrication and assembly and associated cost, dimensions for the feedlines do not correspond exactly to the reference configuration. The effects are considered to be small on the total vehicle aerodynamics. Figure 3 shows the NLS 1½ stage configuration mounted in the MSFC 14-Inch TWT.

The HLLV 0.004 scale model consists of a core vehicle model to which two existing advanced solid rocket booster models are attached. Like the 1½ stage model, the core model is built in two pieces. The aft section is identical to the 1½ stage model requiring only a single set of hardware. The forward section differs only in the payload section that is somewhat longer (3.84 in) and of a noncircular cross-section (0.800 by 0.856 in). This noncircular cross-section in the payload bay area is referred to as a strongback. Figure 4 depicts the HLLV configuration.

Figure 5 shows the NLS HLLV configuration mounted in the MSFC 14- by 14-Inch TWT.

C. Shadowgraph System

The 14-Inch TWT's shadowgraph system consists of a spark source, multiple film canisters, and a mounting bracket for the canisters. The spark source is mounted on one side with the mounting bracket/film holder on the other side of the test section. Glass walls are installed in the transonic test section, while the supersonic test section has built-in glass walls. The spark source is ignited to expose the film, thus producing a shadowgraph. Figure 6 shows a sketch of the shadowgraph setup.

Without flow in the tunnel, the spark source shines through the test section containing stagnant air and illuminates the film with uniform intensity. When the tunnel is started and flow passes through the test section, the light beam will be refracted wherever there is a density gradient. A constant gradient, an empty test section, or no flow through the test section will result in every light ray being reflected evenly producing no change on the film. Only if there is a variation in the density gradient will the light from the spark source converge or diverge. A picture of the instantaneous density gradients will be shown on the film when the spark source is ignited. The shadowgraph easily allows shock waves to be seen. The second derivative of density is positive in the forward region of the shock and negative in the aft region. The shadowgraph film will show the shock wave as a dark line followed by a white line.

The shadowgraph system used for the 14-Inch TWT is explained in detail in reference 5. Reference 5 also explains the theory behind the system and the supporting tests done to initially verify the system. This reference also explains the effects of the glass walls on the shadowgraph. This appears on the shadowgraph to look something like cross hatching in the subsonic and sonic Mach range. Currently only the single film method, not the multiple exposure roll which is also shown in reference 5, is used. Black and white, 8- by 20-inch, Kodak Tri-X™ pan professional film is used for the shadowgraphs.

III. SHADOWGRAPH DESCRIPTION

The shadowgraph is a flow visualization technique that shows the second spatial derivative of the density field or the gradient of the density gradient. The shadowgraph is used to show boundary layers,

flow separation, and shock wave formations. All flow visualization techniques are dependent on variation in the flow fields density. An interferometer measures the density level with regards to a reference. The fringe shifts are counted to obtain the density variations. A Schlieren system shows the gradient in density or the first x derivative. The shadowgraph system is easy to use and the relative shock strengths are easily seen, but the actual density levels cannot be obtained.

Boundary layers and separated regions are easily seen in shadowgraphs if the flow field density is not too low. The density changes across shocks and expansions waves are functions of Mach number and are configuration dependent. The density gradients of the flow are dependent on the ratios of upstream and downstream flow fields. Low-density flow fields are not as discernible as high-density flow in the shadowgraphs. The shadowgraph system and its relation to other optical flow methods are discussed in reference 6. Further details concerning shadowgraphs and their application to launch vehicle aerodynamic studies are found in reference 7.

IV. SHADOWGRAPH ENGINEERING INTERPRETATIONS

These visual representations of the flow have been used in conjunction with launch vehicle aerodynamic analyses to gain a better understanding of the aerothermodynamic environments.

Because of the bluntness of the configurations, the primary bow shock off the vehicles at low supersonic Mach numbers are detached and appear as vertical lines forward of the vehicles. As the Mach number increases, the angle of the shock wave also increases, changing from the appearance of a vertical line, a normal shock, to that of an oblique line, an oblique shock. At approximately Mach 1.96, the bow shock off the noses becomes attached.

At the higher Mach numbers, the shadowgraphs appear to be clearer and the shock waves more pronounced. This is due to the larger density variation fore and aft of the shock.

It can be seen that the strongback present in the payload shroud of the HLLV configuration does not overtly effect the external flow fields of the vehicle payload fairing. This is determined by comparing top and side views of the vehicle, i.e., a shadowgraph at 0° roll and one at 90° roll. The payload fairing is symmetric except for the strongback.

The vehicles engine fairings or engine shrouds cause shock waves to form at transonic and supersonic Mach numbers.

The HLLV and 1½ stage configurations have the same transition and core sections. The only major difference between the two on the core vehicle is the addition of the boosters to the HLLV configuration. The effects of the boosters on the core can be seen by comparing an HLLV and a 1½ stage shadowgraph taken at the same conditions. From these comparisons, it can be seen that the boosters cause a shock off the boosters nose cap to intersect the interstage of the vehicle core. This shock results in higher loading of the intertank region and a large pressure gradient over the intertank region.

The flow phenomena around the reference configurations are shown and labeled in a typical shadowgraph. Figure 7 represents a typical 1½ stage shadowgraph, and figure 8 represents a typical HLLV shadowgraph. These figures are the same as shadowgraphs in figure 18 and 73, respectfully.

V. CONCLUSIONS

Shadowgraphs for the NLS 1½ stage configuration and HLLV configuration taken in the MSFC's 14-Inch TWT are presented herein. These shadowgraphs present a pictorial view of the flow fields for the two configurations. The shadowgraphs are used in conjunction with launch vehicle aerodynamic analyses to gain a better understanding of the aerothermodynamic environments.

This report presents the shadowgraphs for two NLS configurations in a concise format, offers a means of easy transfer of the data to interested parties, and documents the results for future study.

REFERENCES

1. Springer, A.M., and Pokora, Darlene C.: "A Shadowgraph Study of Two Proposed Shuttle-C Launch Vehicle Configurations." NASA RP 1303, May 1993.

2. Springer, A.M.: "A Shadowgraph Study of Space Transportation System (STS); The Space Shuttle Launch Vehicle (SSLV)." NASA RP TBD, 1994.

3. Pokora, Darlene C.: "Posttest Report for the National Launch System (NLS) 1.5 Stage, Heavy Lift Launch Vehicle, and Early Lift Launch Vehicle Configurations in the MSFC 14-Inch Trisonic Wind Tunnel." ED35-04-93, April 26, 1993.

4. Simon, E.H.: "The George C. Marshall Space Flight Center's 14×14 Inch Trisonic Wind Tunnel Technical Handbook." NASA TMX-64624, November 5, 1971.

5. Clark, J., Heaman, J.P., and Stewart, D.L.: "14-Inch Wind Tunnel Spark Shadowgraph System." NASA TM X-53195, January 22, 1965.

6. Shapiro, A.H.: "The Dynamics and Thermodynamics of Compressible Fluid Flow Volume I." 1953, John Wiley and Sons, Inc., Chapter 3.7. Optical Methods of Investigation, pp. 59-68.

7. Andrews, C.D., and Carlson, D.R.: "Shadowgraph Study of the Upper Stage Flow Fields of Some Saturn V Study Configurations in the Transonic Mach Number Range." NASA TN D-2755, April 1965.

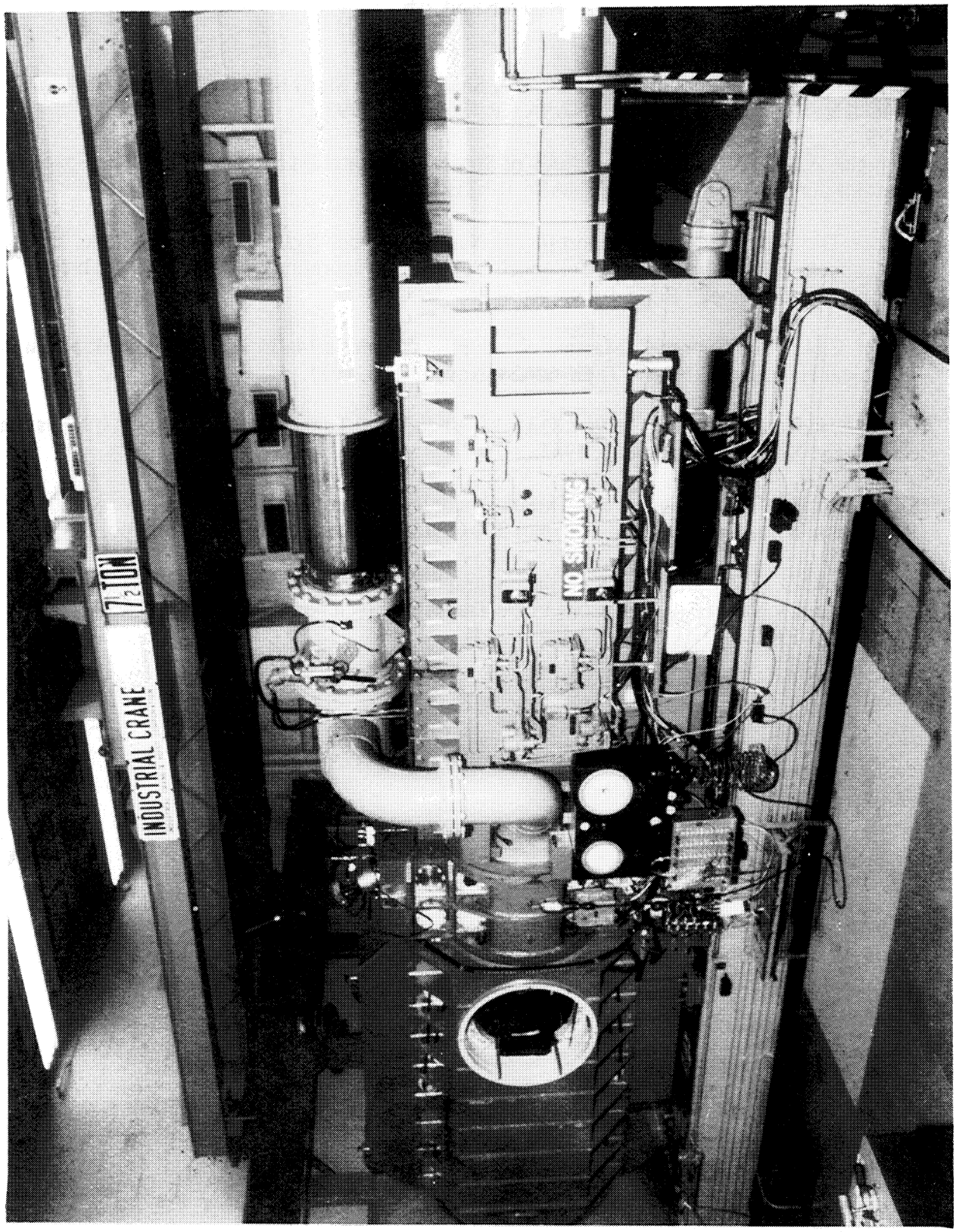

Figure 1. MSFC 14- by 14-Inch TWT.

AREF=593.96 sq. ft.
DREF=27. 5 ft.

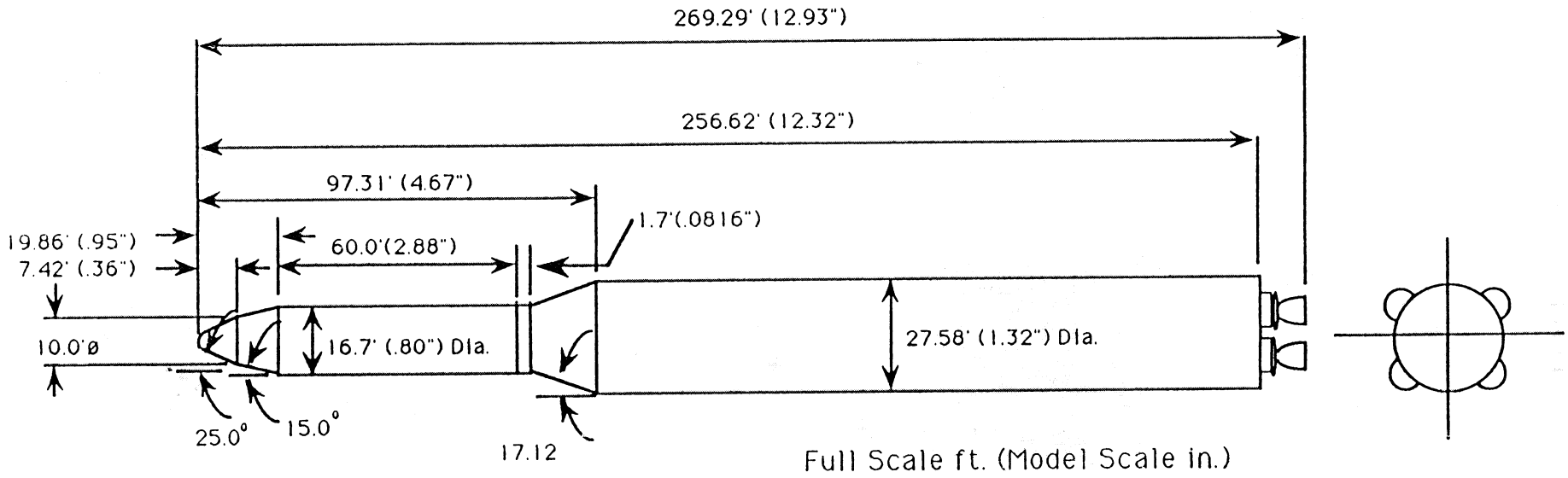

Figure 2. NLS 1½ stage configuration.

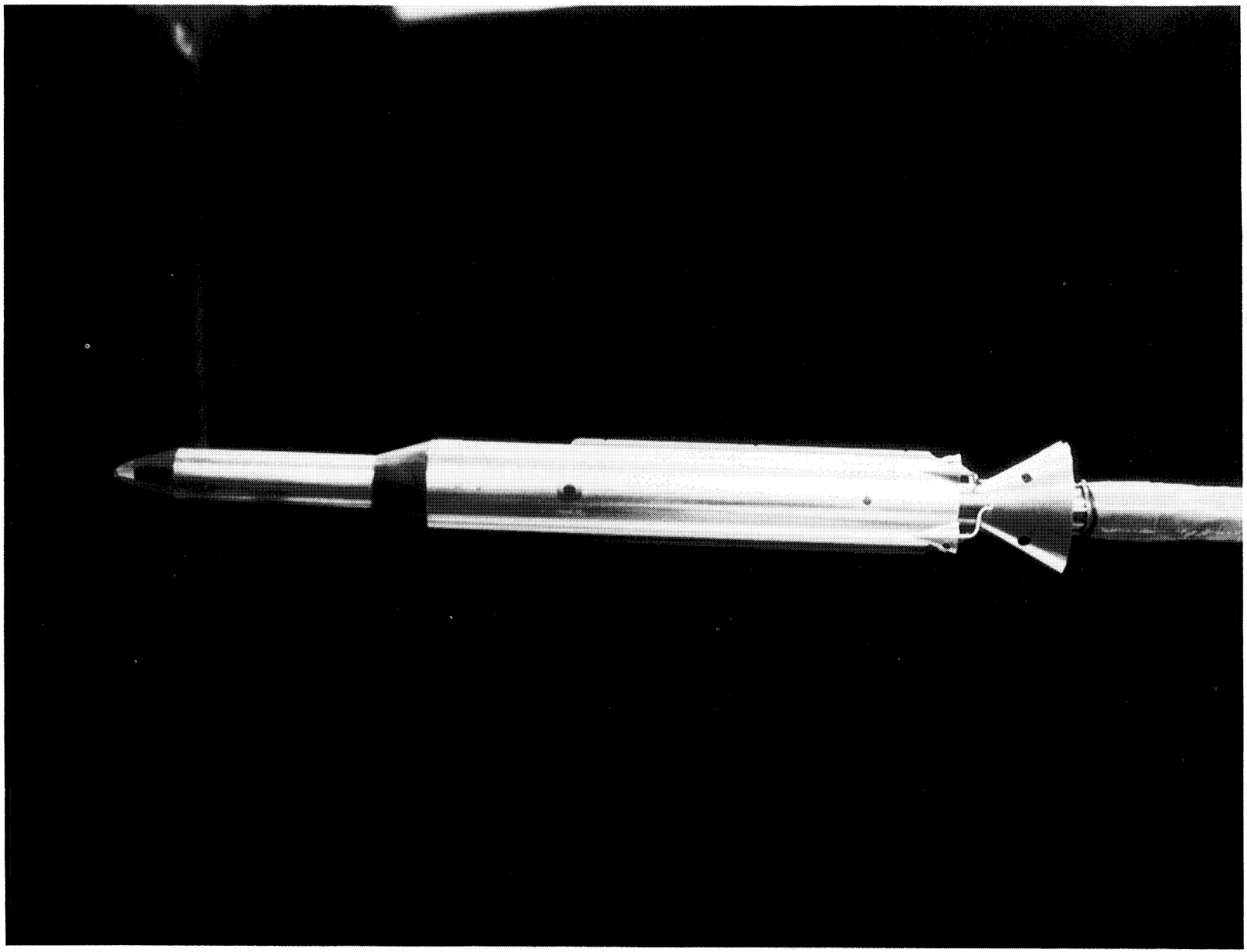

Figure 3. 1½ stage configuration mounted in MSFC 14- by 14- Inch TWT.

AREF = 593.96 SQ FT
DREF = 27.5 FT

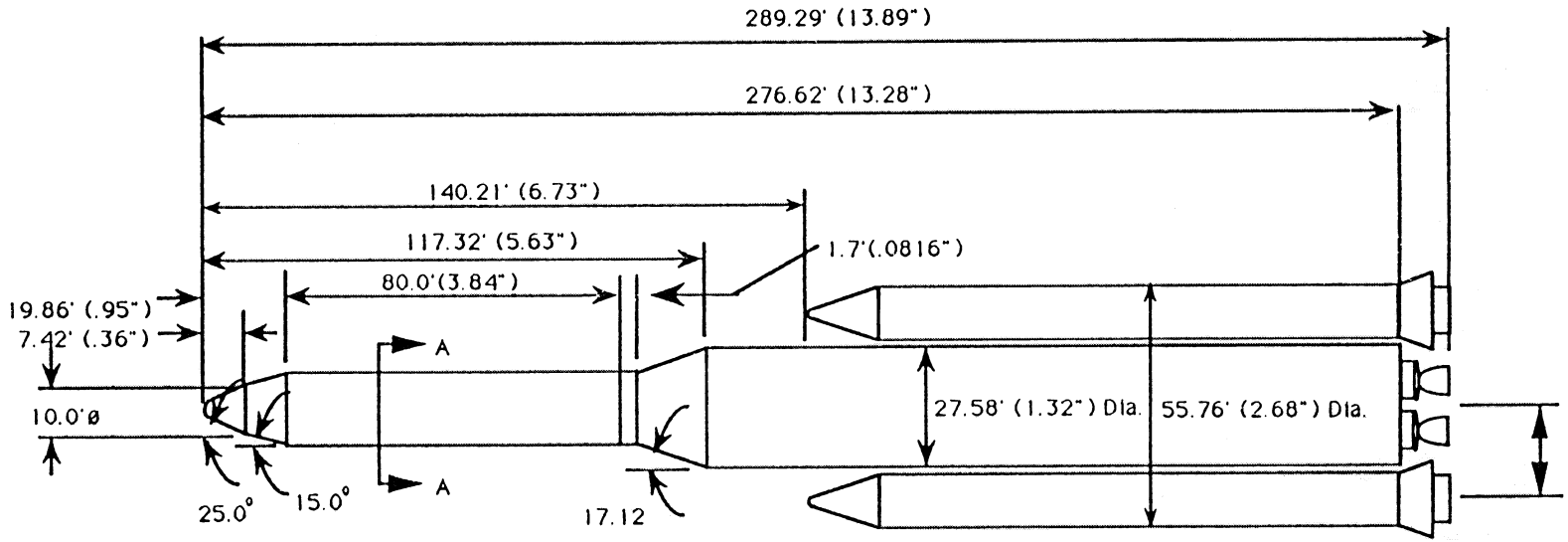

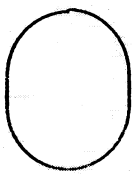

Figure 4. NLS HLLV.

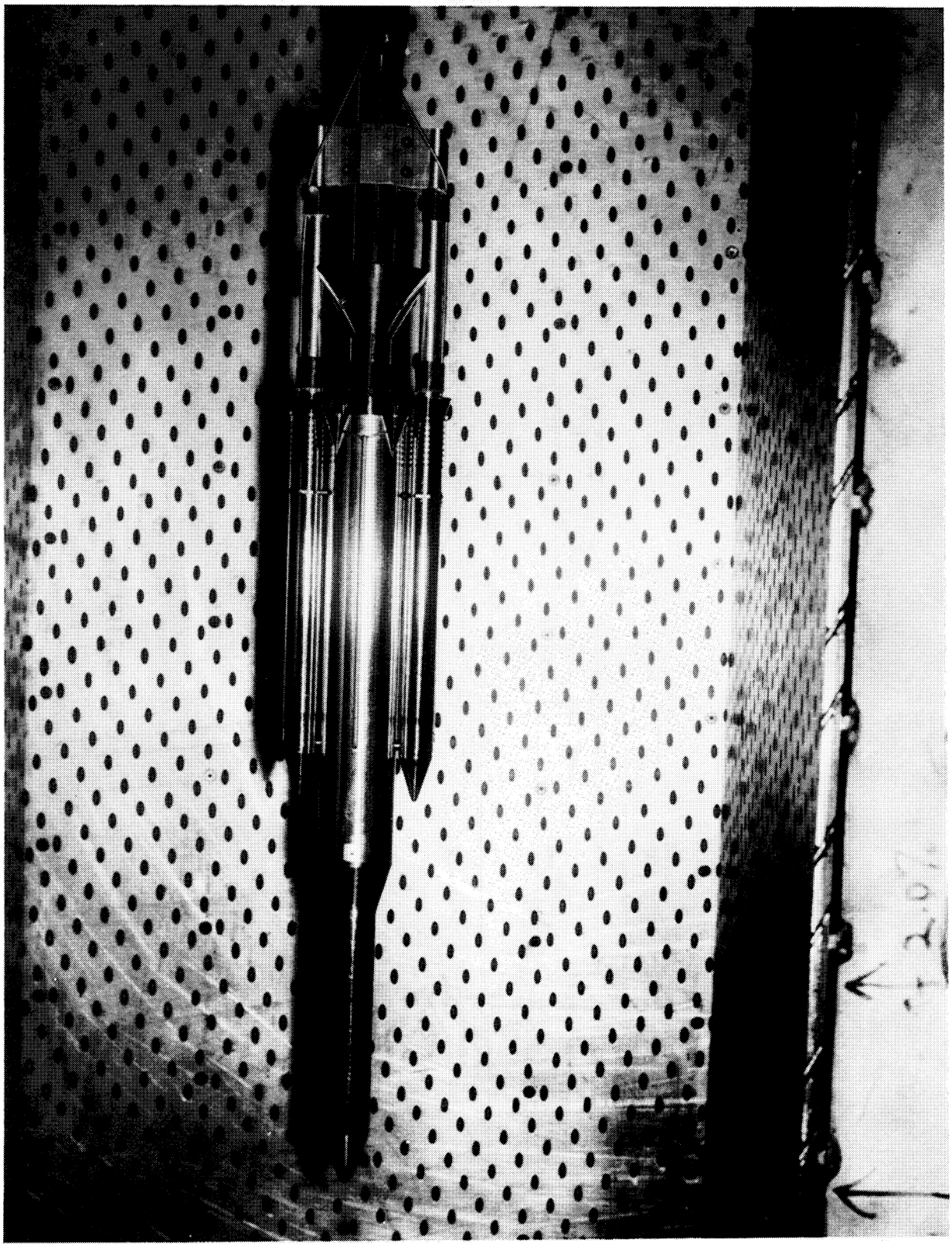

Figure 5. HLLV mounted in MSFC 14- by 14-Inch TWT.

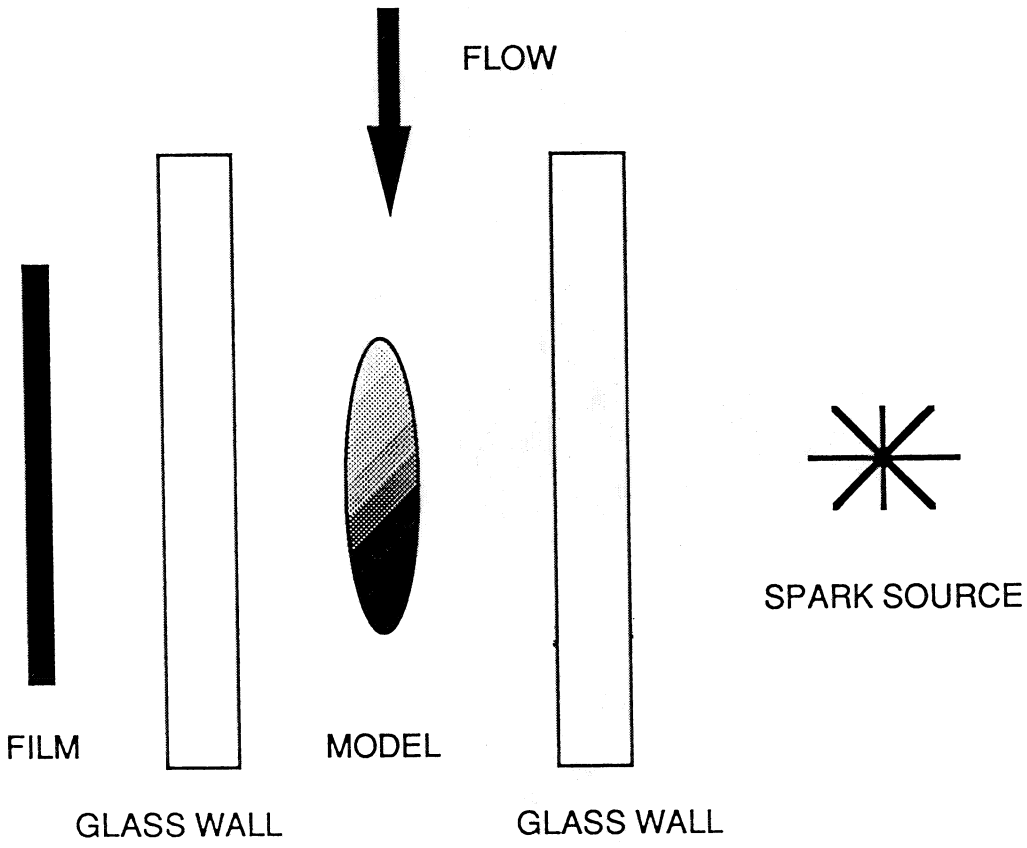

Figure 6. Shadowgraph setup.

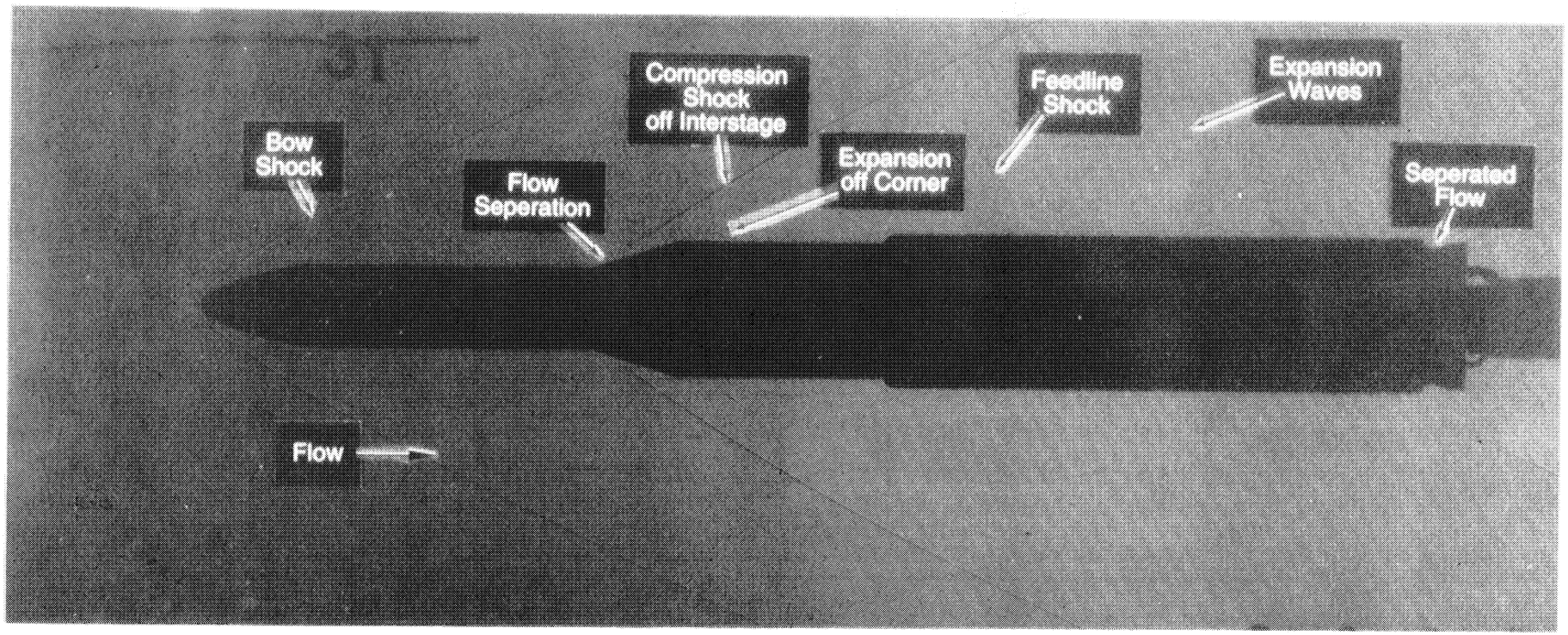

Figure 7. 1½ stage typical flow phenomena Mach 1.96, alpha = 0° and beta = 0°.

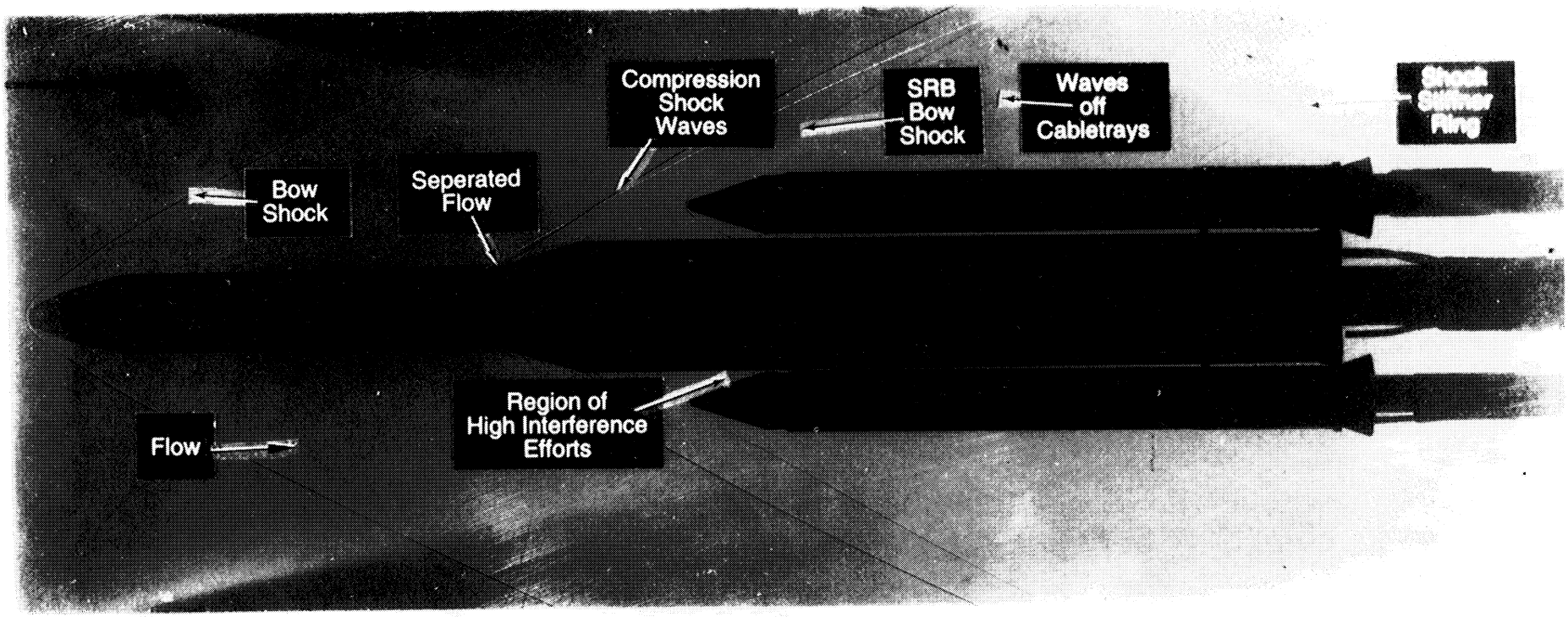

Figure 8. HLLV typical flow phenomena Mach 2.74, roll = 90°, alpha = 4°, beta = 0°.

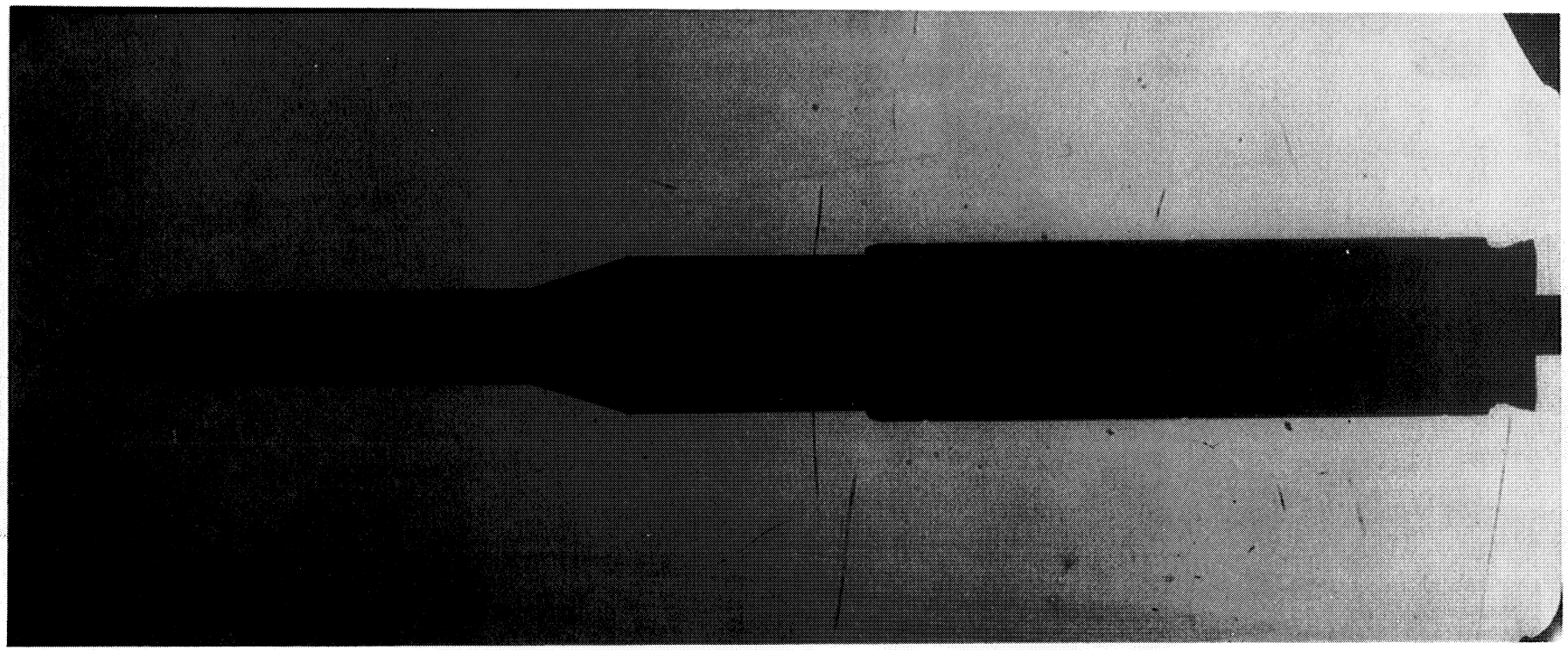

Figure 9. 1½ stage configuration Mach 0.6, alpha = 0° and beta = 0°.

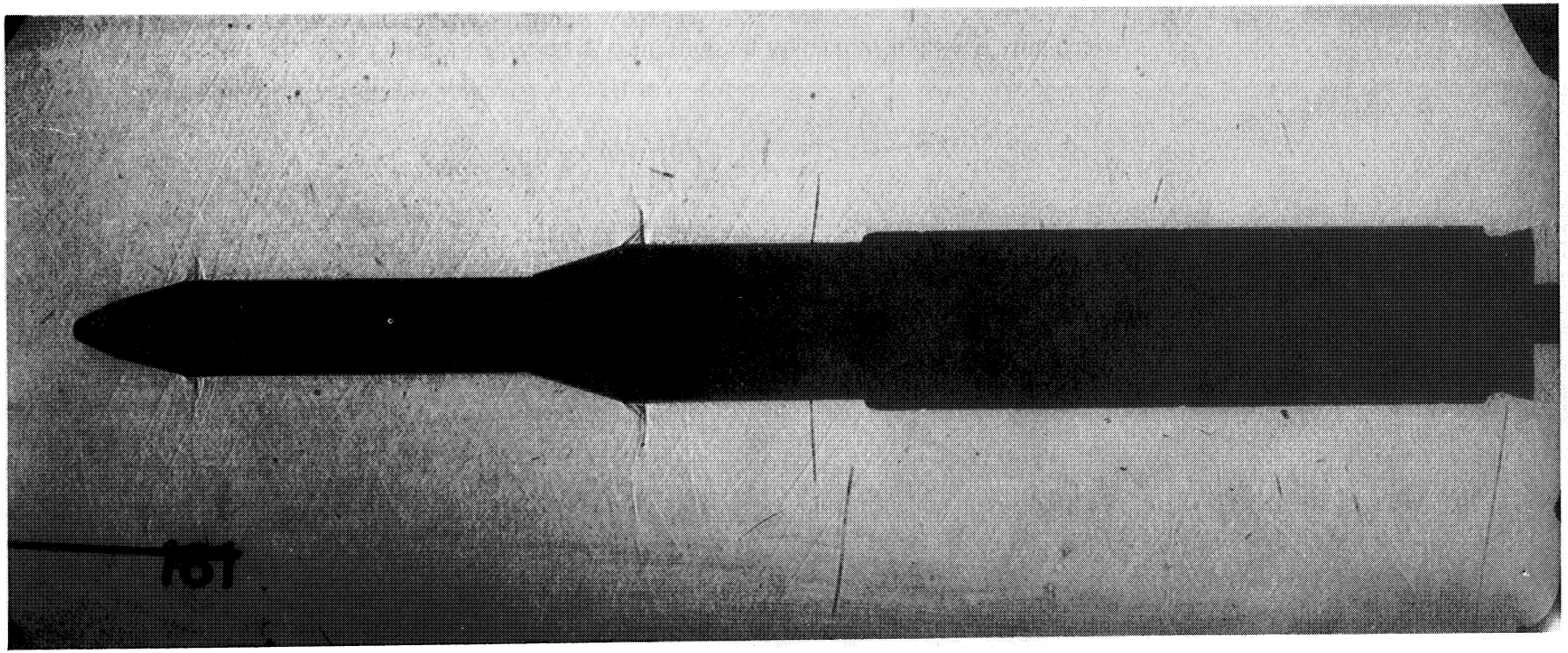

Figure 10. 1½ stage configuration Mach 0.8, alpha = 0° and beta = 0°.

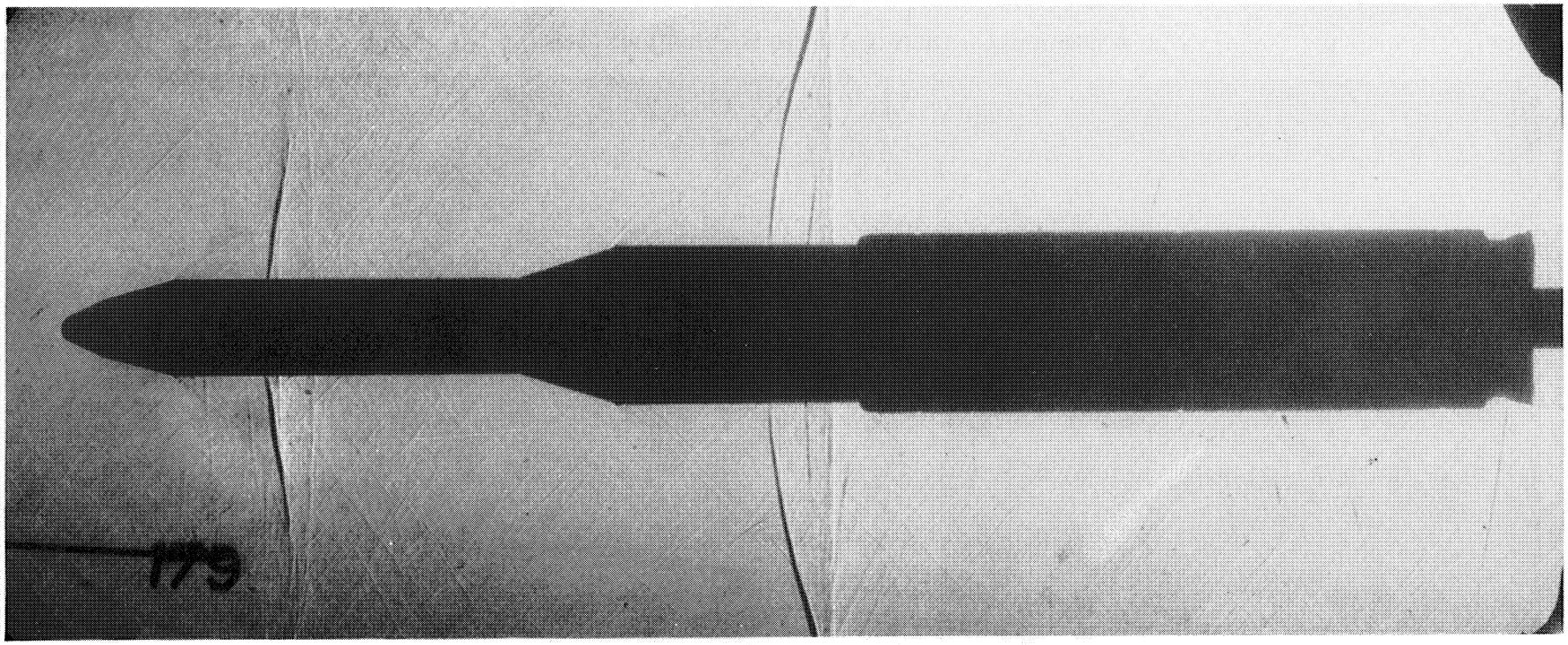

Figure 11. 1½ stage configuration Mach 0.9, alpha = 0° and beta = 0°.

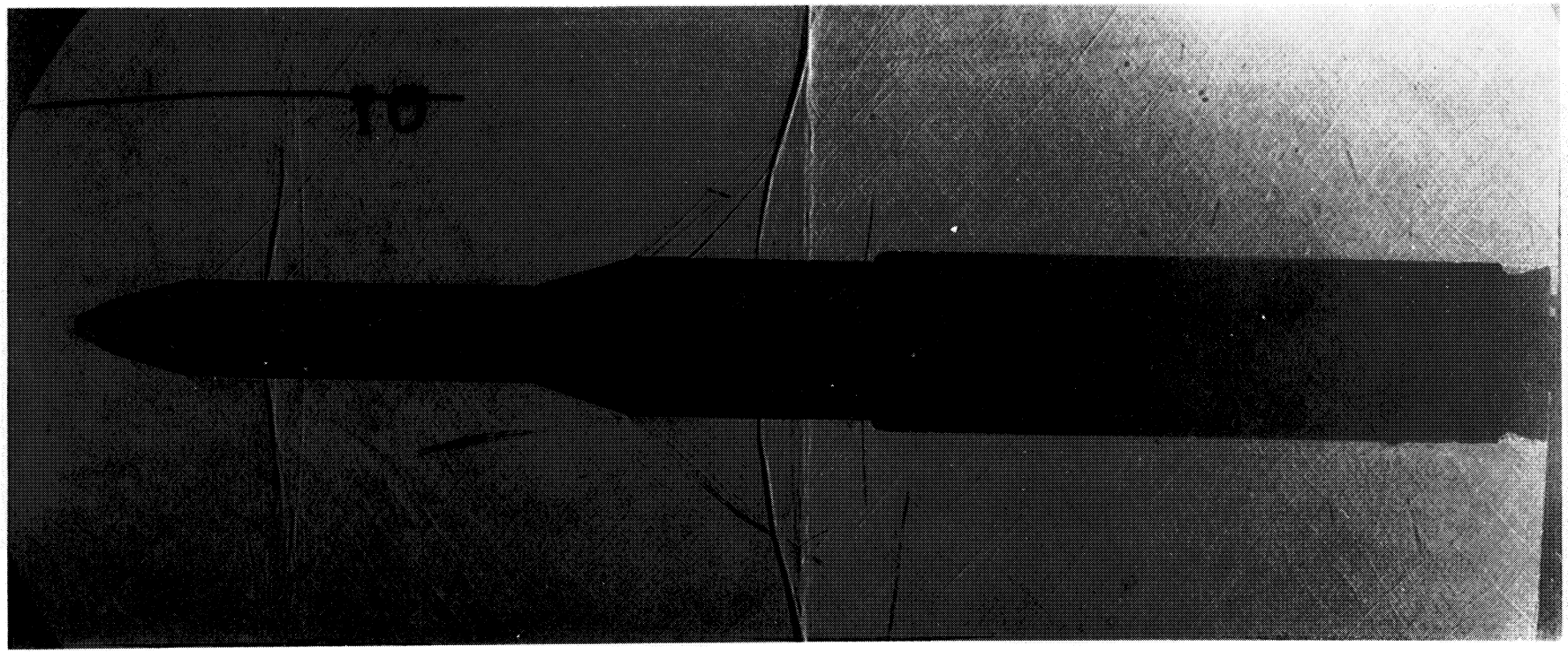

Figure 12. 1½ stage configuration Mach 0.95, alpha = 0° and beta = 0°.

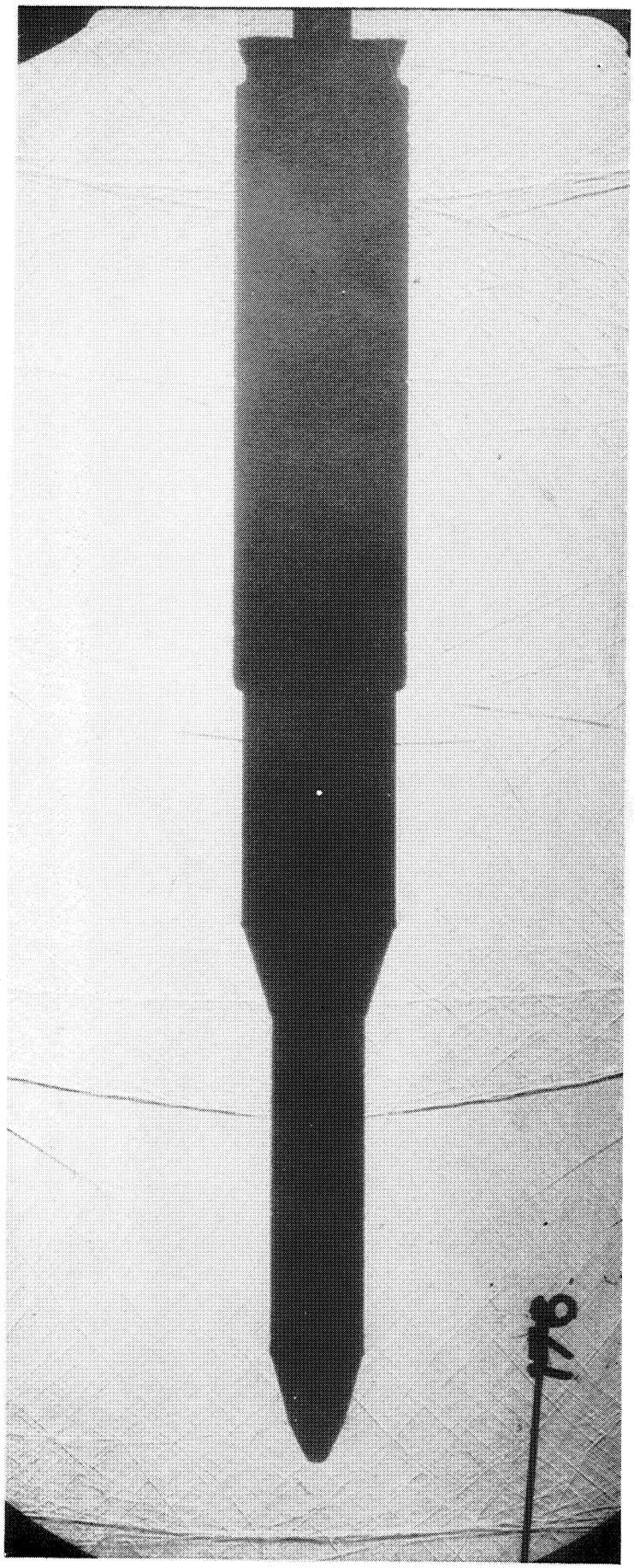

Figure 13. 1½ stage configuration Mach 1.05, alpha = 0° and beta = 0°.

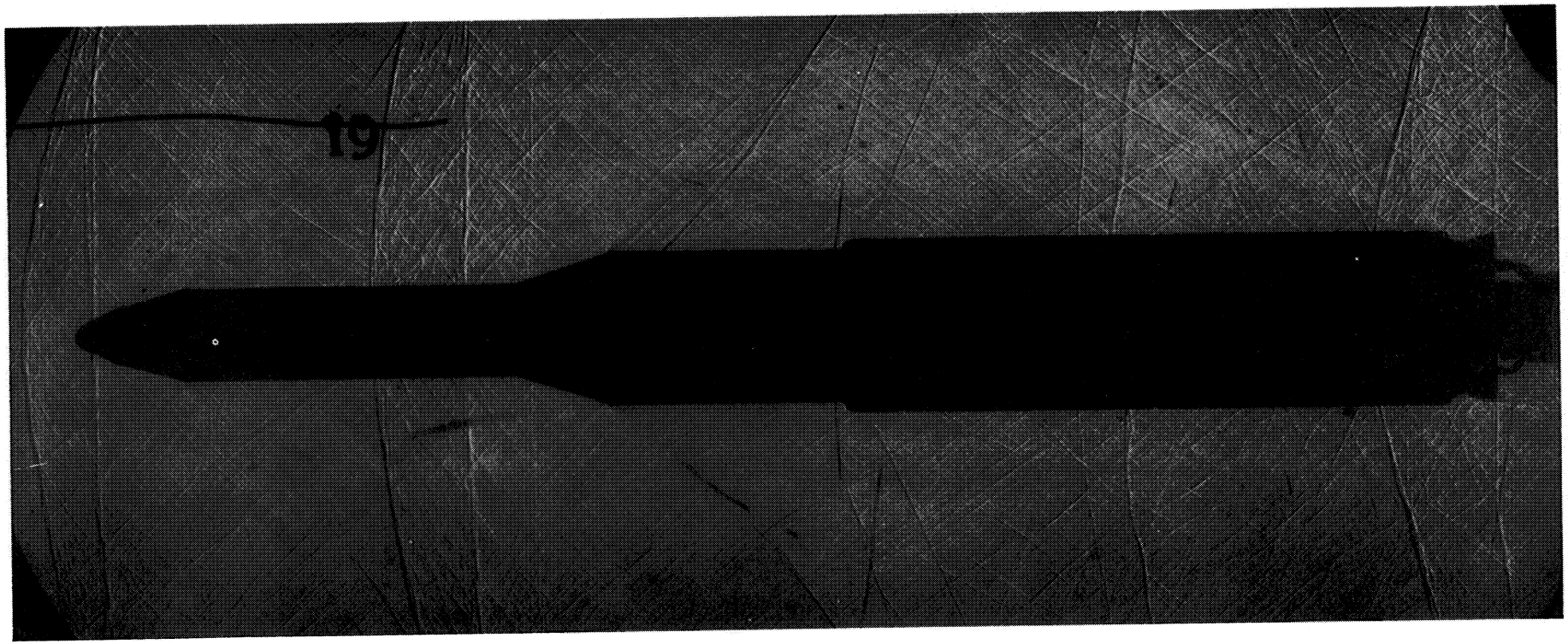

Figure 14. 1½ stage configuration Mach 1.10, alpha = 0° and beta = 0°.

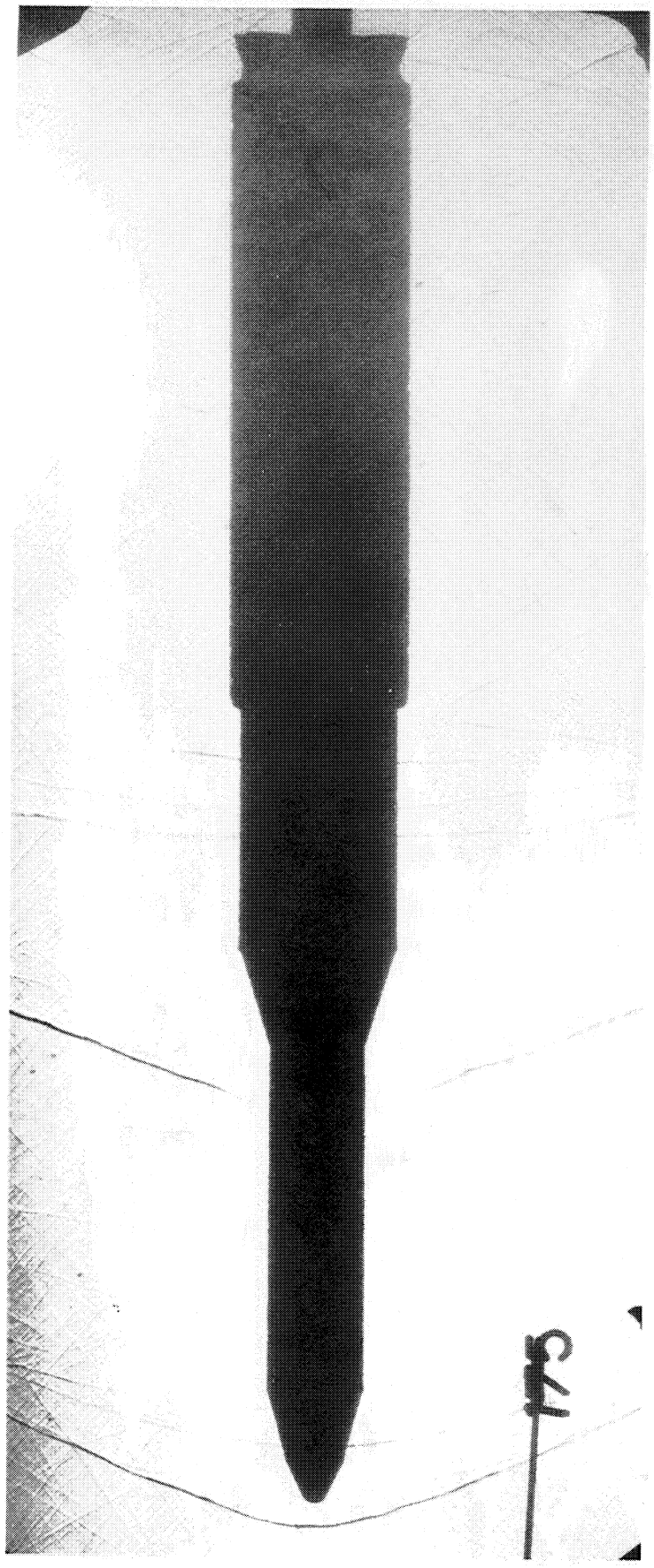

Figure 15. 1½ stage configuration Mach 1.15, alpha = 0° and beta = 0°.

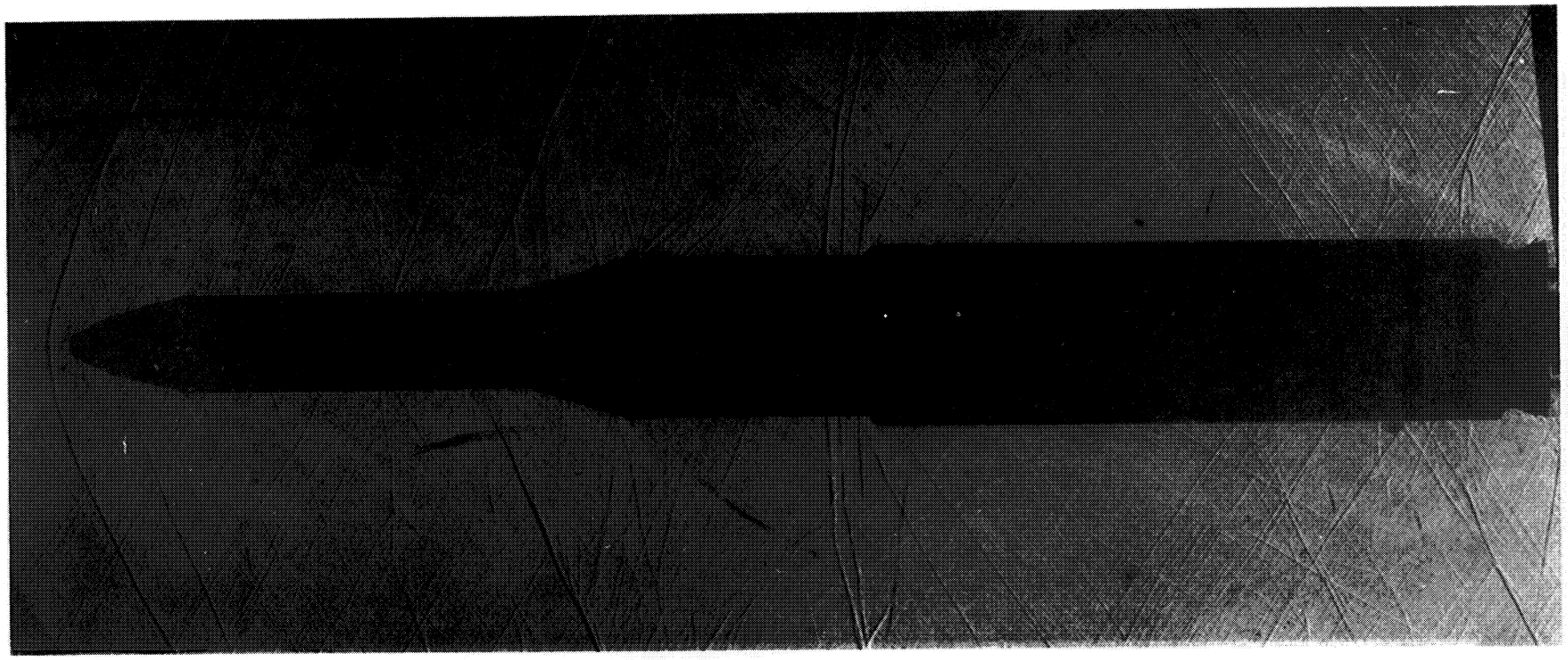

Figure 16. 1½ stage configuration Mach 1.25, alpha = 0° and beta = 0°.

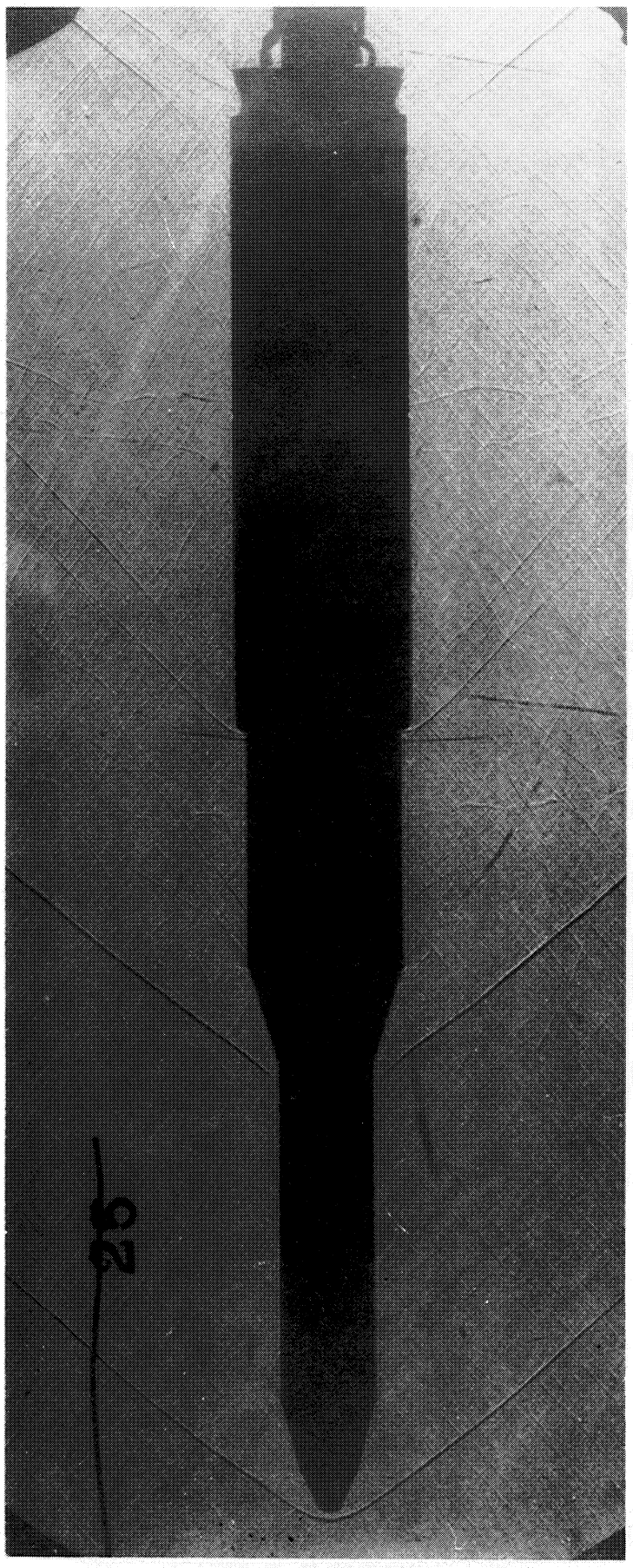

Figure 17. 1½ stage configuration Mach 1.46, alpha = 0° and beta = 0°.

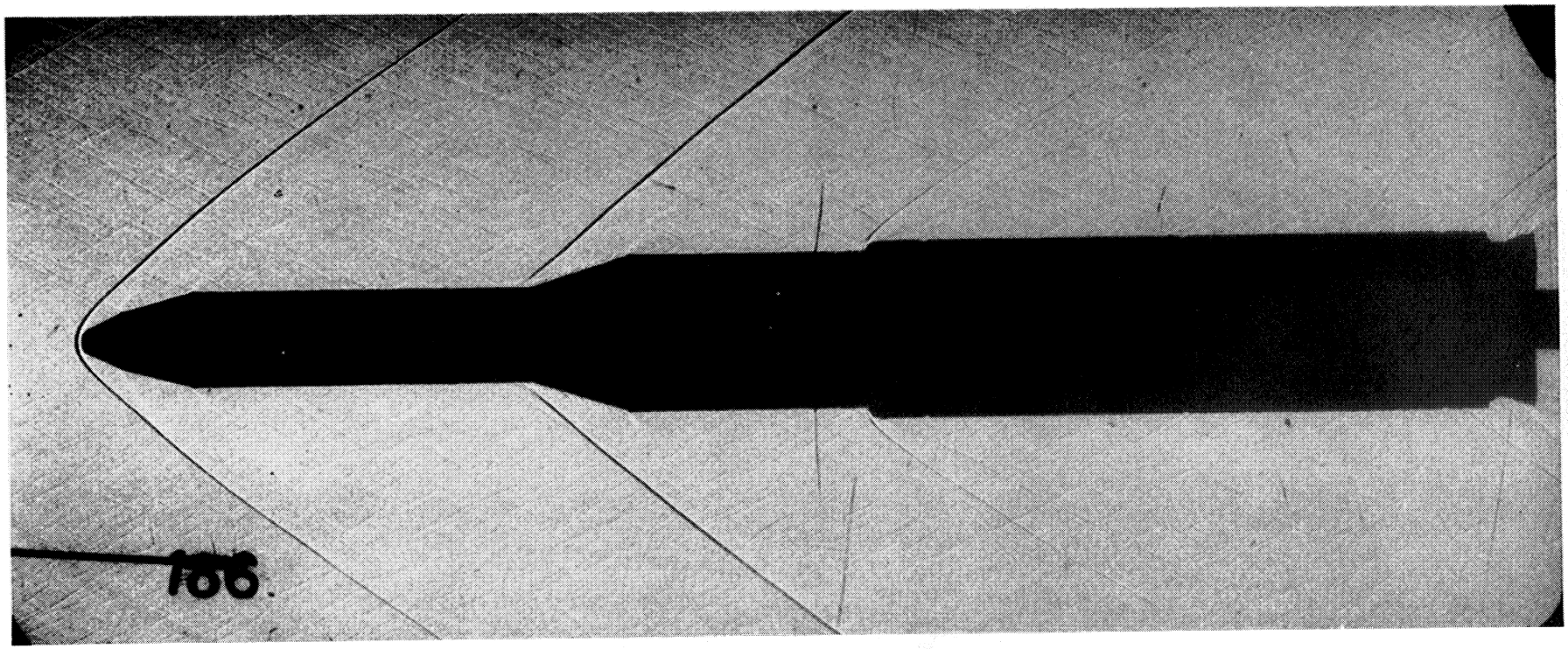

Figure 18. 1½ stage configuration Mach 1.96, alpha = 0° and beta = 0°.

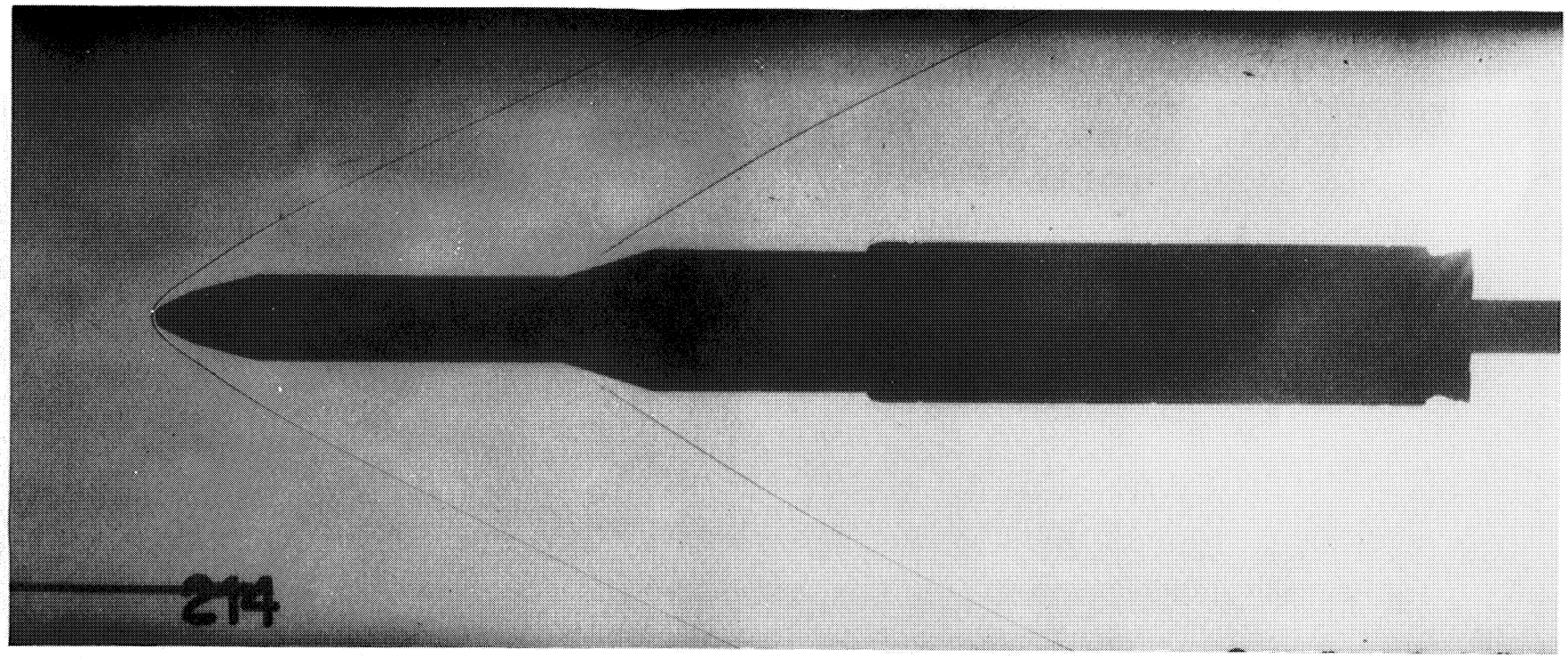

Figure 19. 1½ stage configuration Mach 2.74, alpha = 0° and beta = 0°.

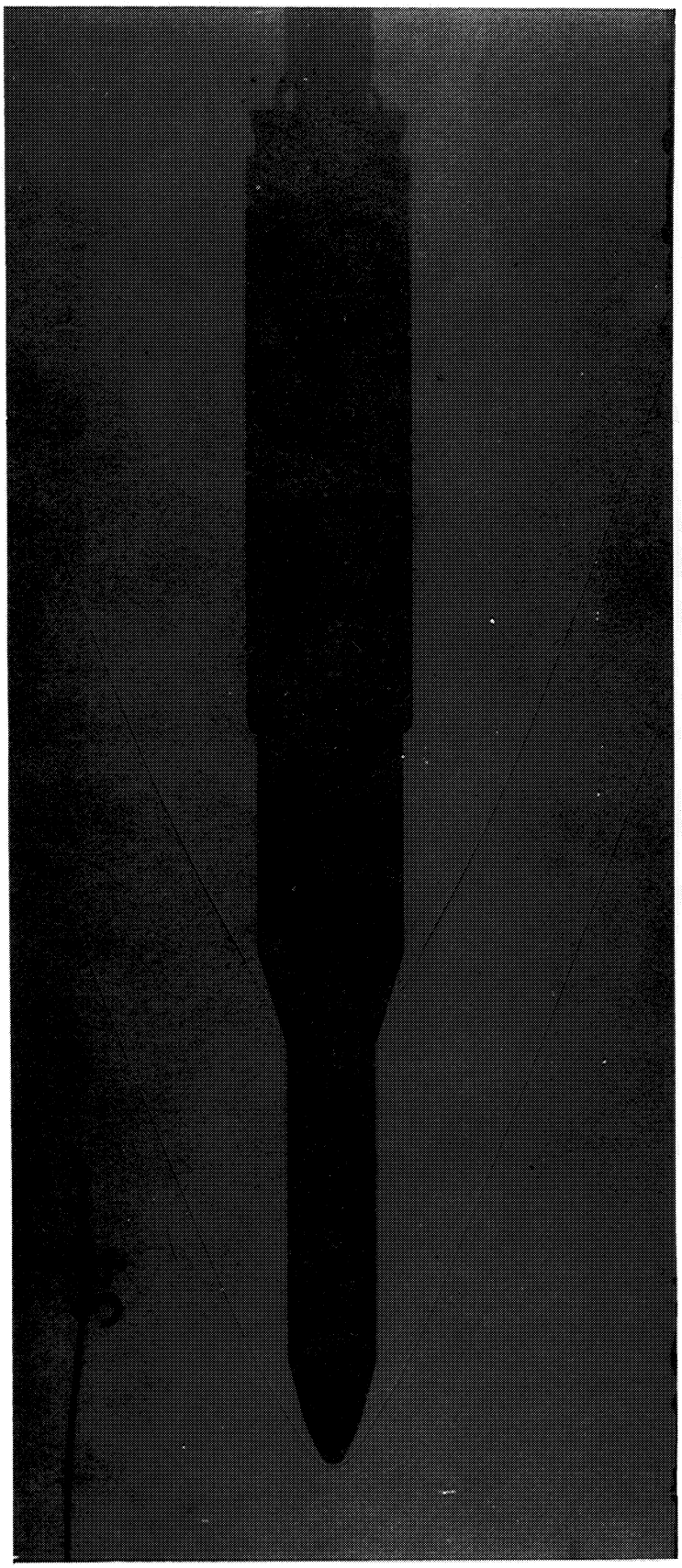

Figure 20. 1½ stage configuration Mach 3.48, alpha = 0° and beta = 0°.

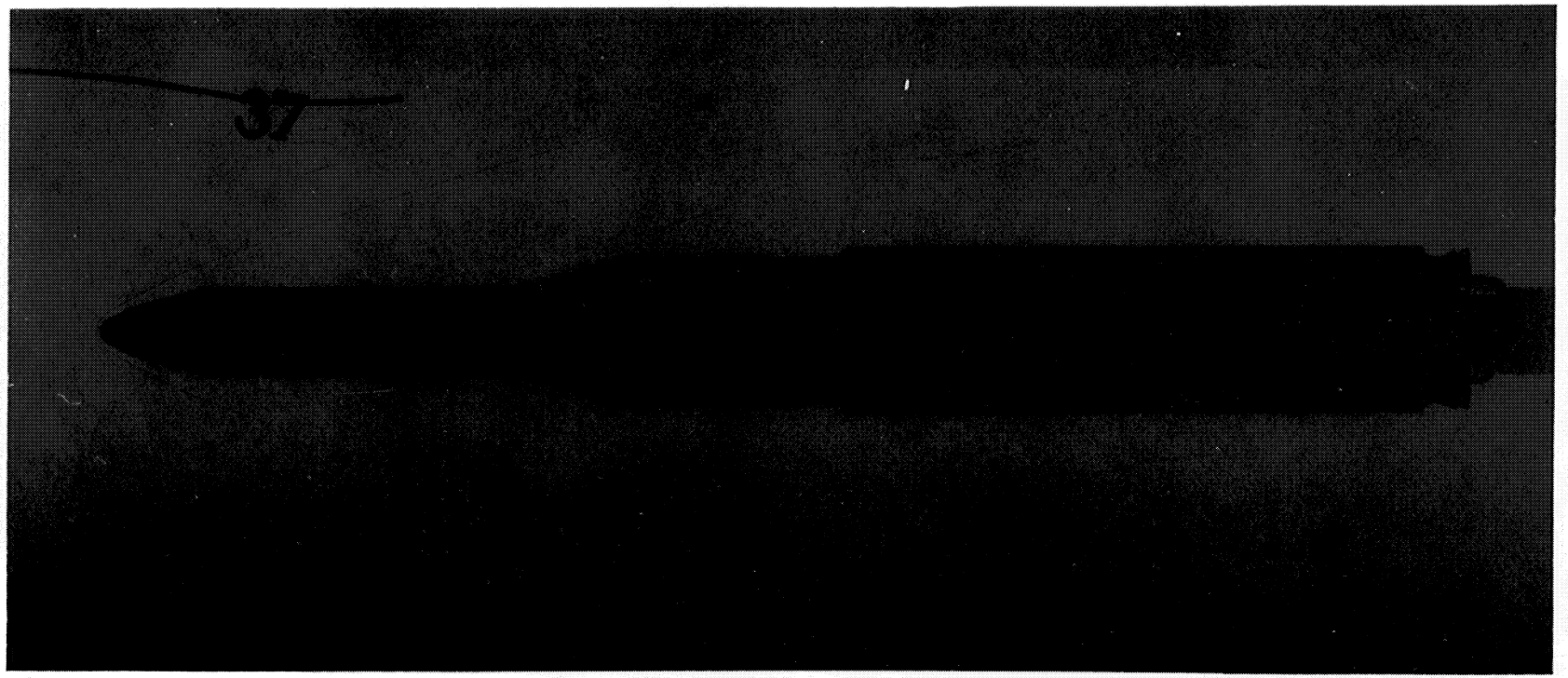

Figure 21. 1½ stage configuration Mach 4.96, alpha = 0° and beta = 0°.

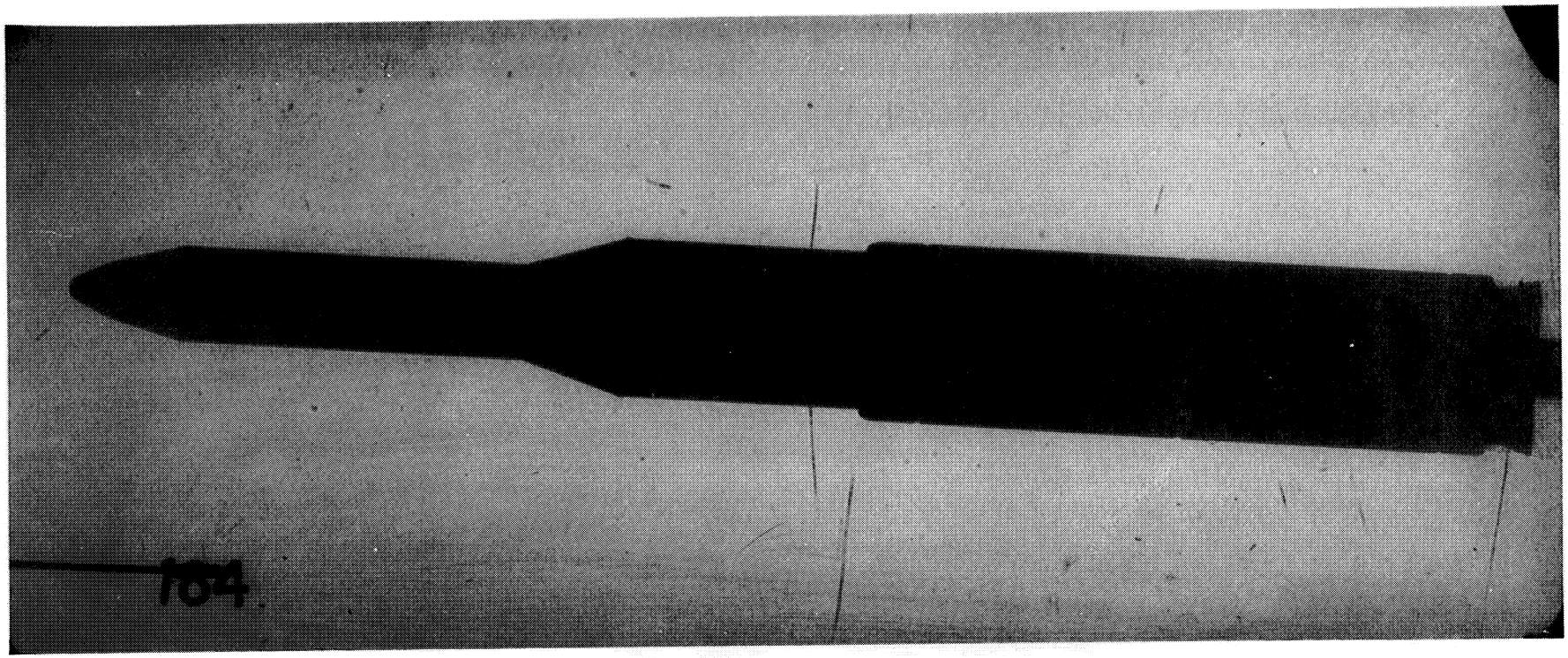

Figure 22. 1½ stage configuration Mach 0.6, alpha = 4° and beta = 0°.

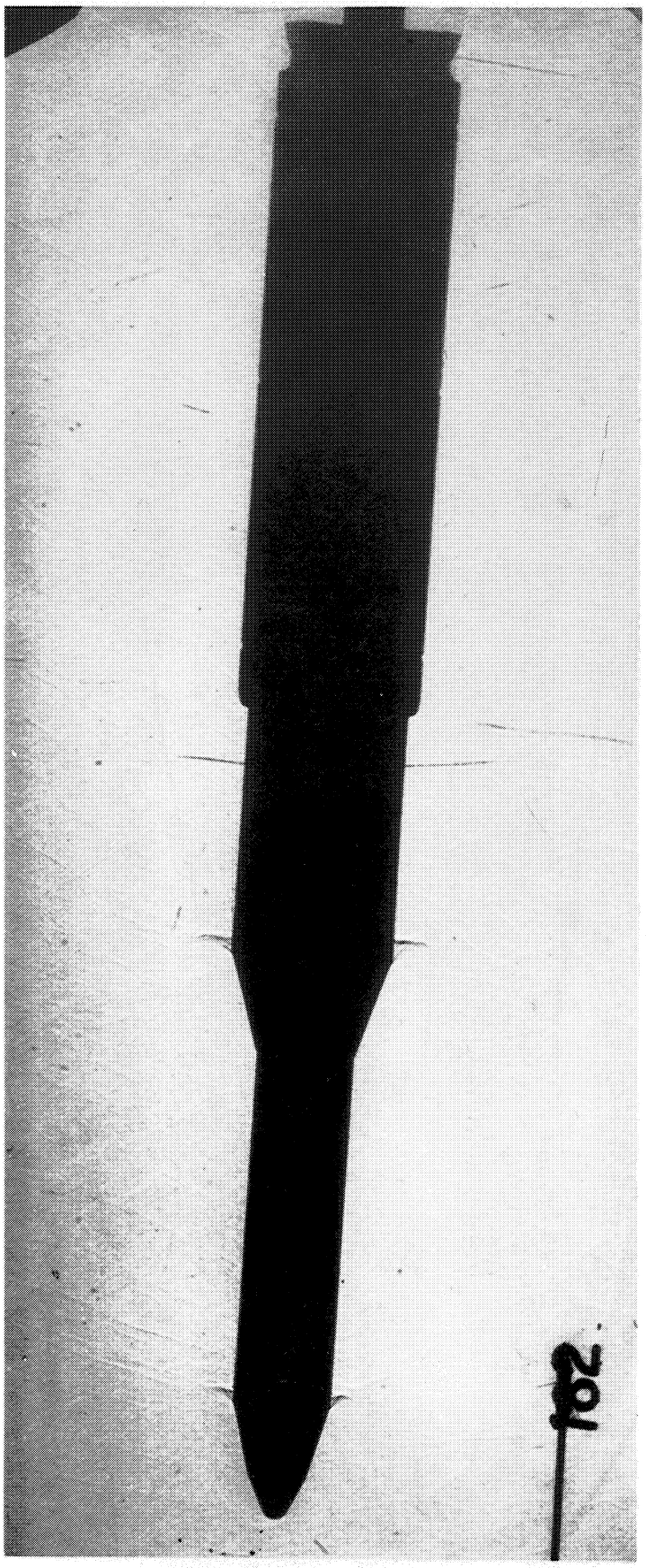

Figure 23. 1½ stage configuration Mach 0.8, alpha = 4° and beta = 0°.

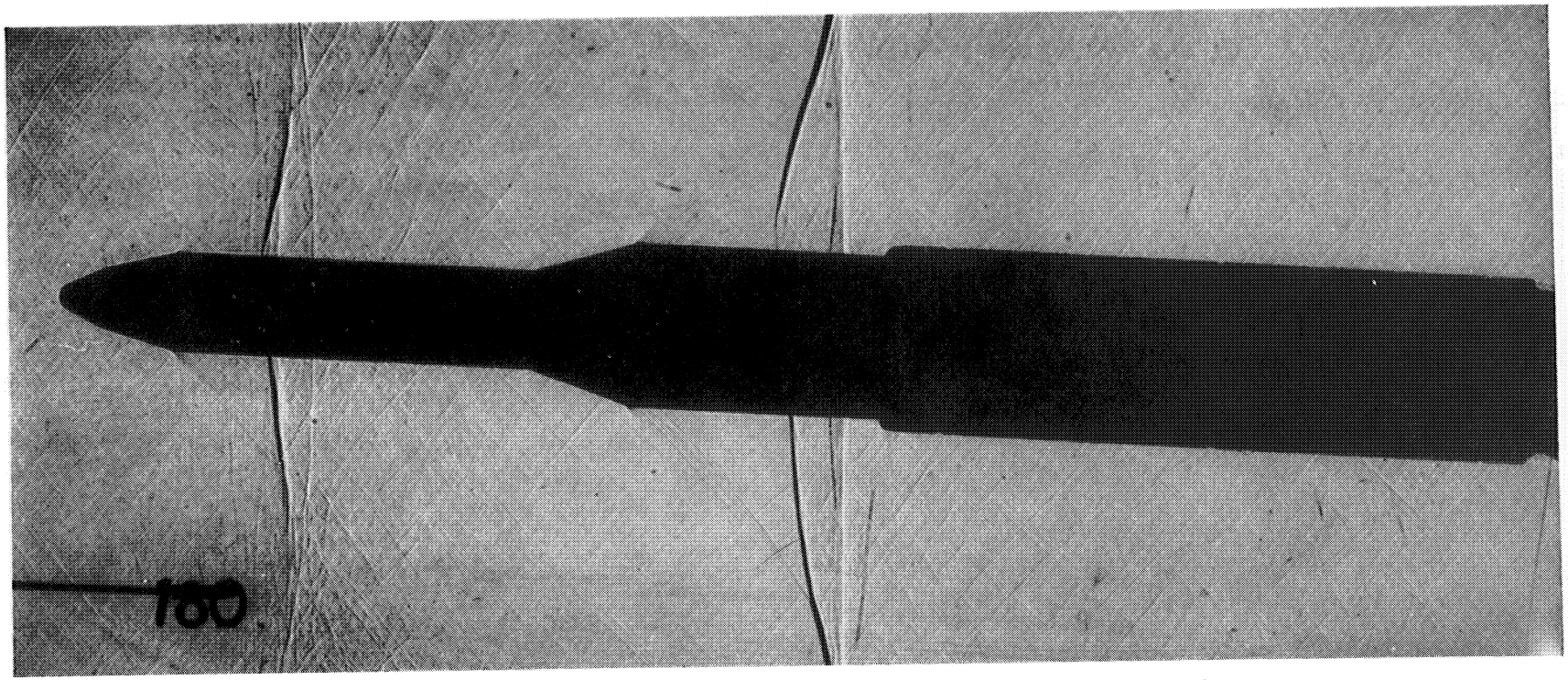

Figure 24. 1½ stage configuration Mach 0.9, alpha = 4° and beta = 0°.

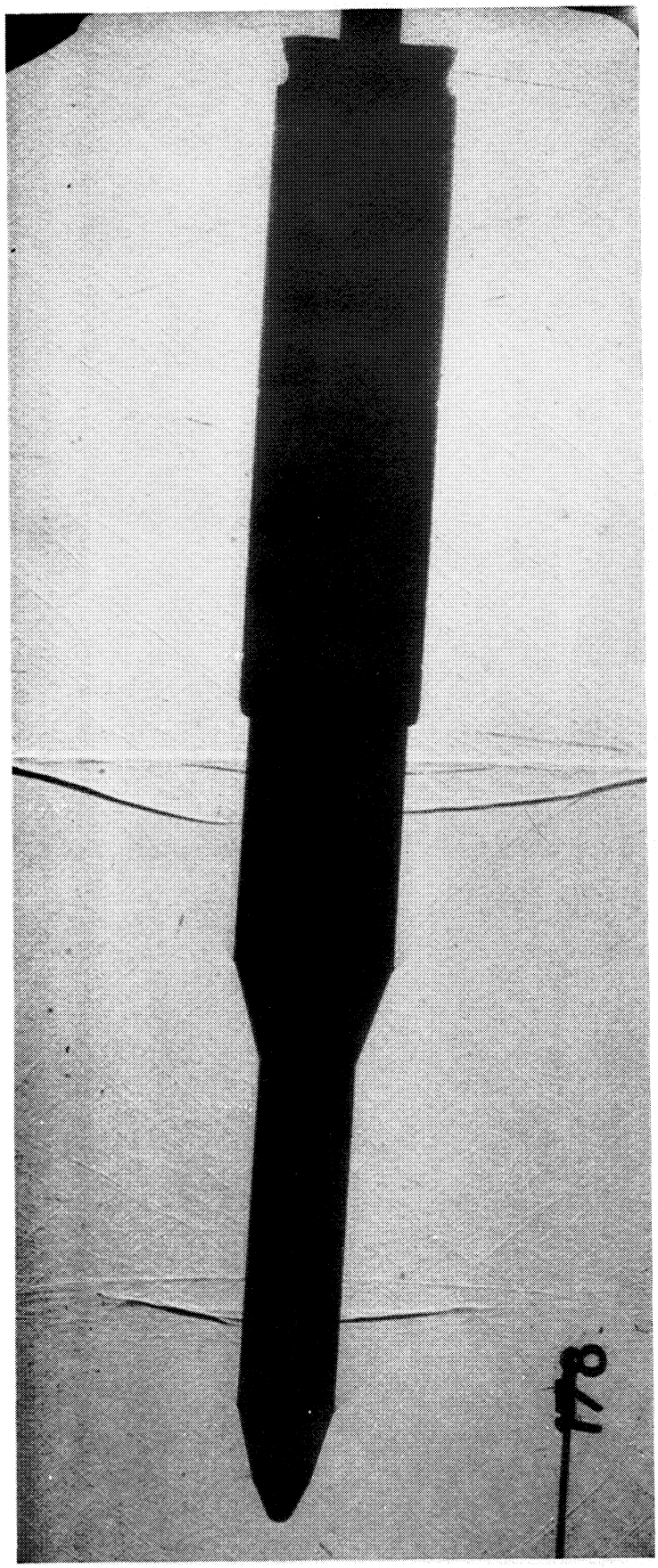

Figure 25. 1½ stage configuration Mach 0.95, alpha = 4° and beta = 0°.

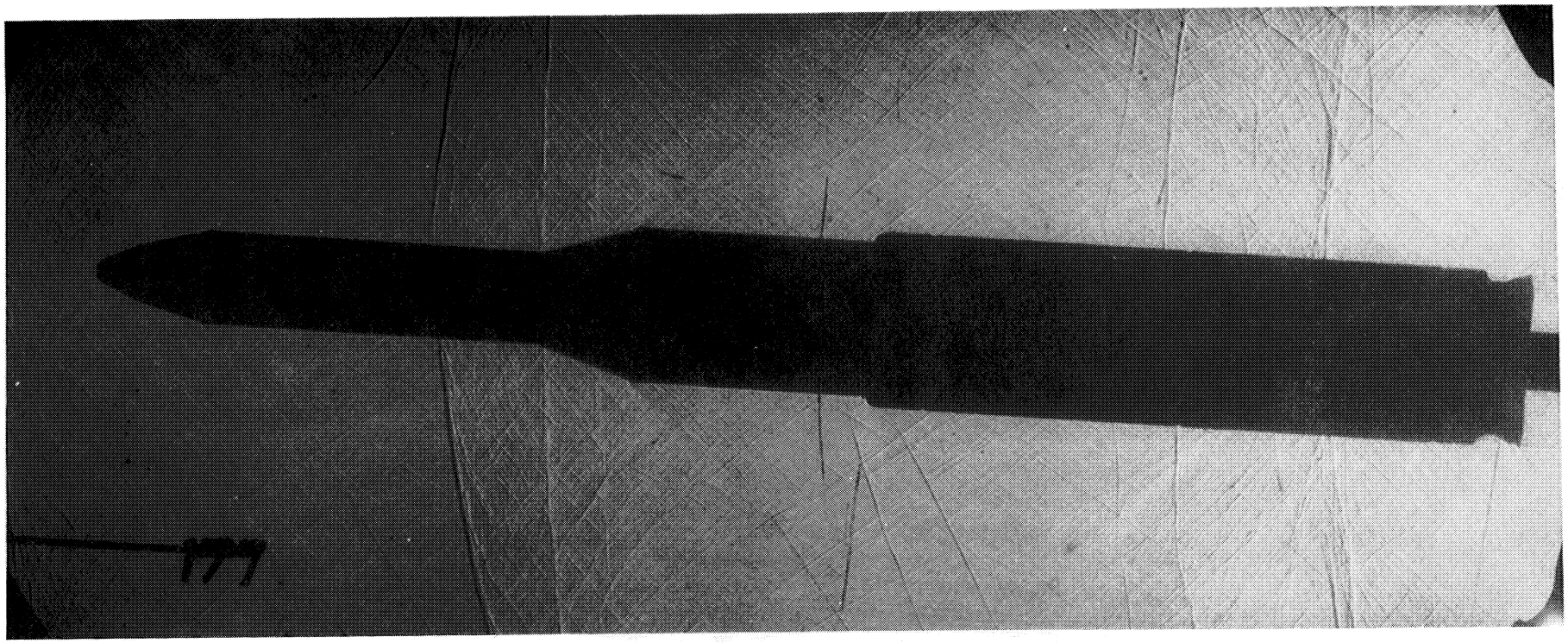

Figure 26. 1½ stage configuration Mach 1.05, alpha = 4° and beta = 0°.

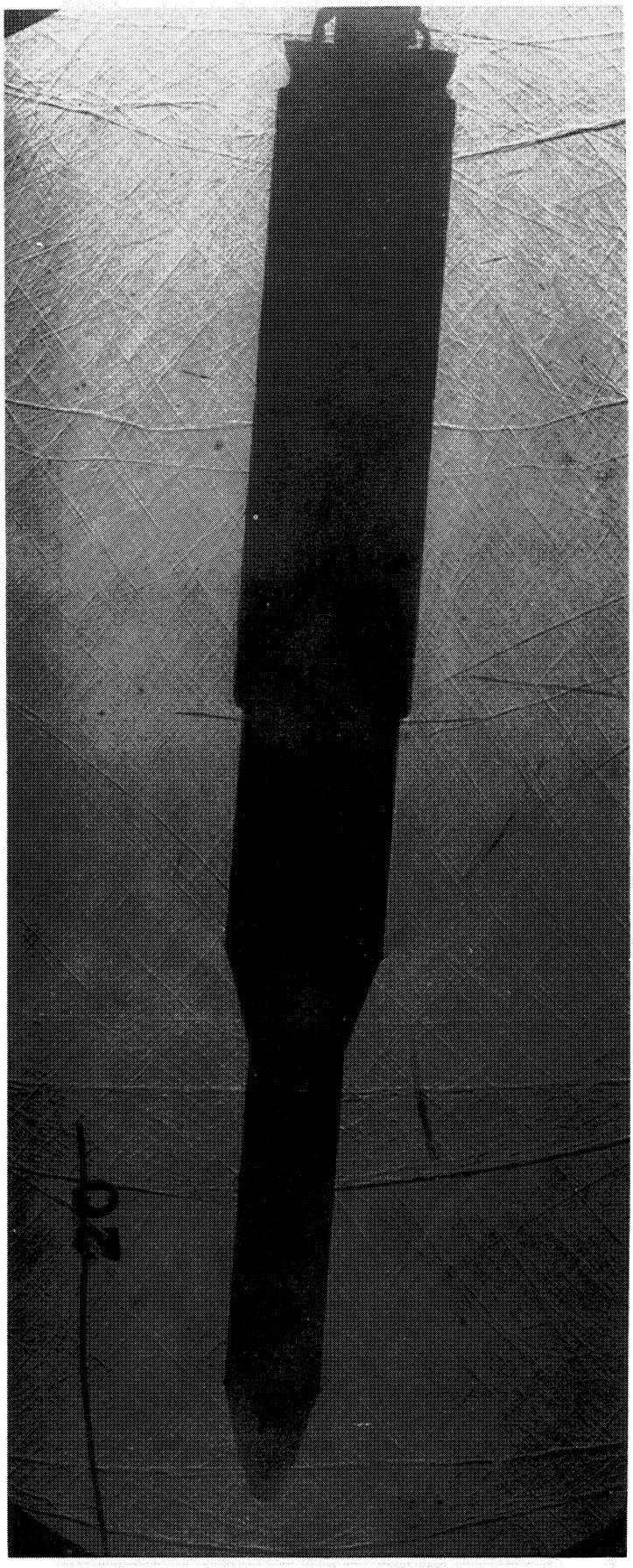

Figure 27. 1½ stage configuration Mach 1.10, alpha = 4° and beta = 0°.

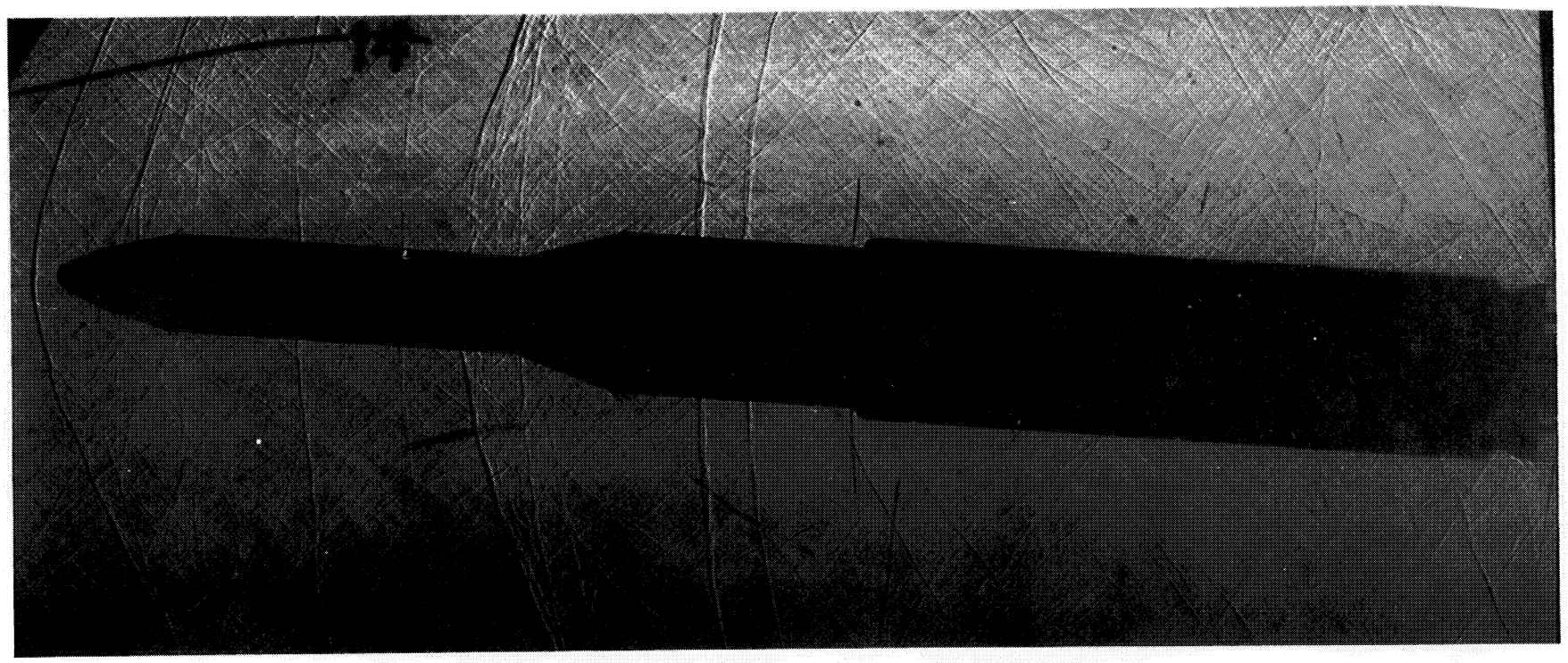

Figure 28. 1½ stage configuration Mach 1.15, alpha = 4° and beta = 0°.

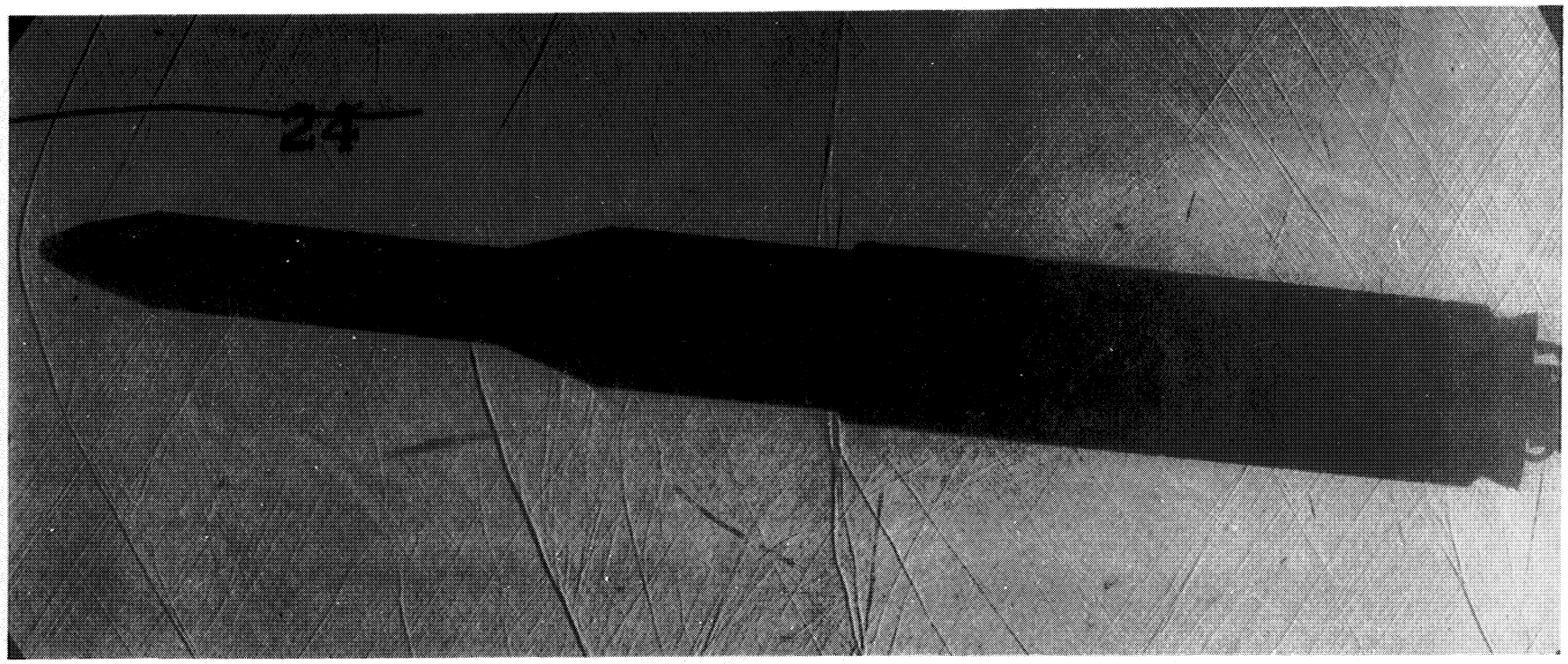

Figure 29. 1½ stage configuration Mach 1.25, alpha = 4° and beta = 0°.

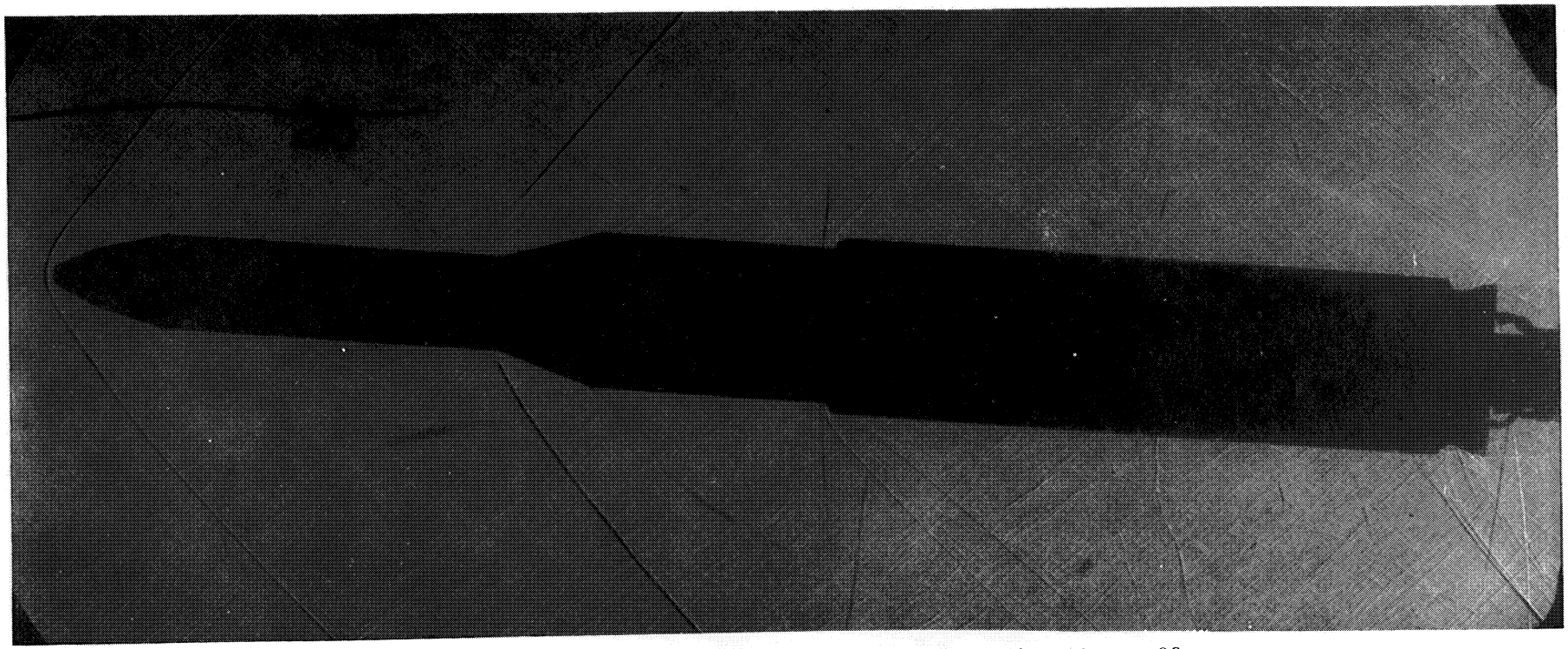

Figure 30. 1½ stage configuration Mach 1.46, alpha = 4° and beta = 0°.

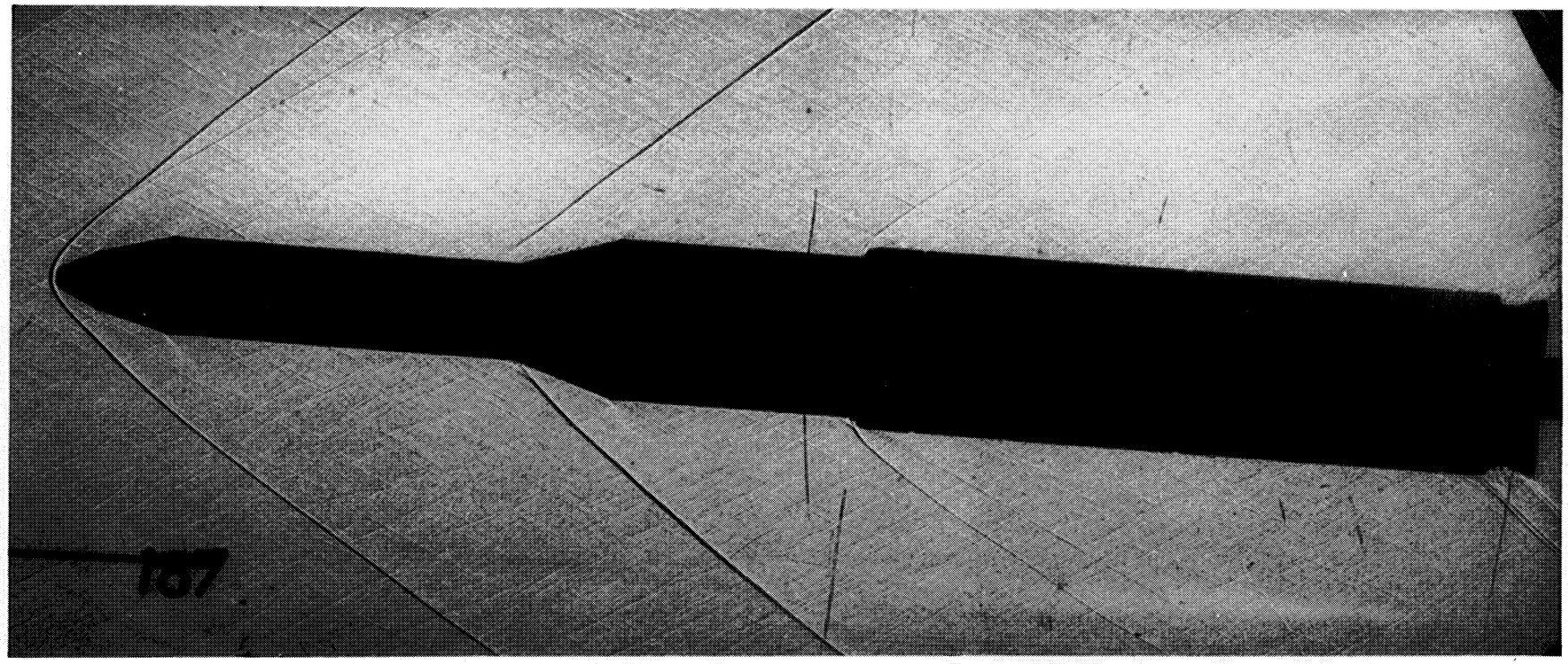

Figure 31. 1½ stage configuration Mach 1.96, alpha = 4° and beta = 0°.

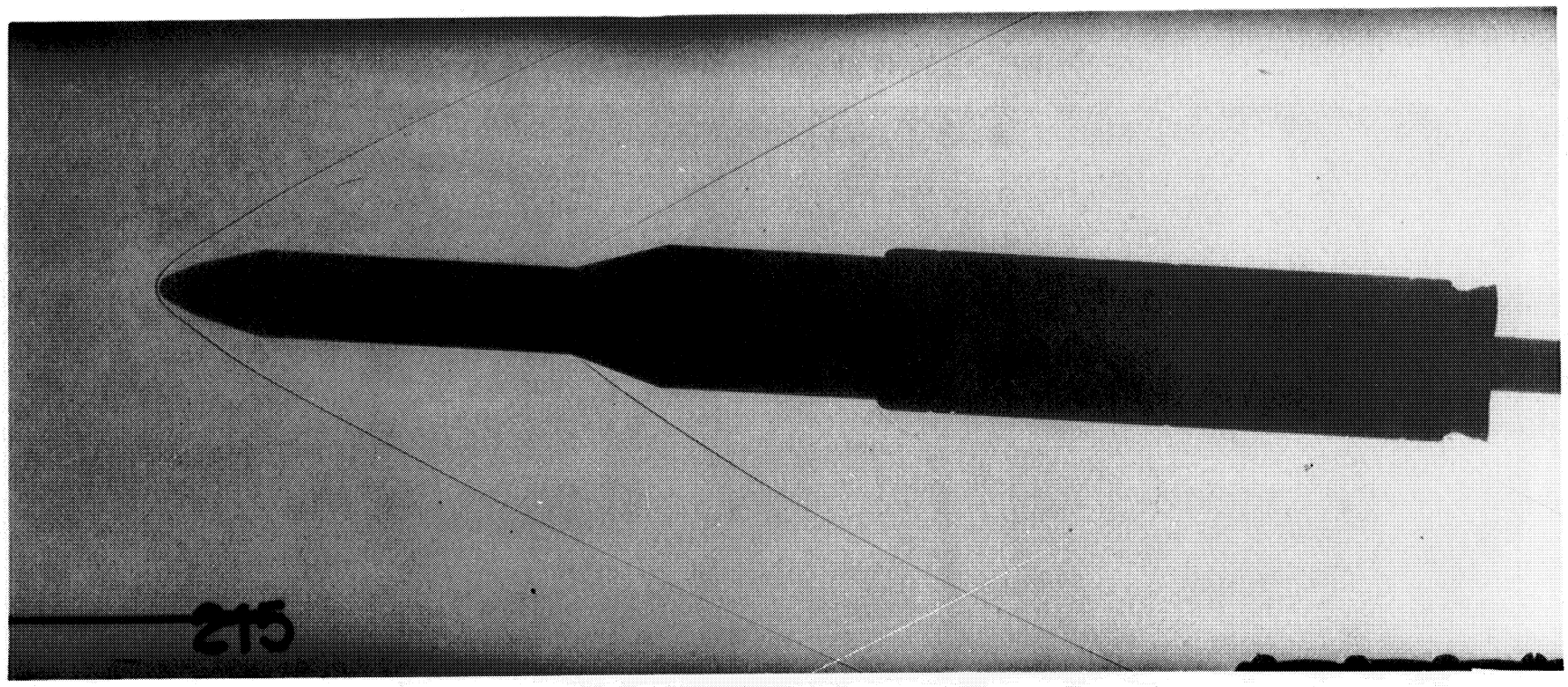

Figure 32. 1½ stage configuration Mach 2.74, alpha = 4° and beta = 0°.

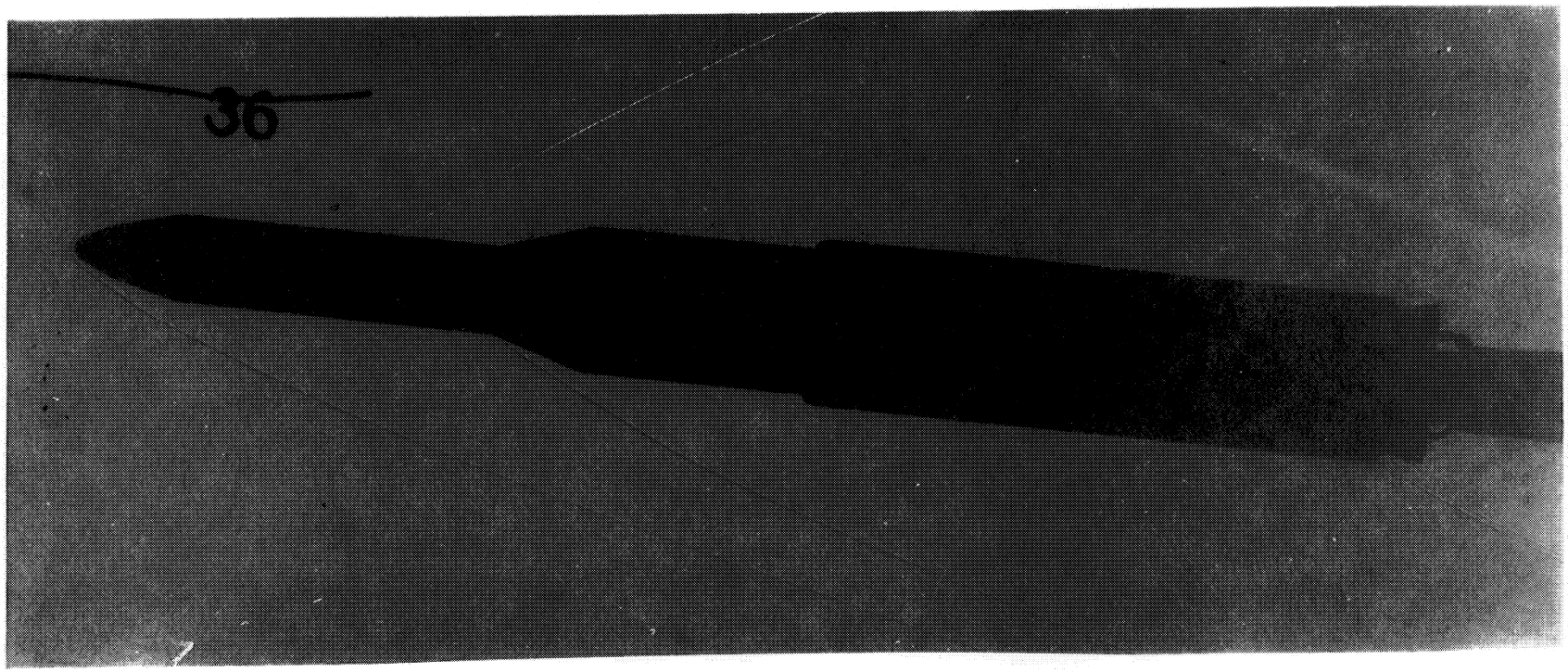

Figure 33. 1½ stage configuration Mach 3.48, alpha = 4° and beta = 0°.

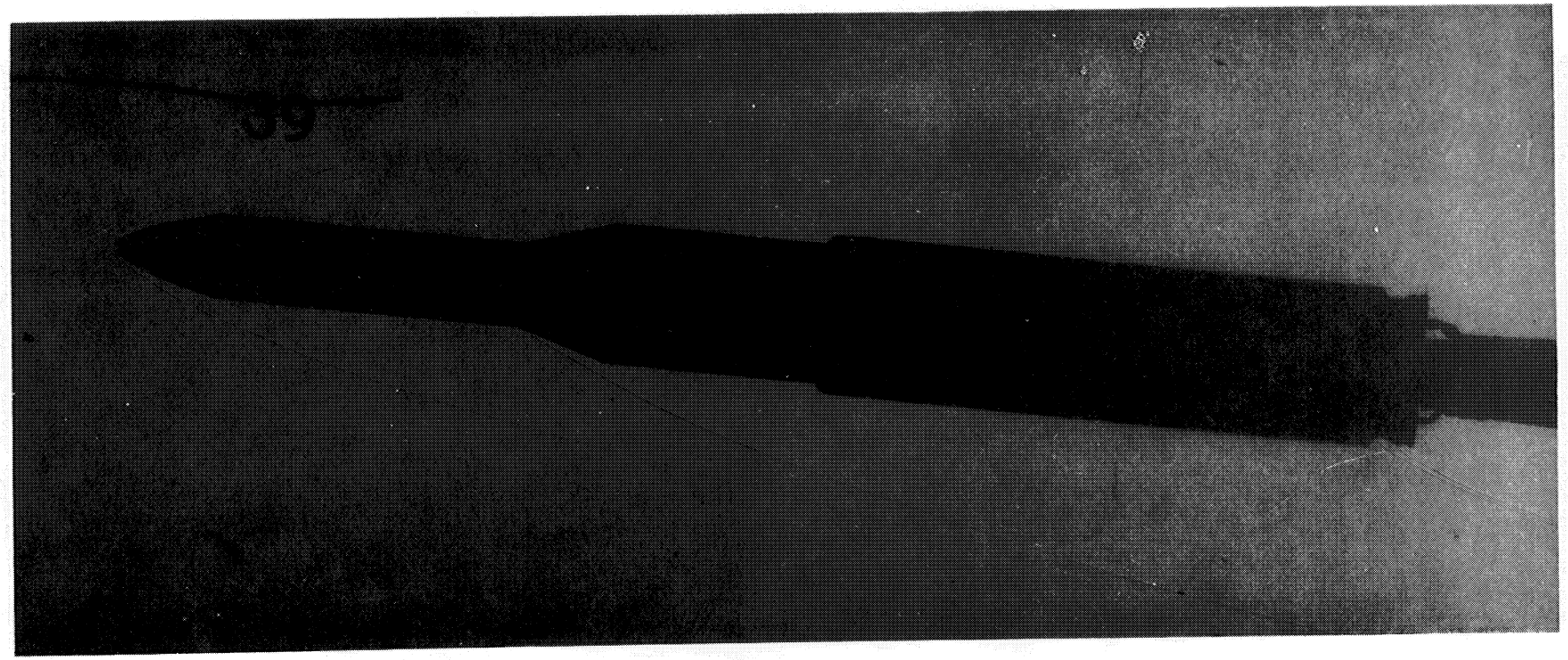

Figure 34. 1½ stage configuration Mach 4.96, alpha = 4° and beta = 0°.

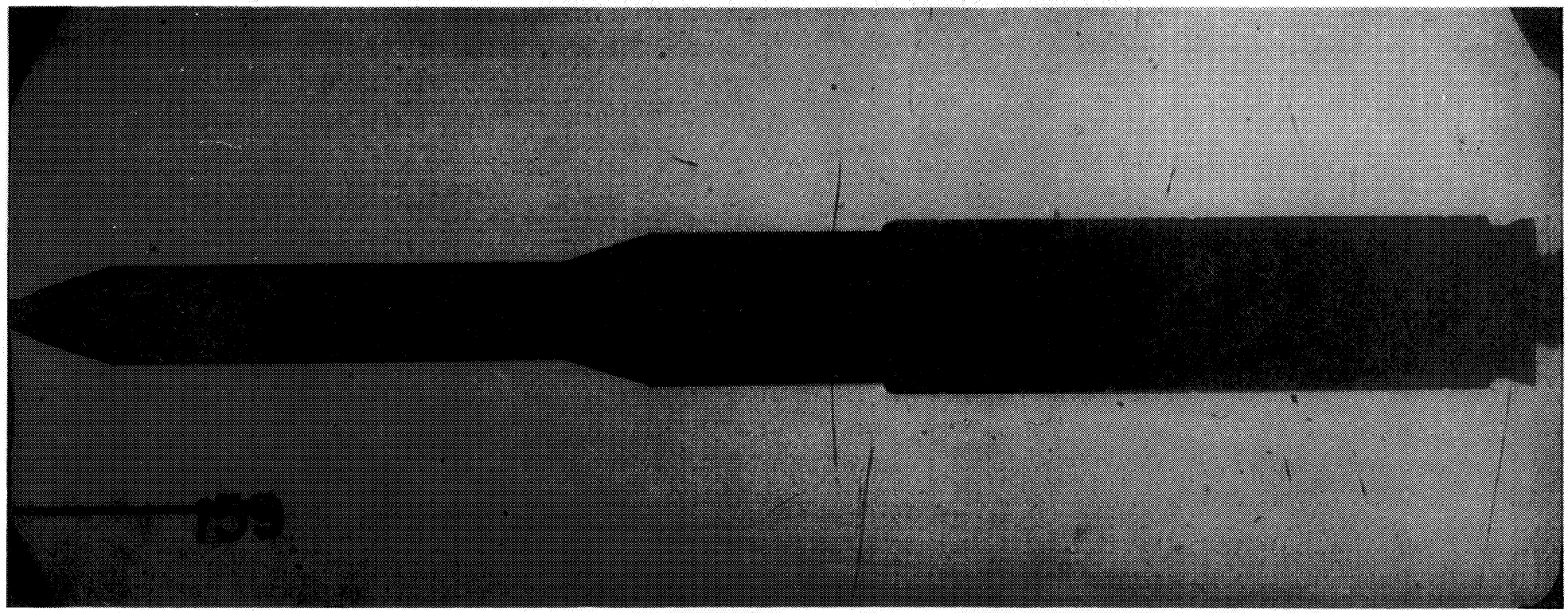

Figure 35. HLLV Mach 0.6, alpha = 0° and beta = 0°.

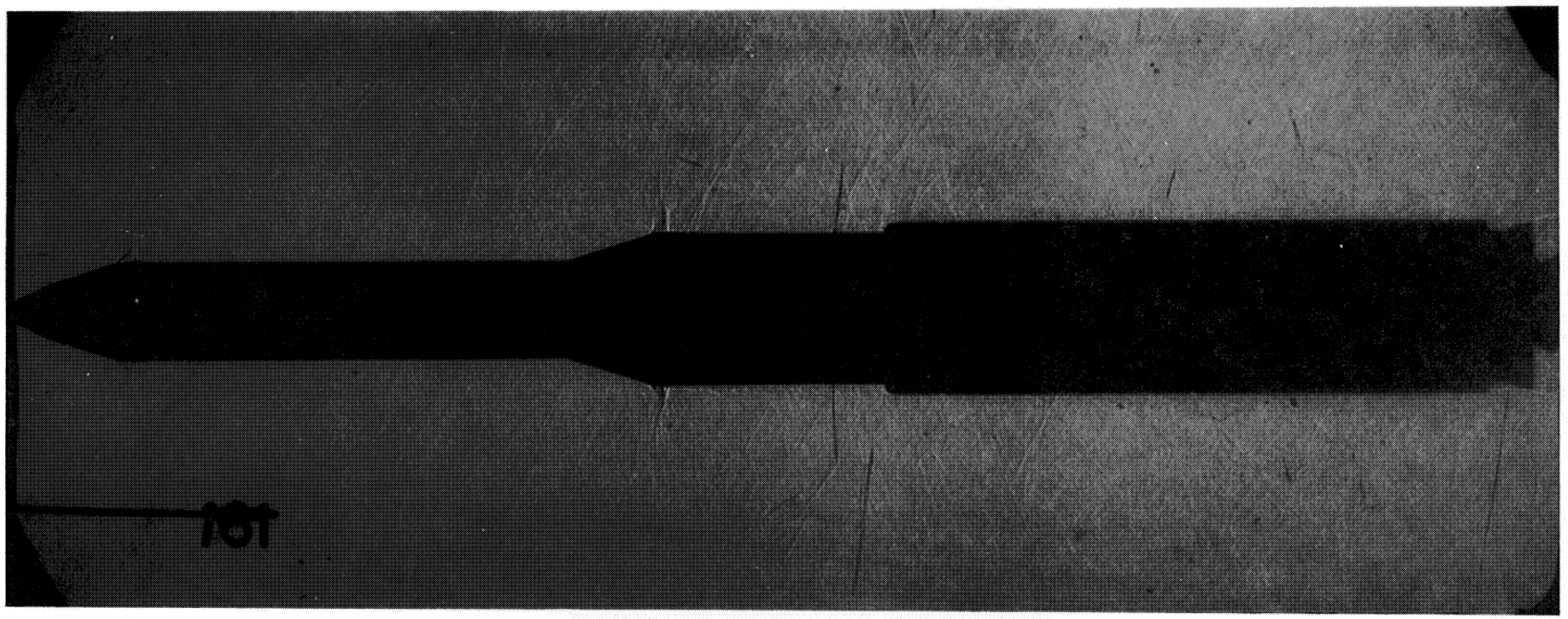

Figure 36. HLLV Mach 0.8, alpha = 0° and beta = 0°.

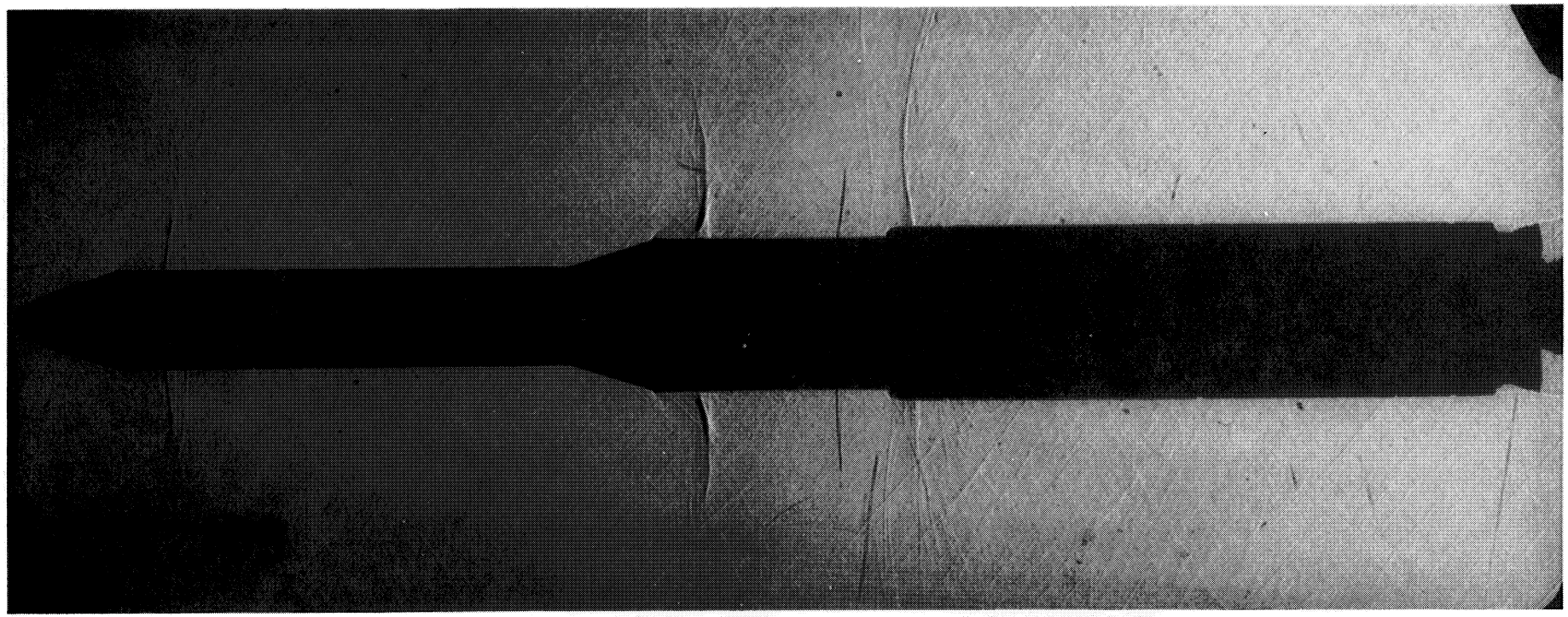

Figure 37. HLLV Mach 0.9, alpha = 0° and beta = 0°.

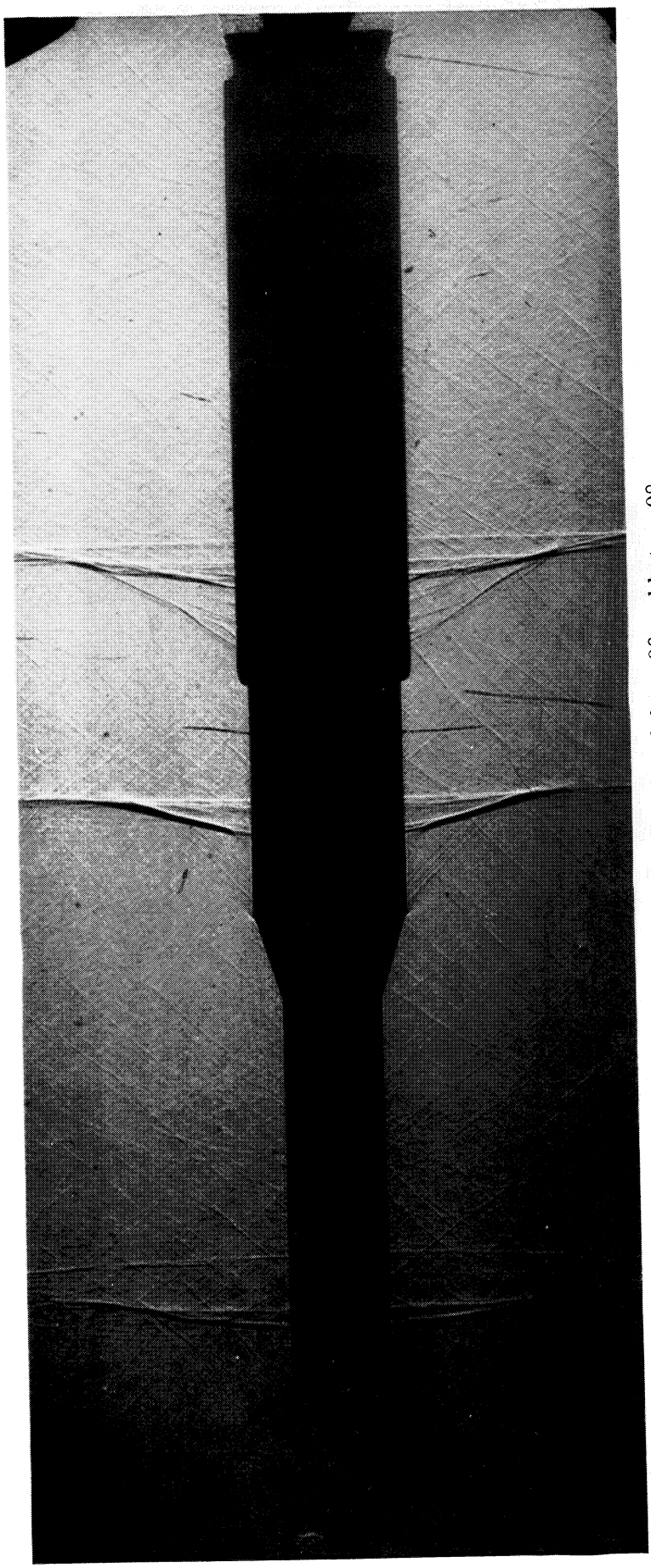

Figure 38. HLLV Mach 0.95, alpha = 0° and beta = 0°.

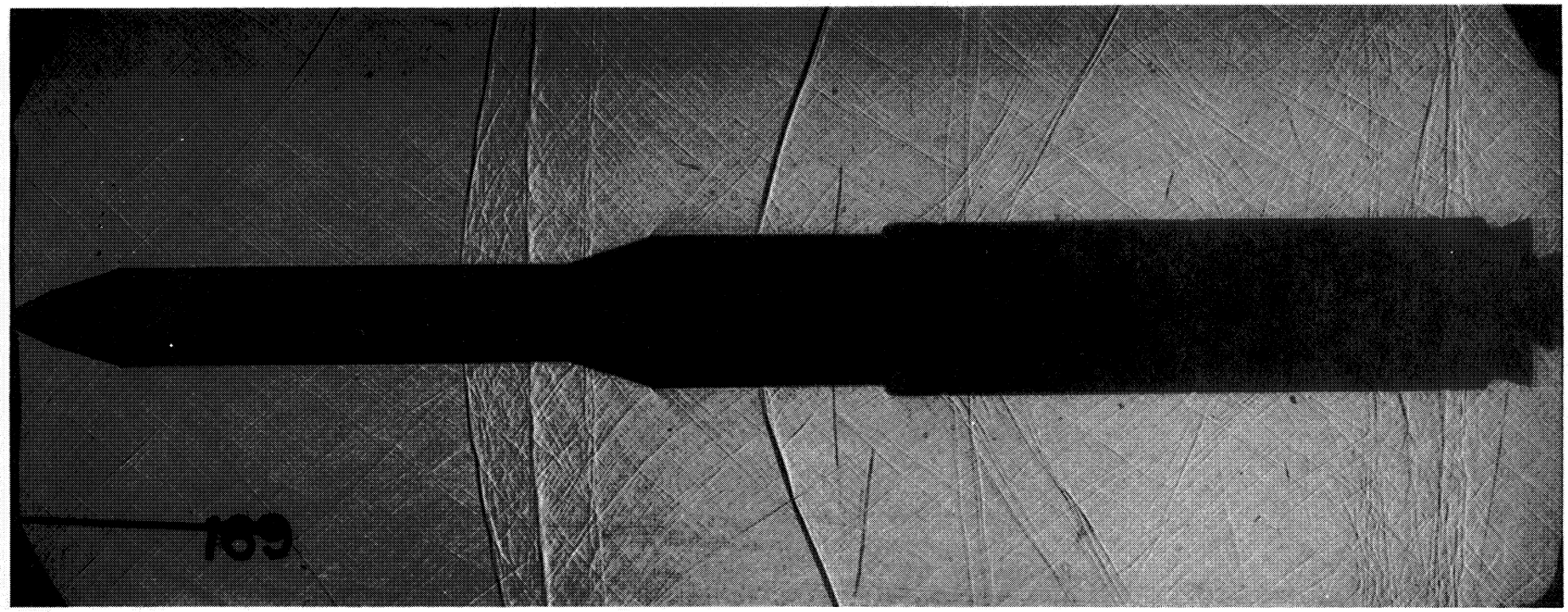

Figure 39. HLLV Mach 1.05, alpha = 0° and beta = 0°.

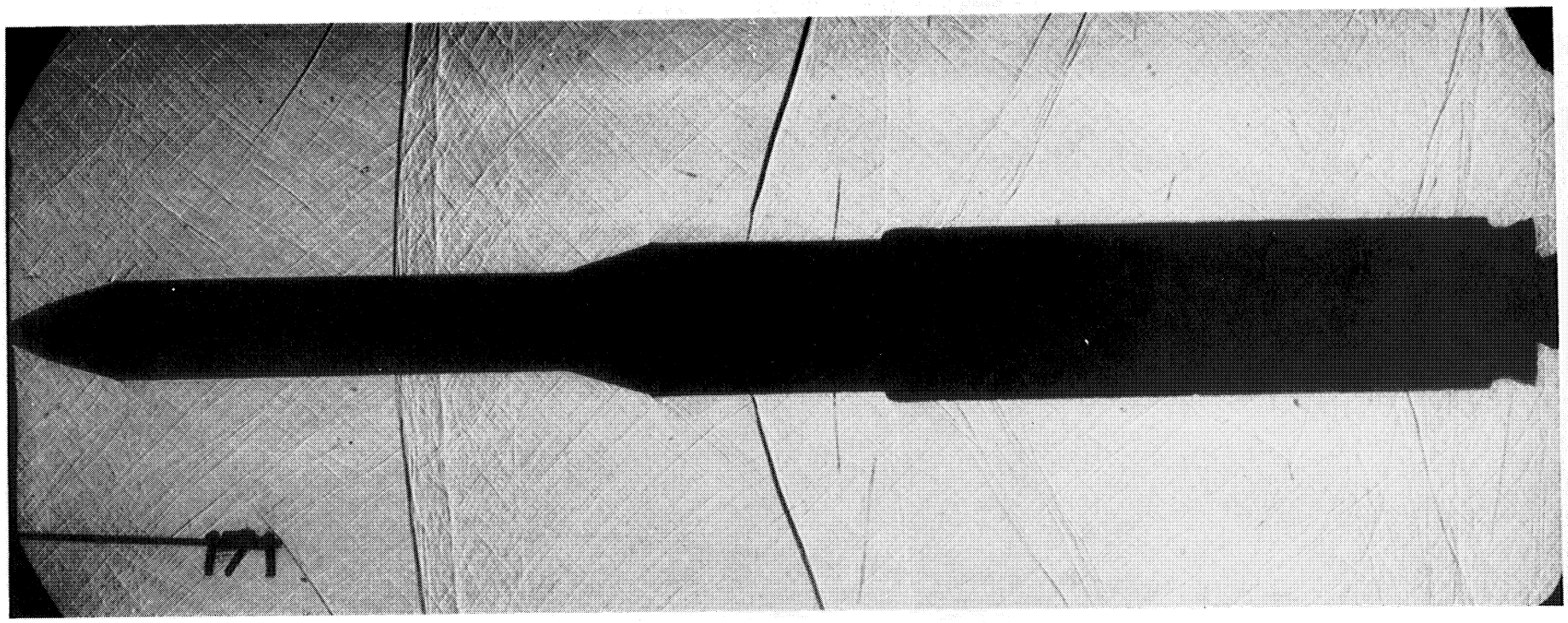

Figure 40. HLLV Mach 1.10, alpha = 0° and beta = 0°.

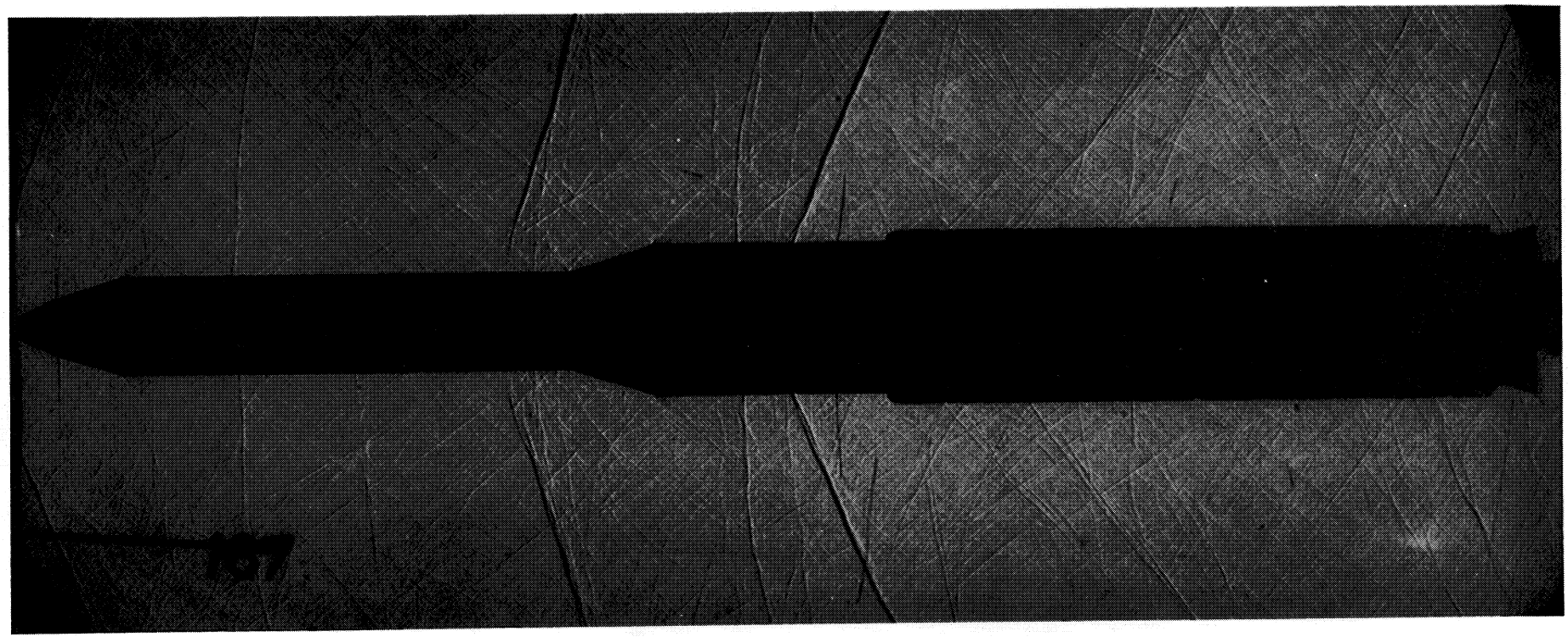

Figure 41. HLLV Mach 1.15, alpha = 0° and beta = 0°.

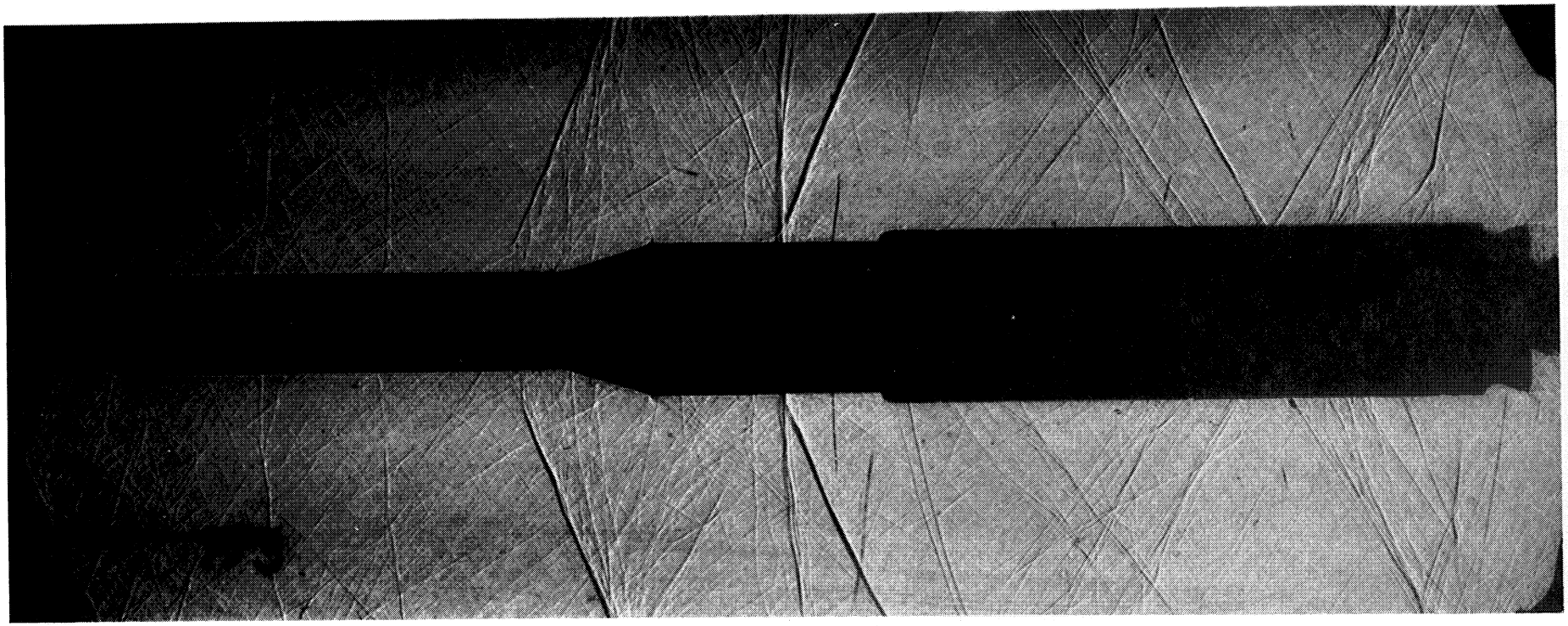

Figure 42. HLLV Mach 1.25, alpha = 0° and beta = 0°.

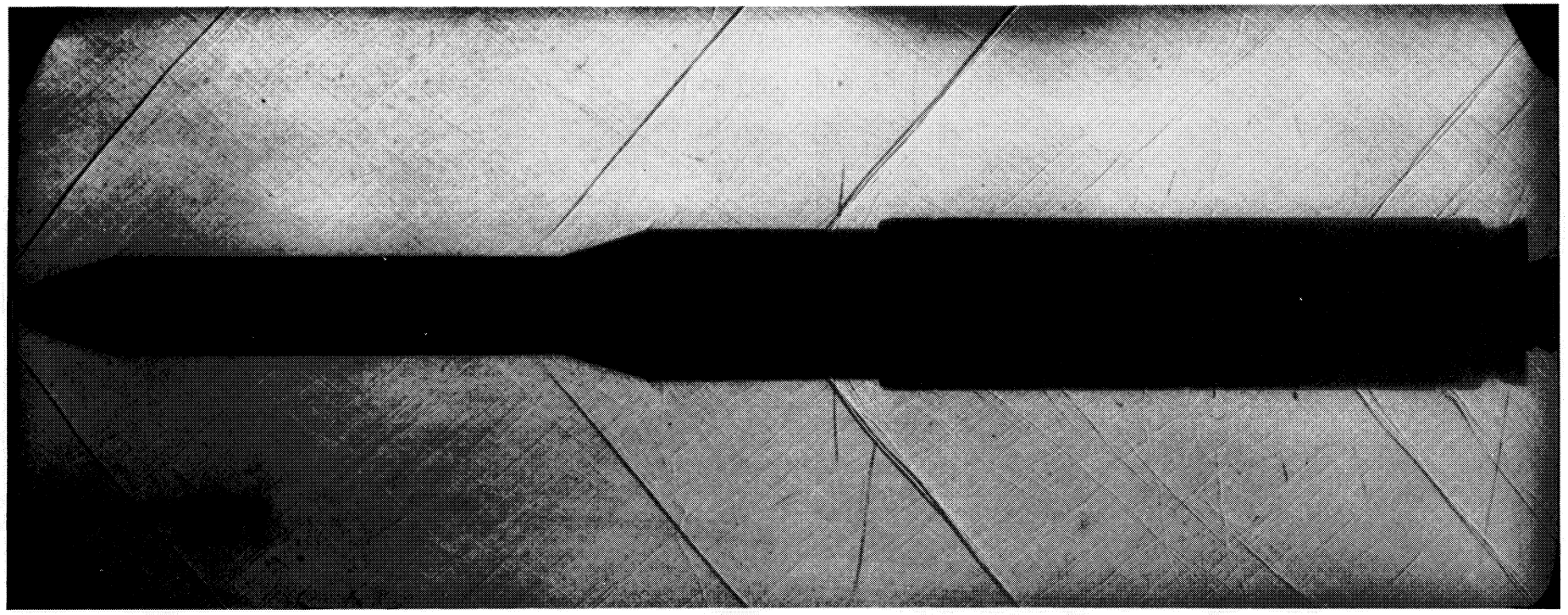

Figure 43. HLLV Mach 1.46, alpha = 0° and beta = 0°.

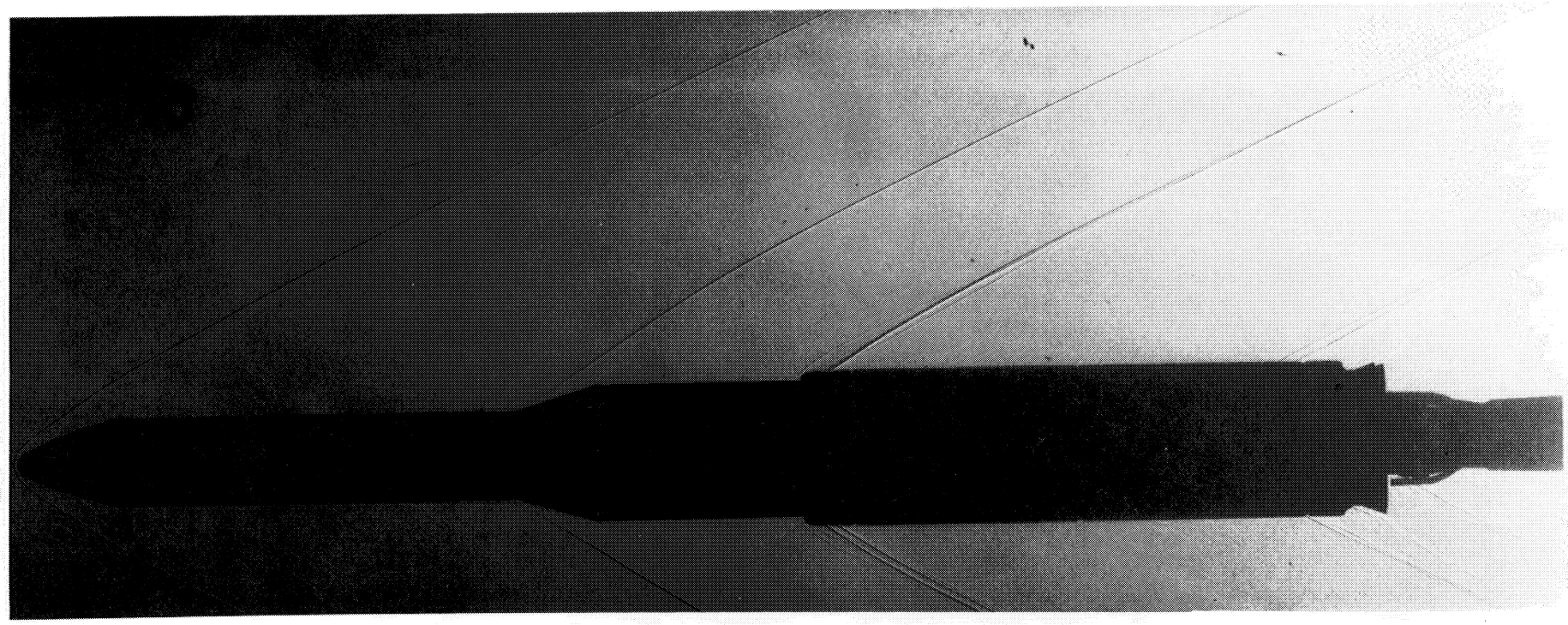

Figure 44. HLLV Mach 2.74, alpha = 0° and beta = 0°.

Figure 45. HLLV Mach 3.48, alpha = 0° and beta = 0°.

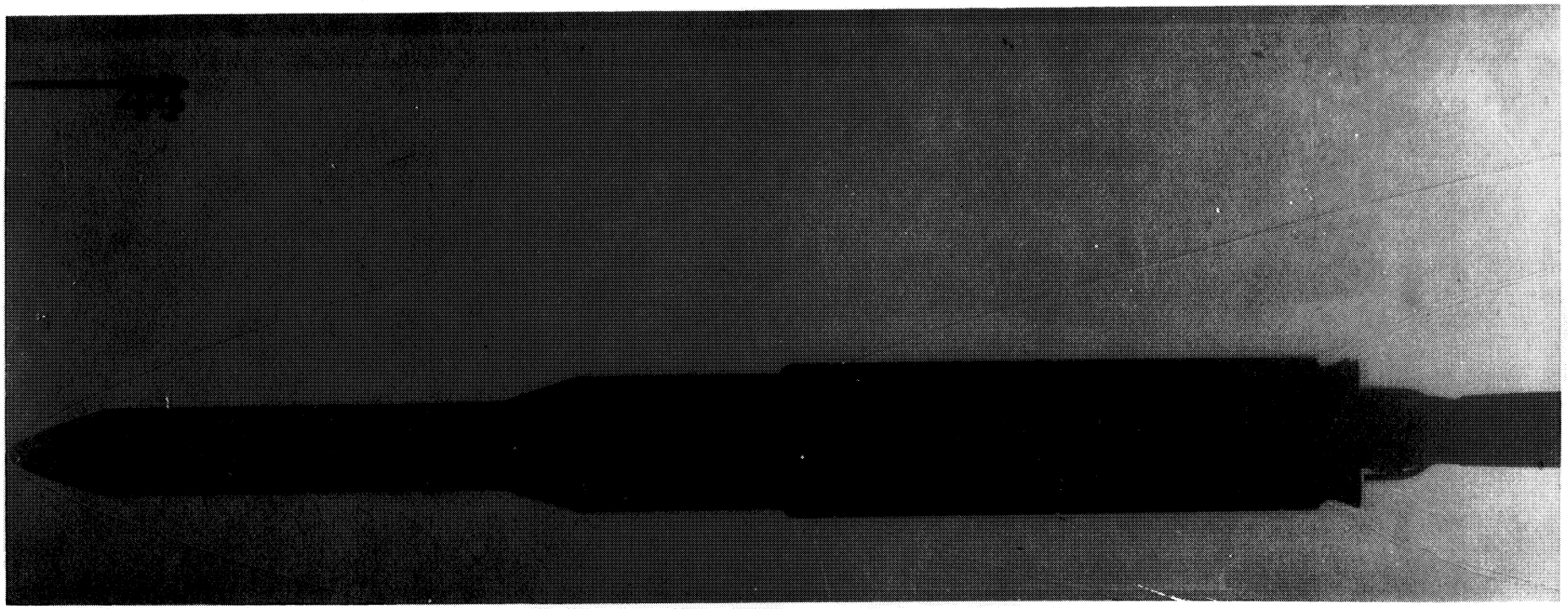

Figure 46. HLLV Mach 4.96, alpha = 0° and beta = 0°.

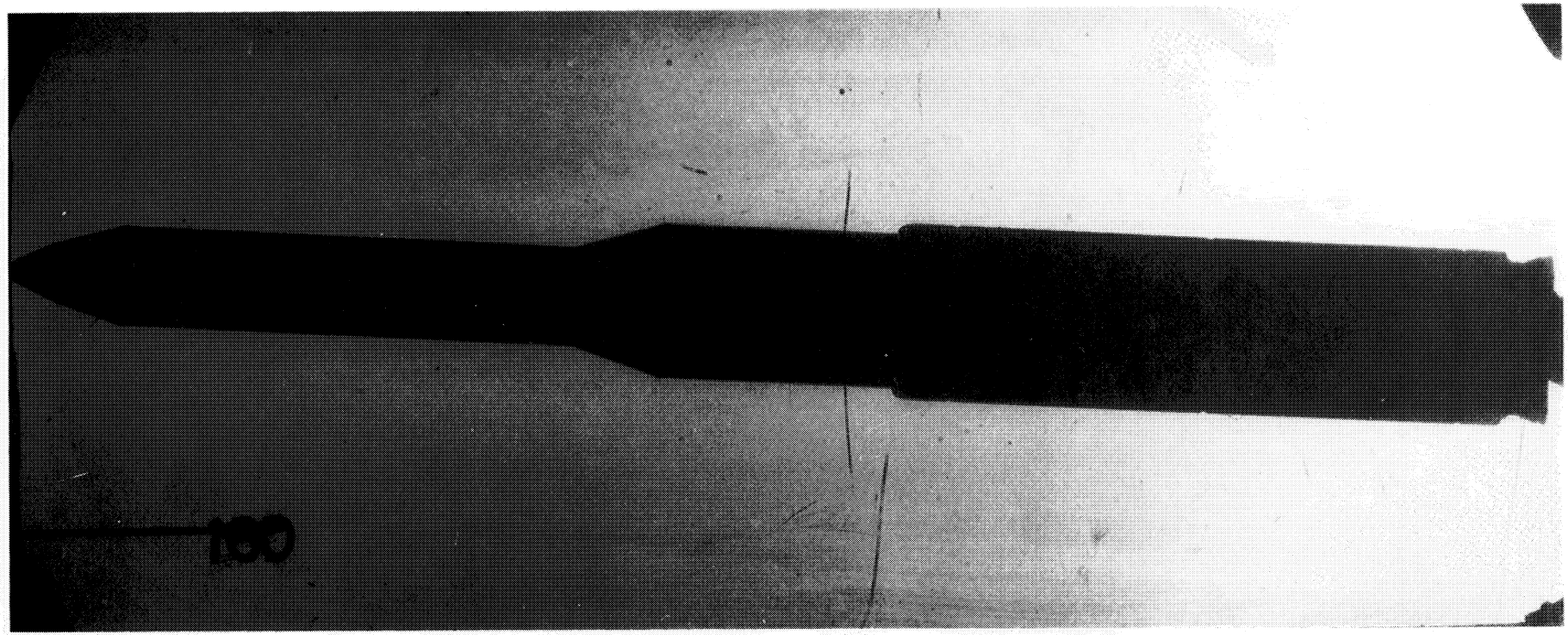

Figure 47. HLLV Mach 0.6, alpha = 4° and beta = 0°.

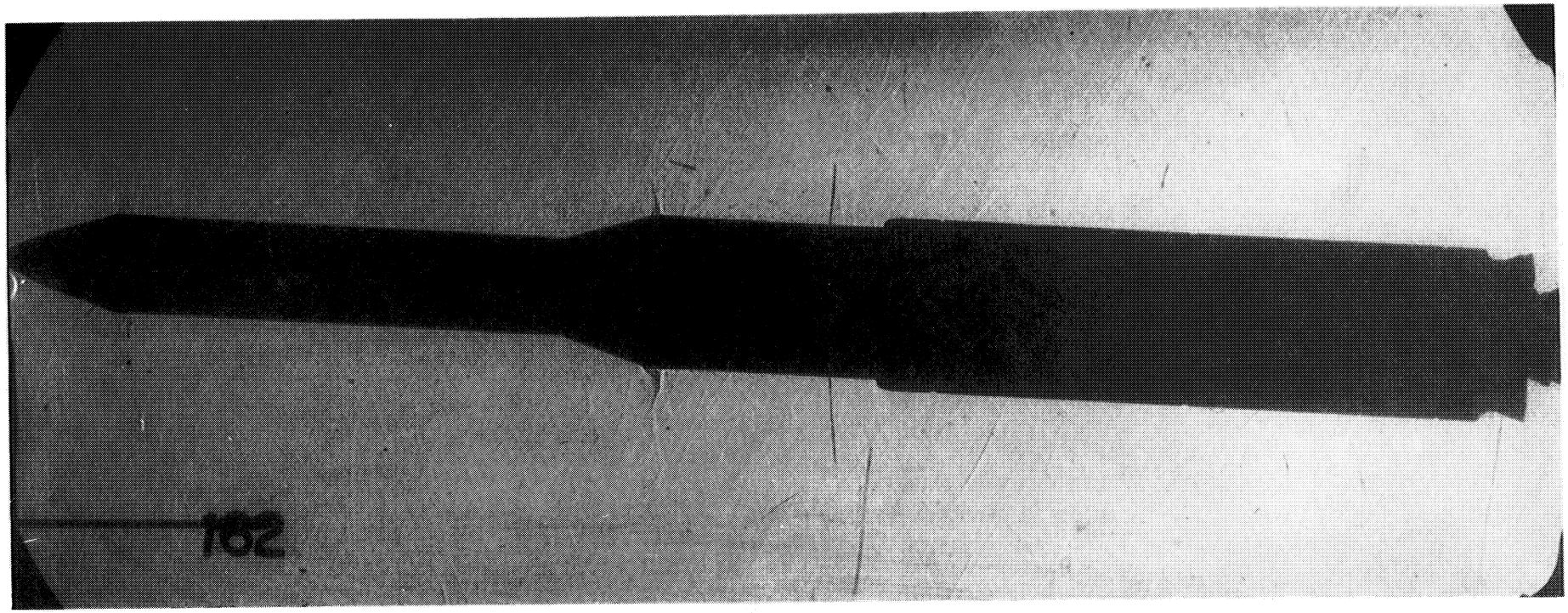

Figure 48. HLLV Mach 0.8, alpha = 4° and beta = 0°.

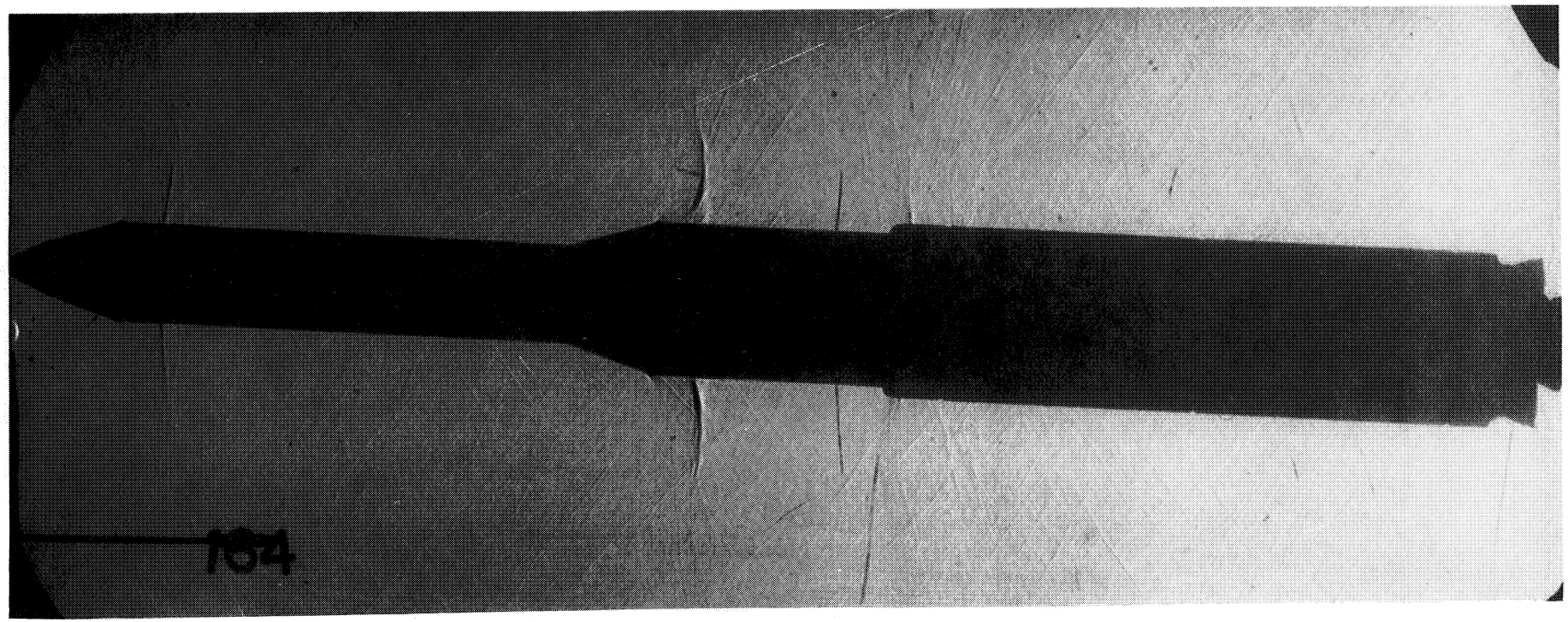

Figure 49. HLLV Mach 0.9, alpha = 4° and beta = 0°.

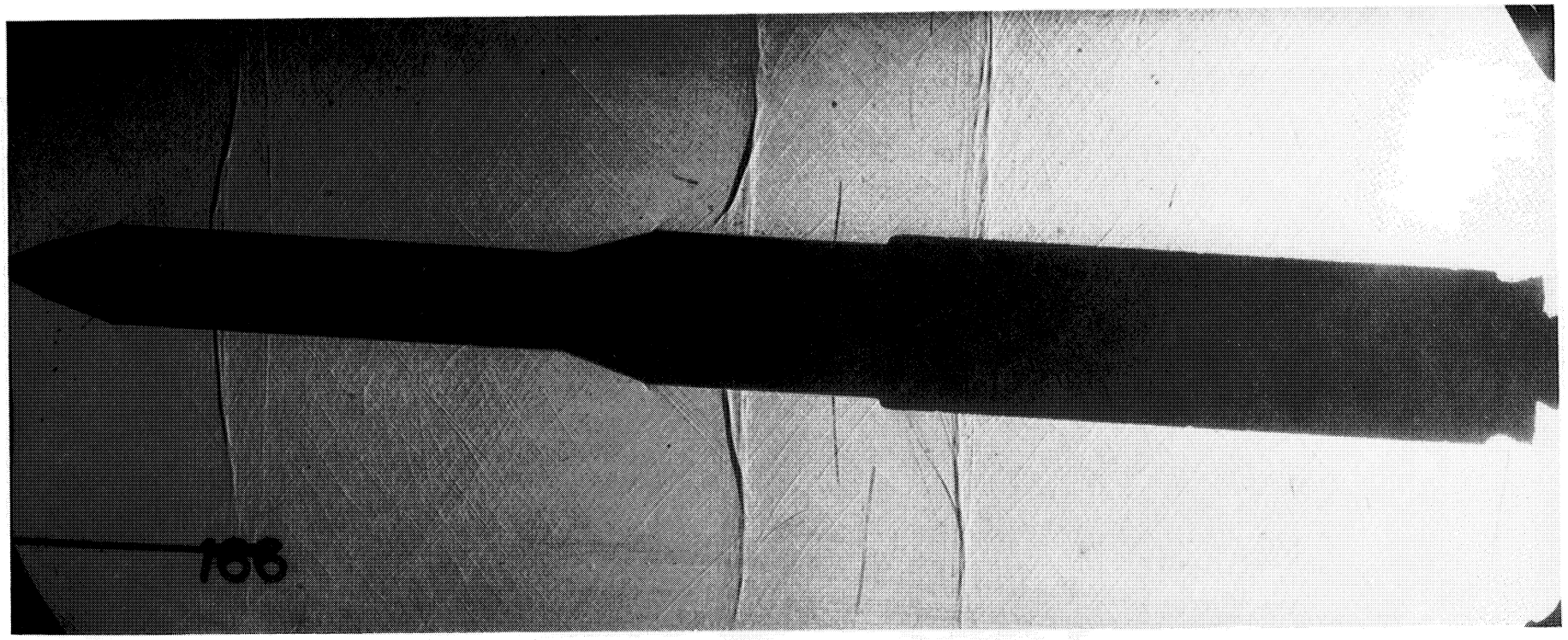

Figure 50. HLLV Mach 0.95, alpha = 4° and beta = 0°.

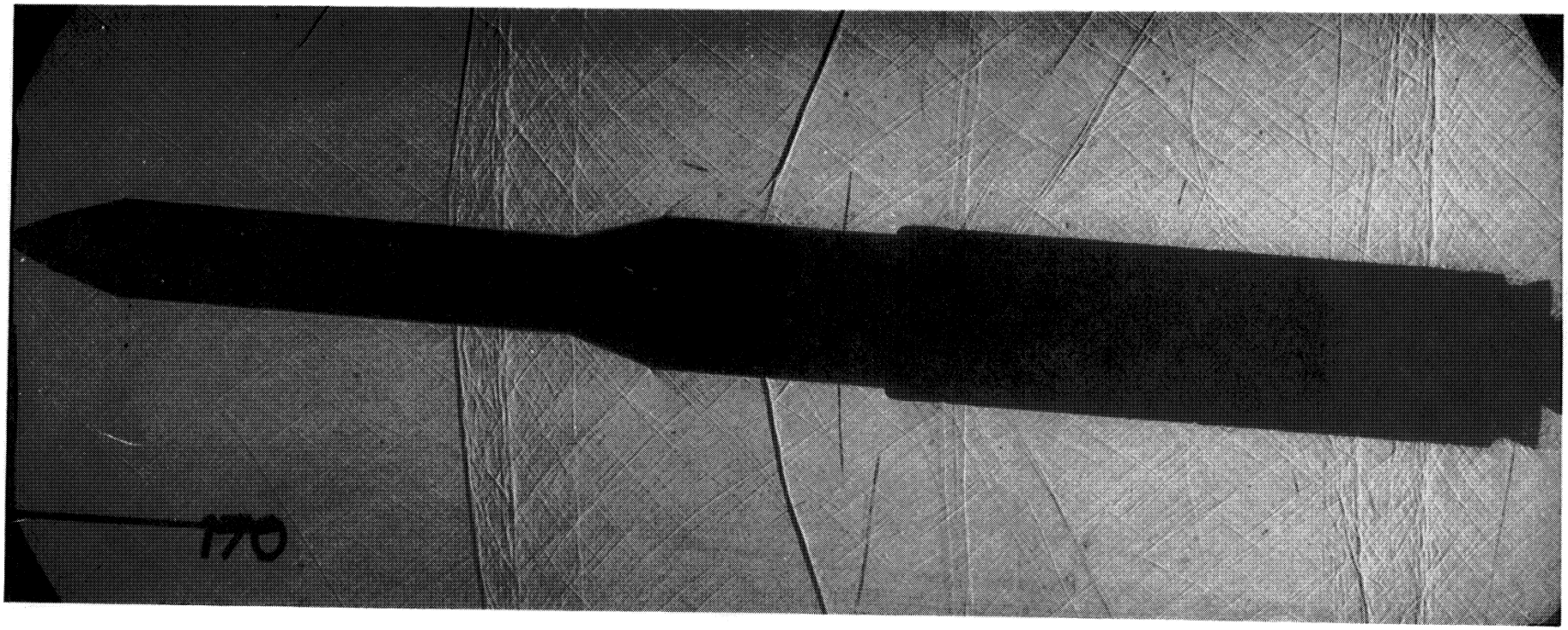

Figure 51. HLLV Mach 1.05, alpha = 4° and beta = 0°.

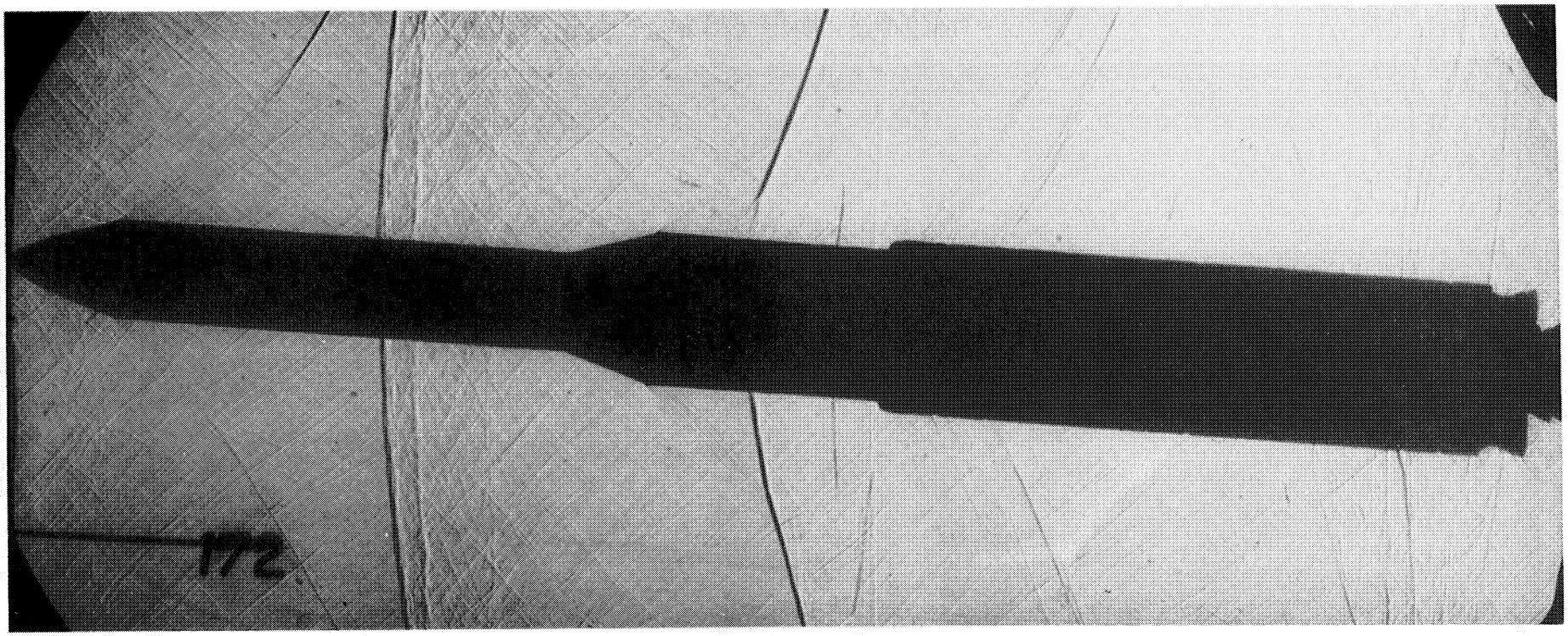

Figure 52. HLLV Mach 1.10, alpha = 4° and beta = 0°.

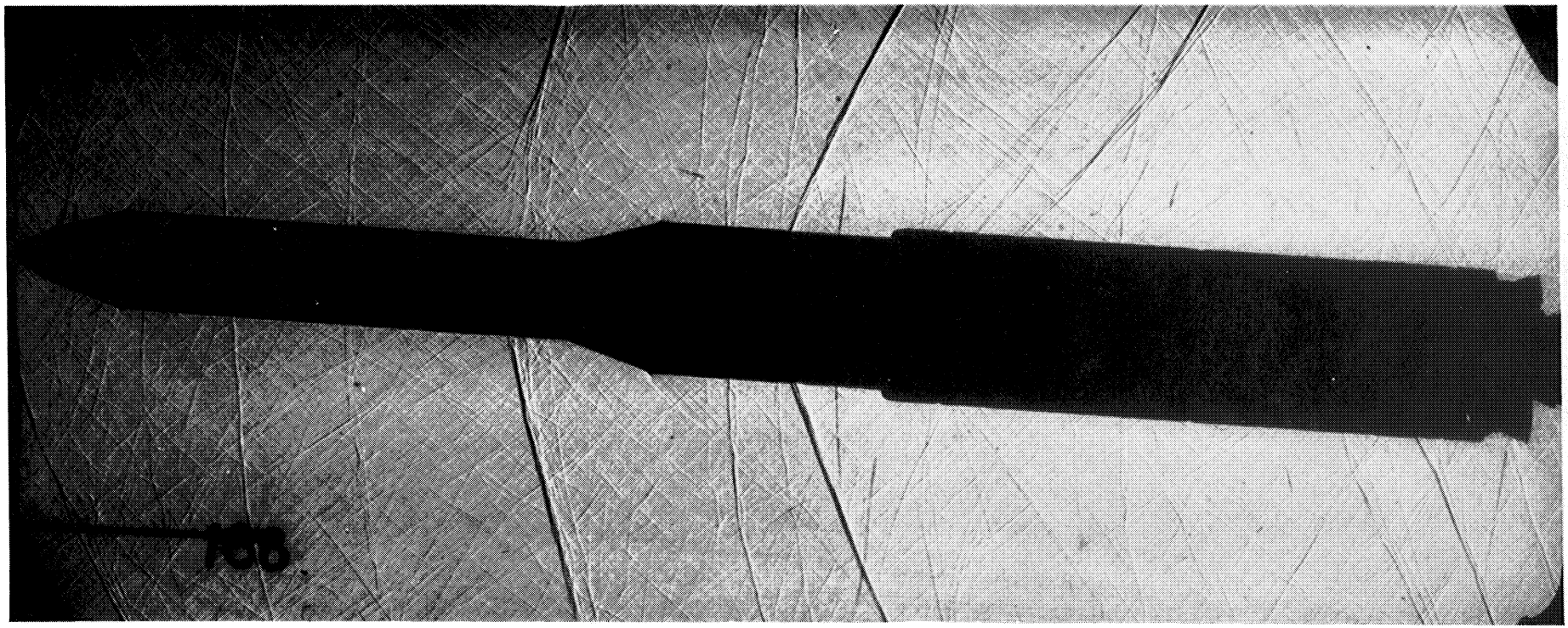

Figure 53. HLLV Mach 1.15, alpha = 4° and beta = 0°.

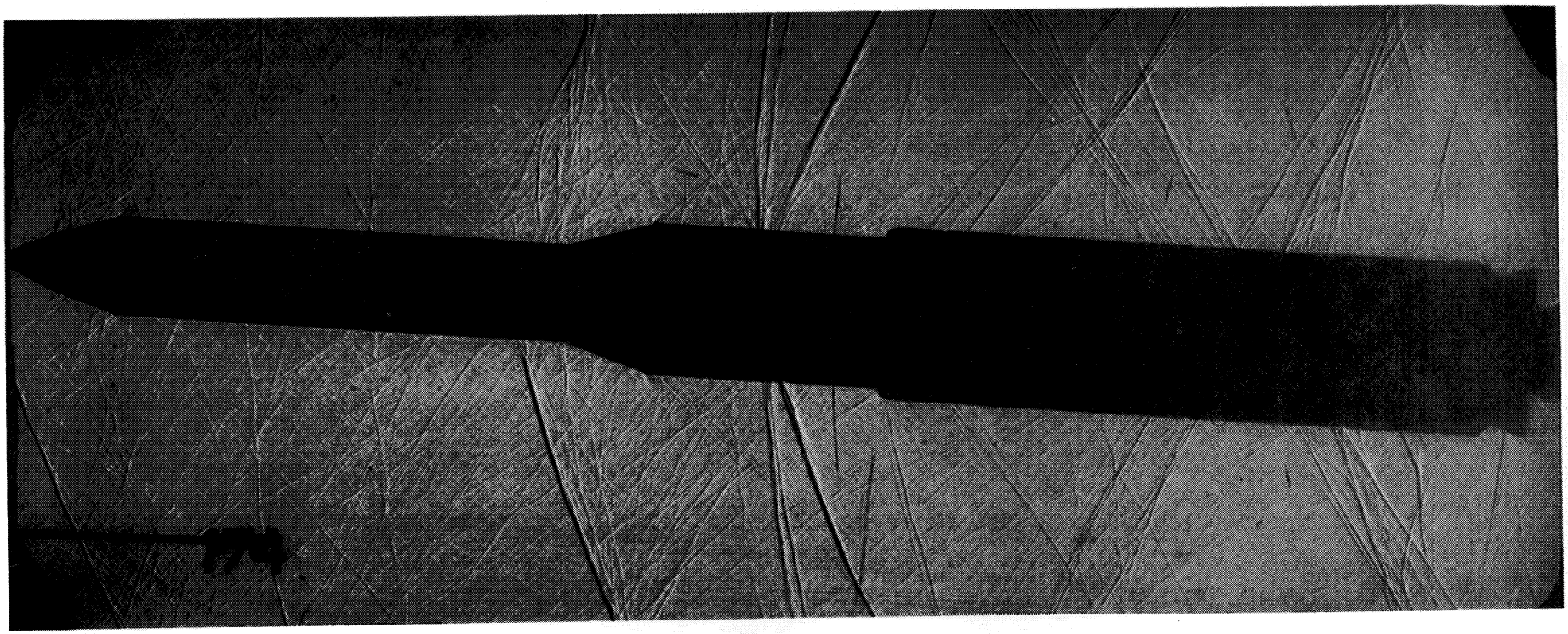

Figure 54. HLLV Mach 1.25, alpha = 4° and beta = 0°.

Figure 55. HLLV Mach 1.46, alpha = 4° and beta = 0°.

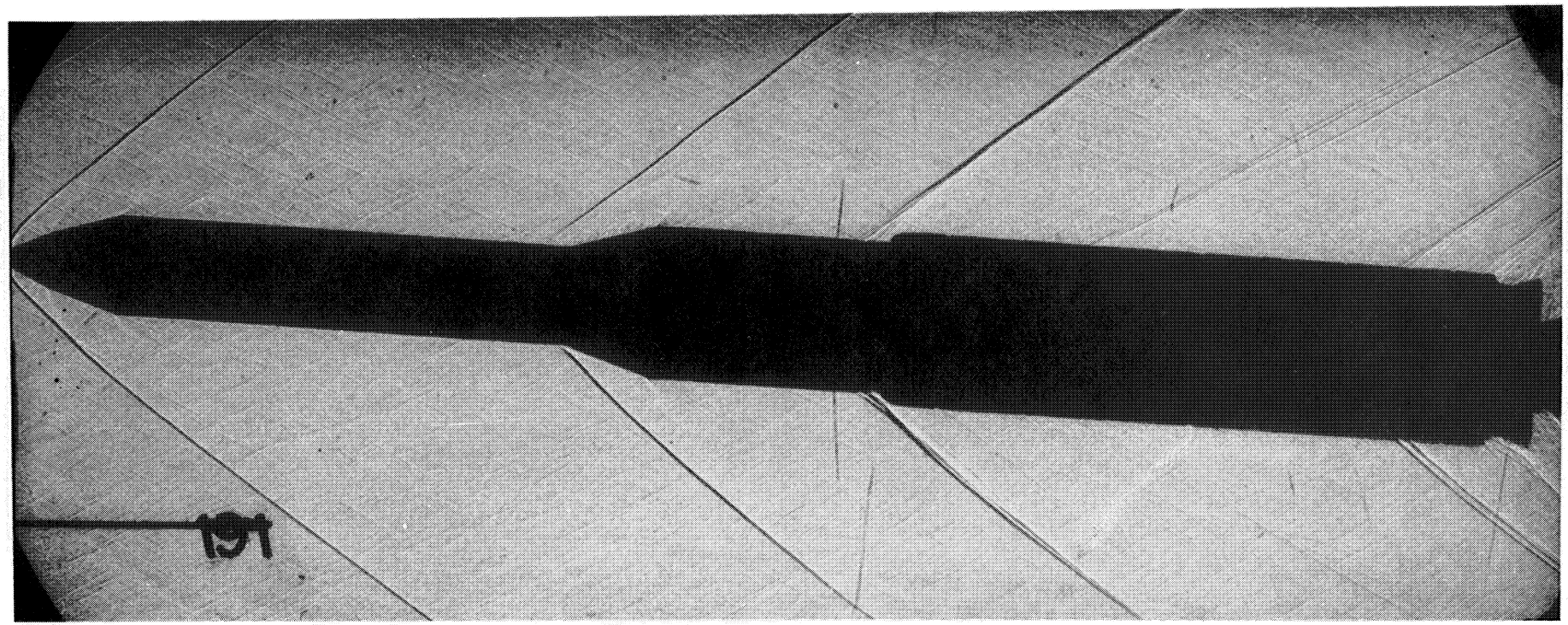

Figure 56. HLLV Mach 1.96, alpha = 4° and beta = 0°.

Figure 57. HLLV Mach 2.74, alpha = 4° and beta = 0°.

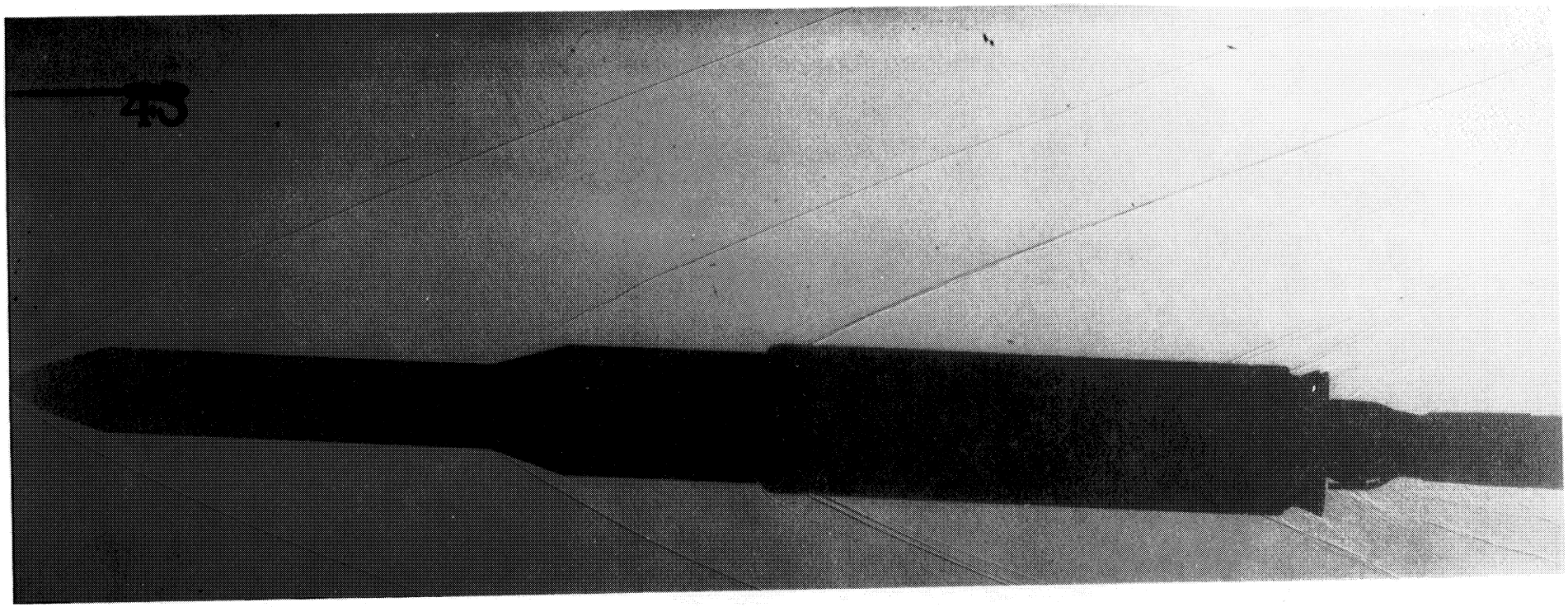

Figure 58. HLLV Mach 3.48, alpha = 4° and beta = 0°.

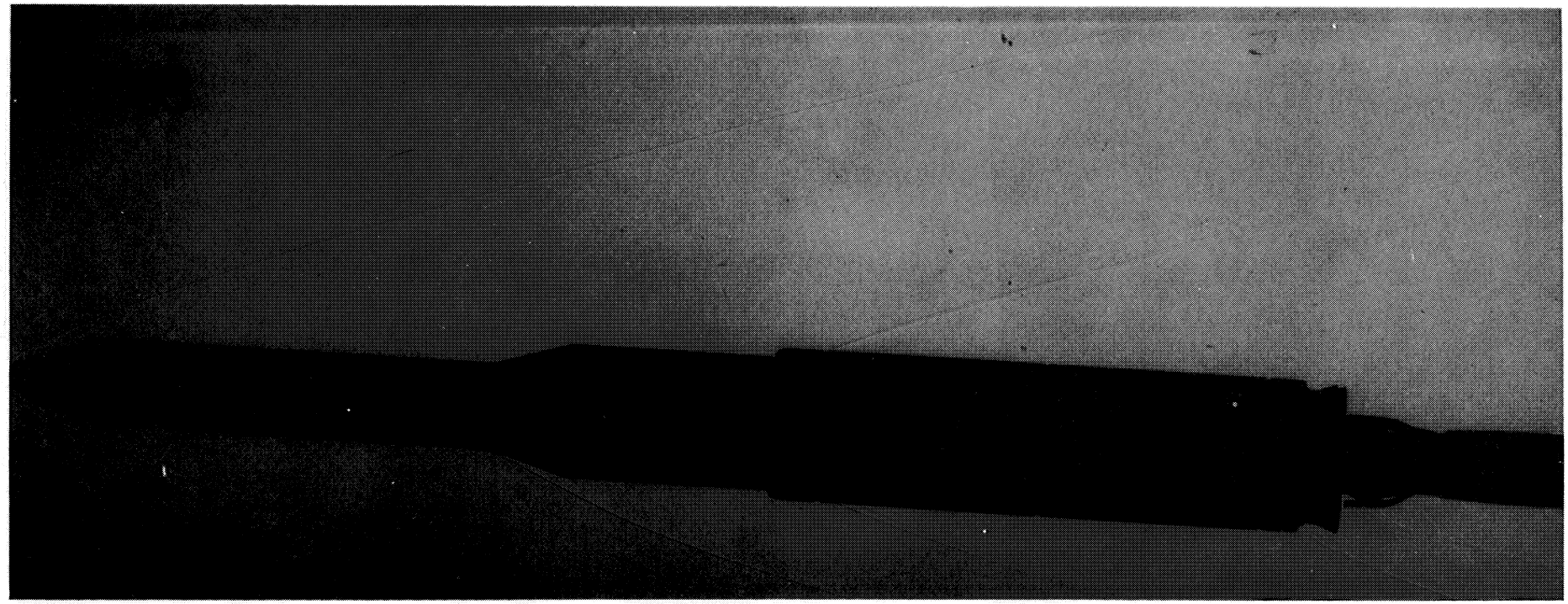

Figure 59. HLLV Mach 4.96, alpha = 4° and beta = 0°.

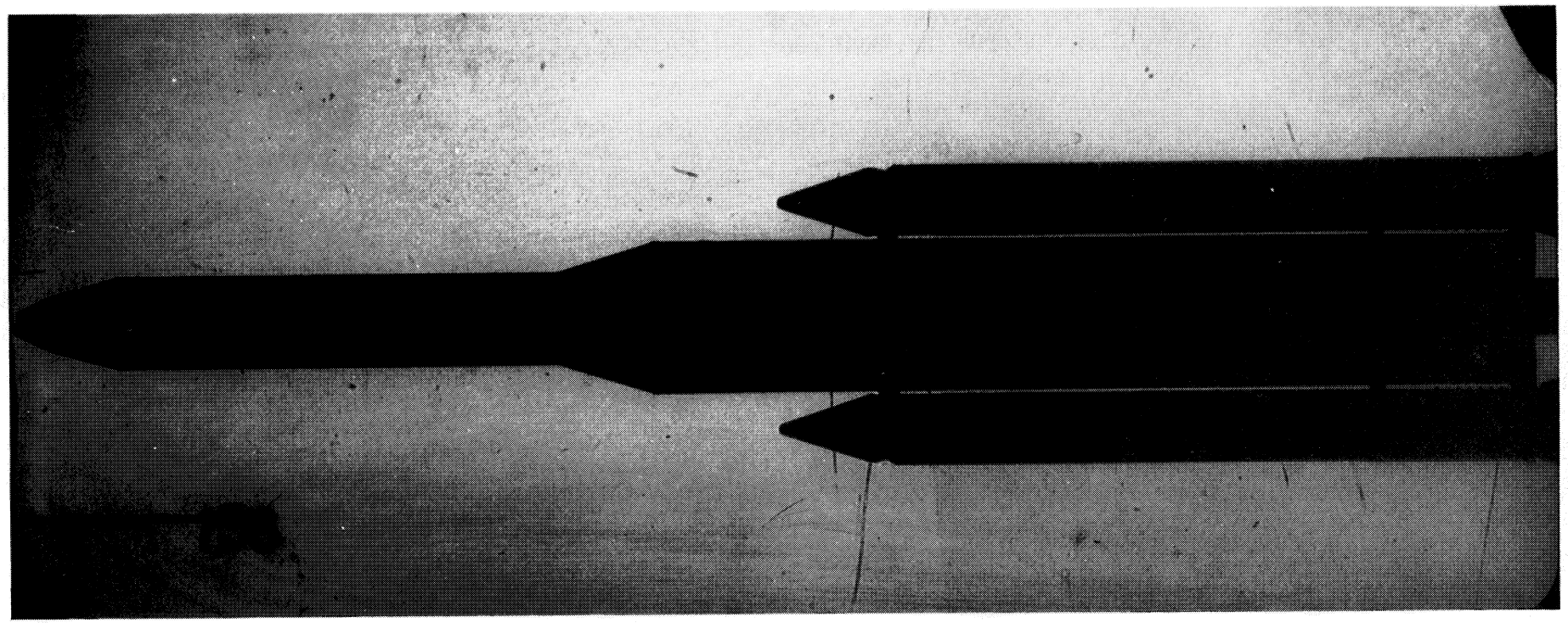

Figure 60. HLLV Mach 0.6, roll = 90°, alpha = 0°, and beta = 0°.

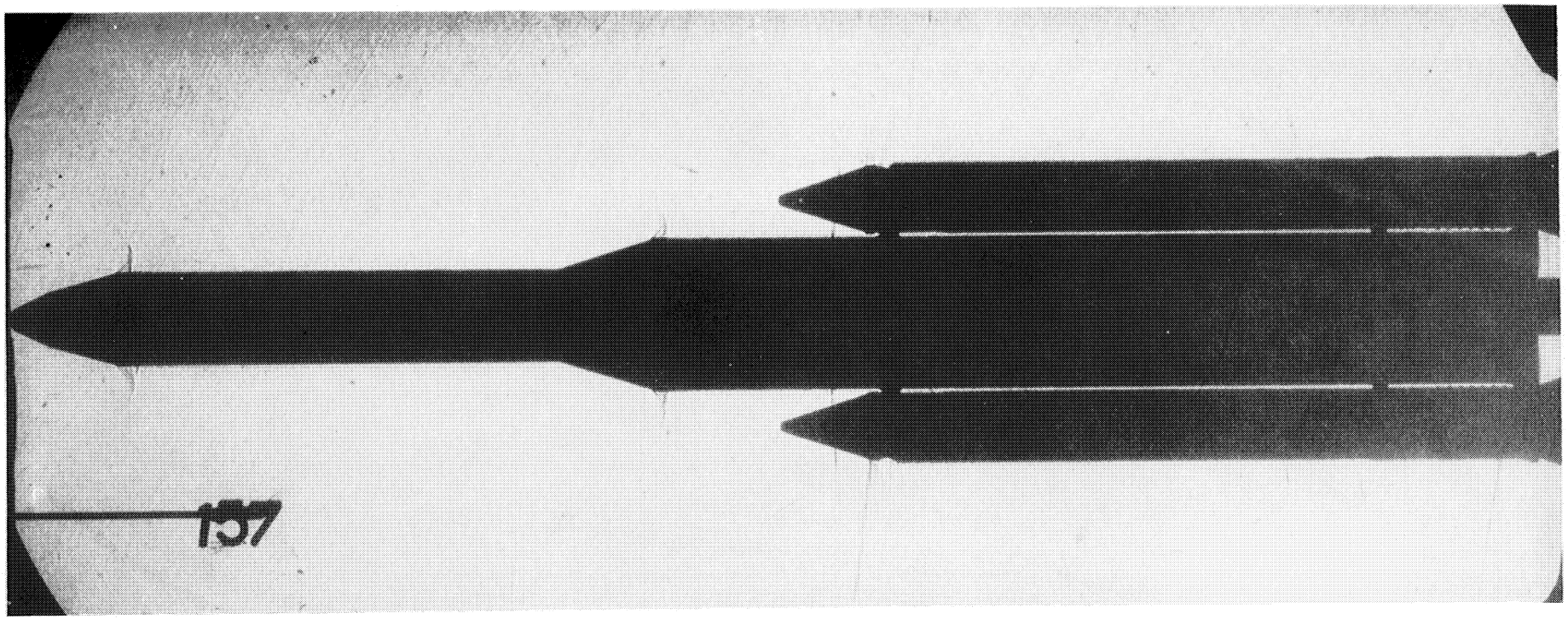

Figure 61. HLLV Mach 0.8, roll = 90°, alpha = 0°, and beta = 0°.

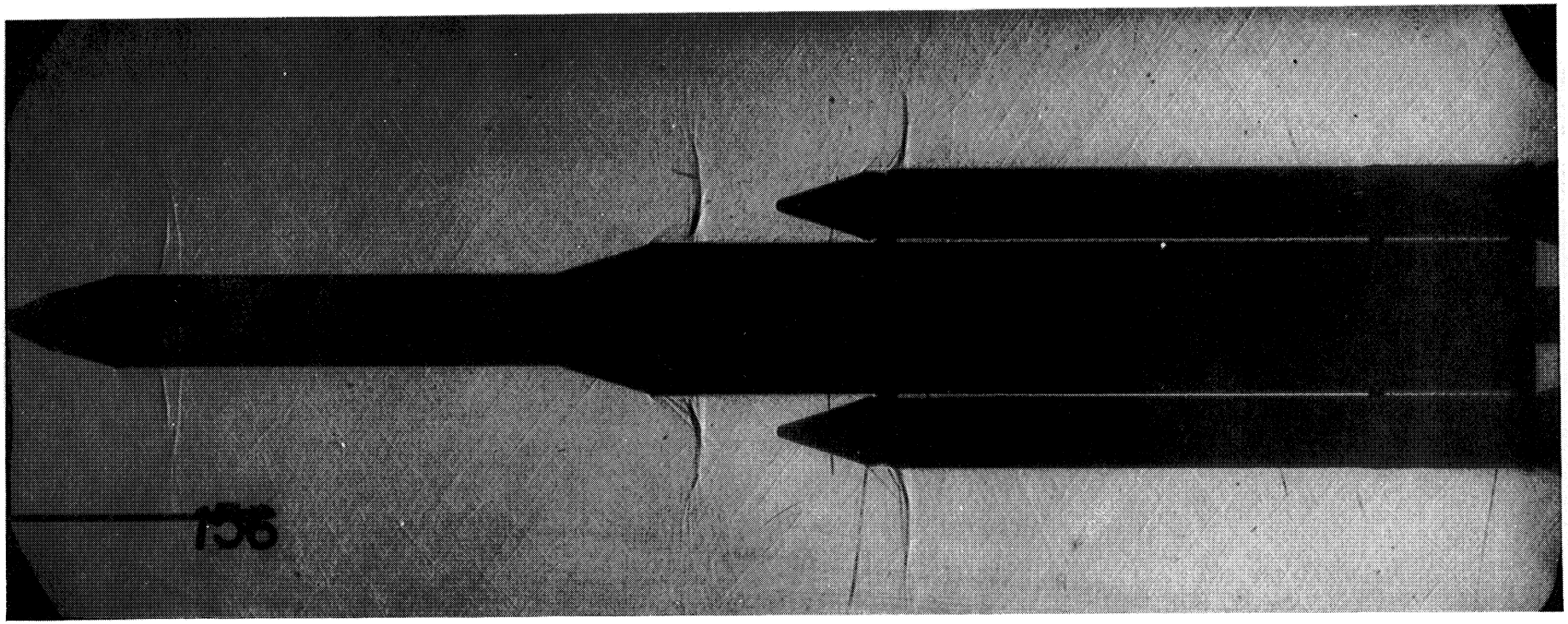

Figure 62. HLLV Mach 0.9, roll = 90°, alpha = 0°, and beta = 0°.

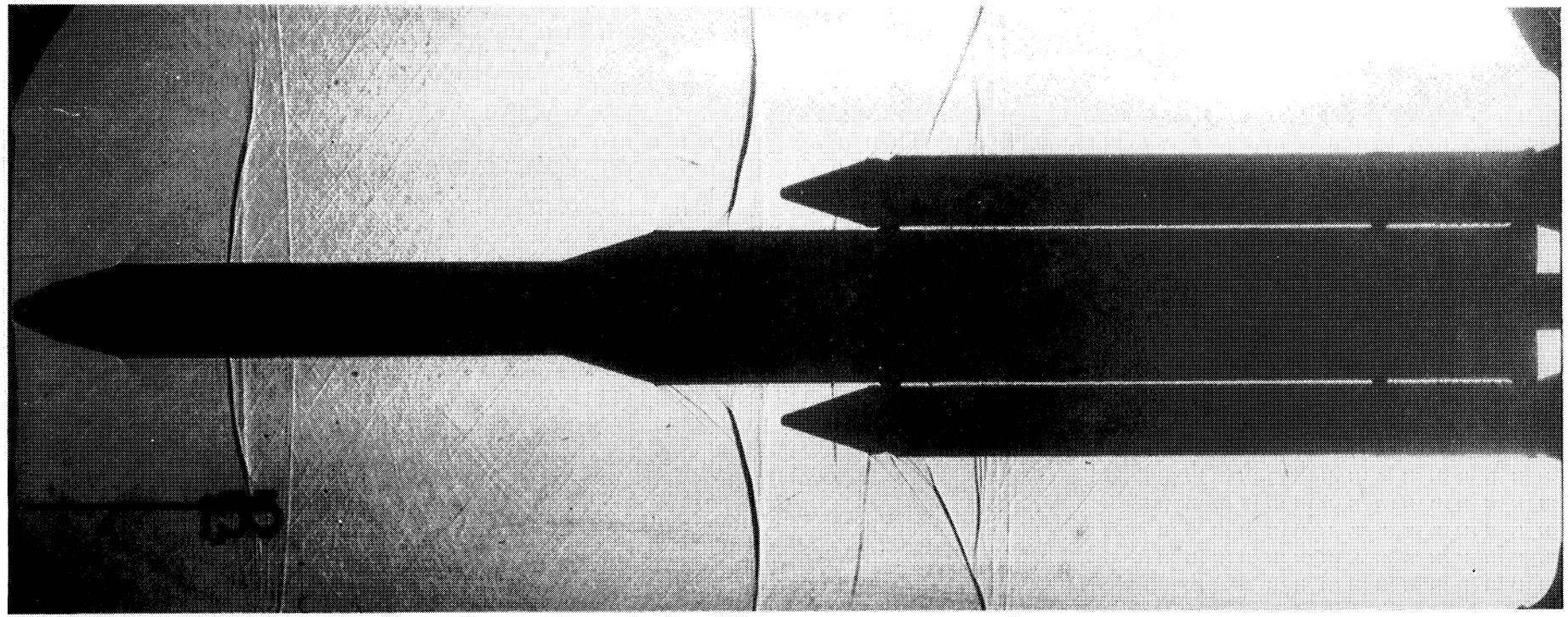

Figure 63. HLLV Mach 0.95, roll = 90°, alpha = 0°, and beta = 0°.

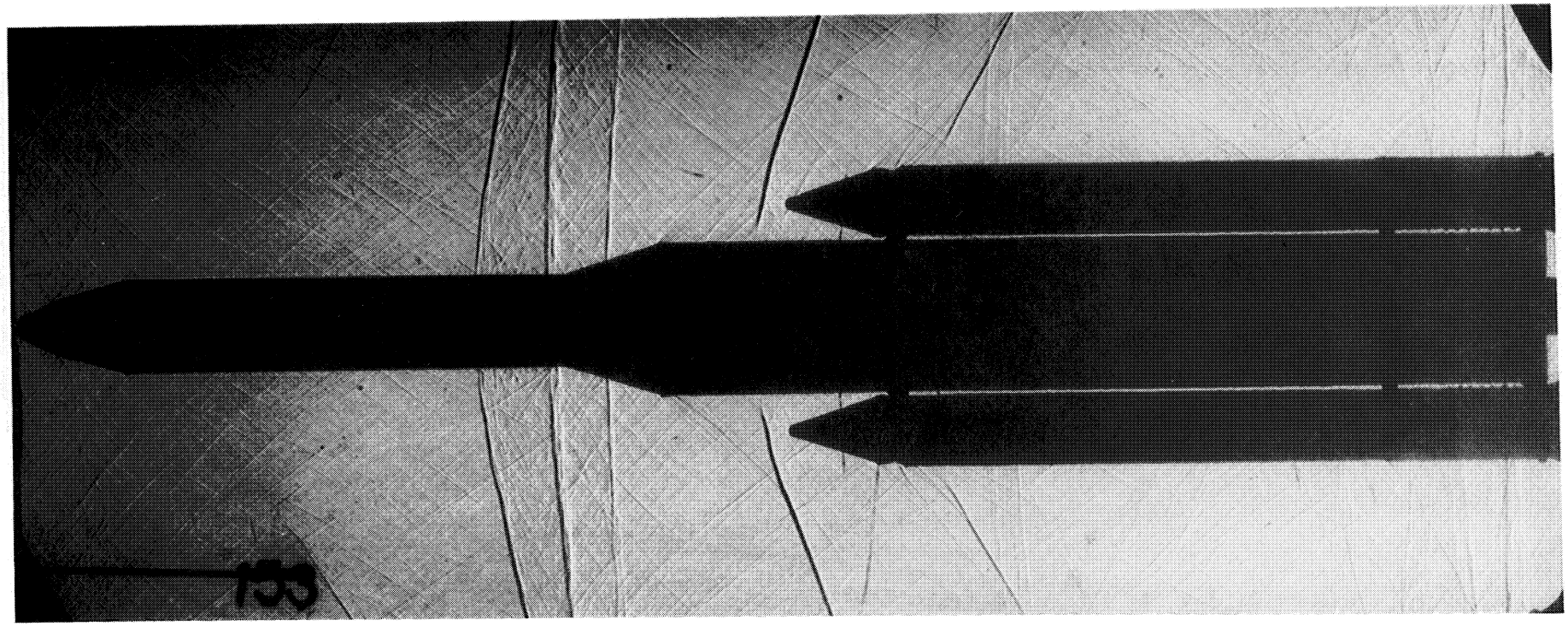

Figure 64. HLLV Mach 1.05, roll = 90°, alpha = 0°, and beta = 0°.

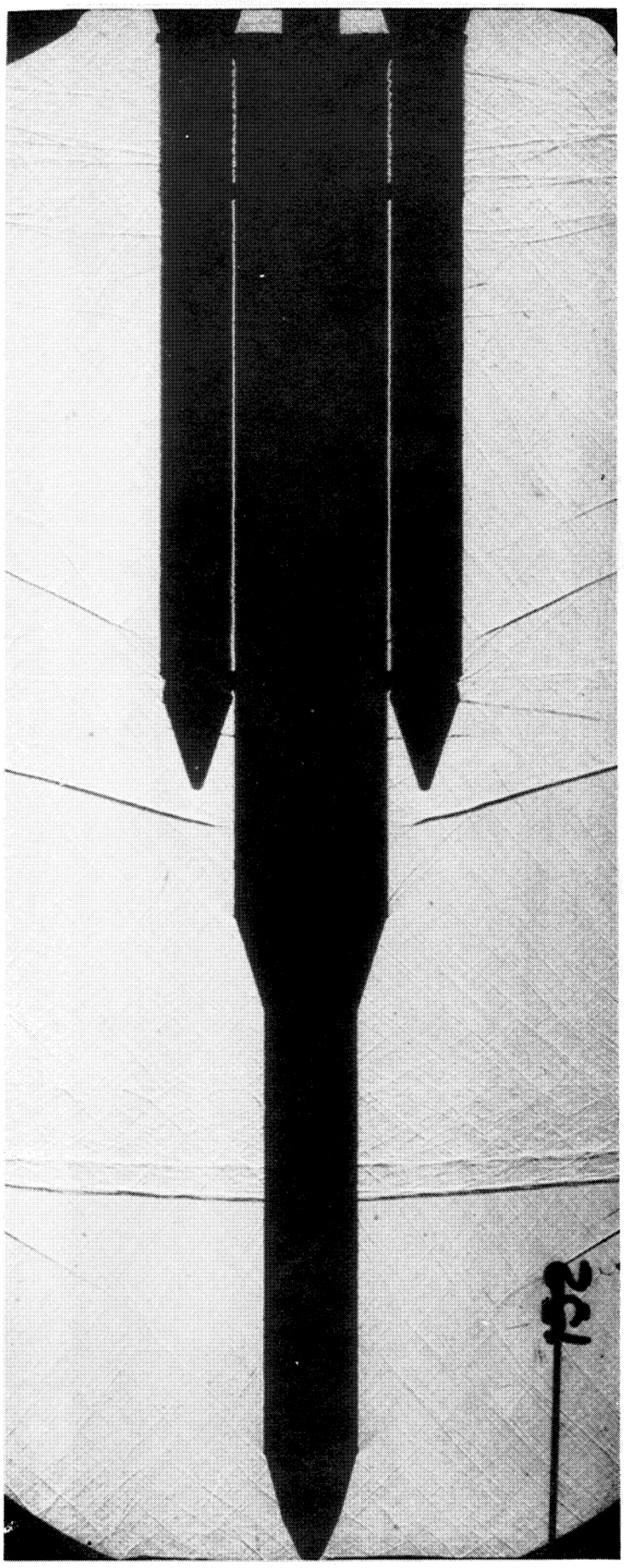

Figure 65. HLLV Mach 1.10, roll = 90°, alpha = 0°, and beta = 0°.

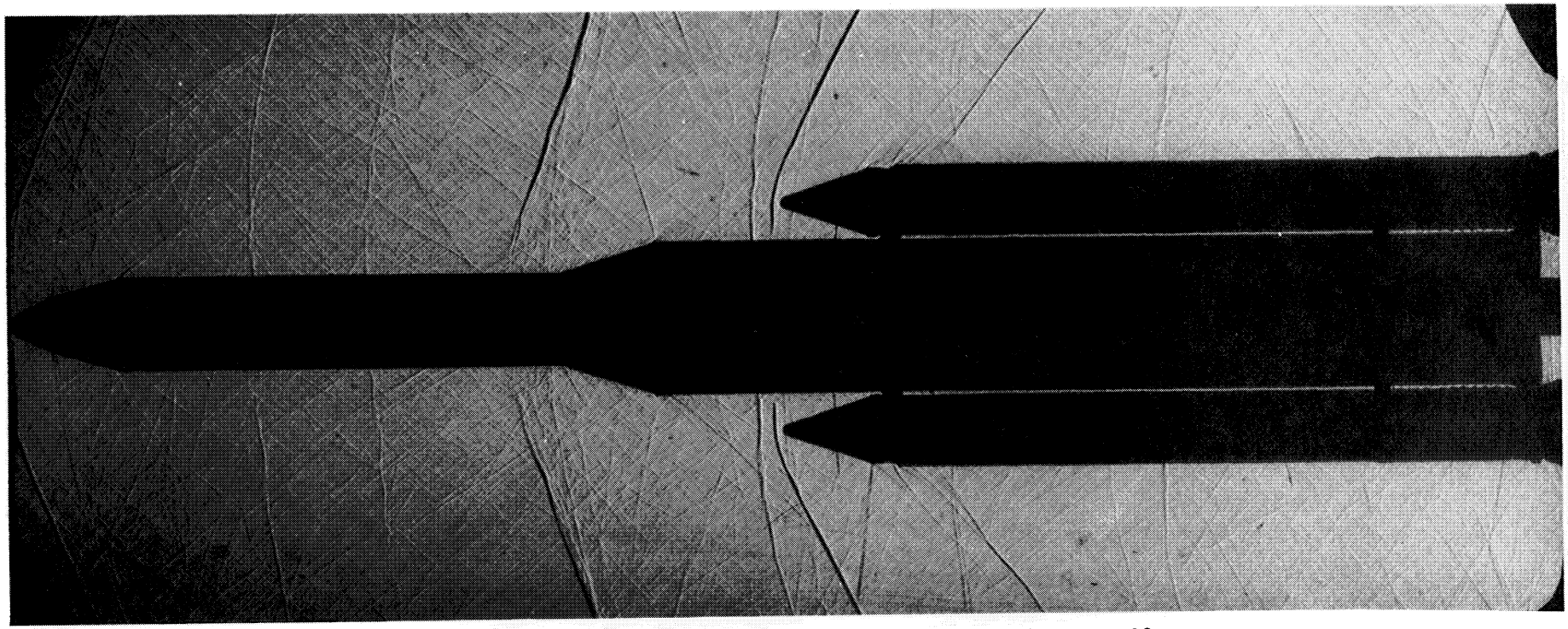

Figure 66. HLLV Mach 1.15, roll = 90°, alpha = 0°, and beta = 0°.

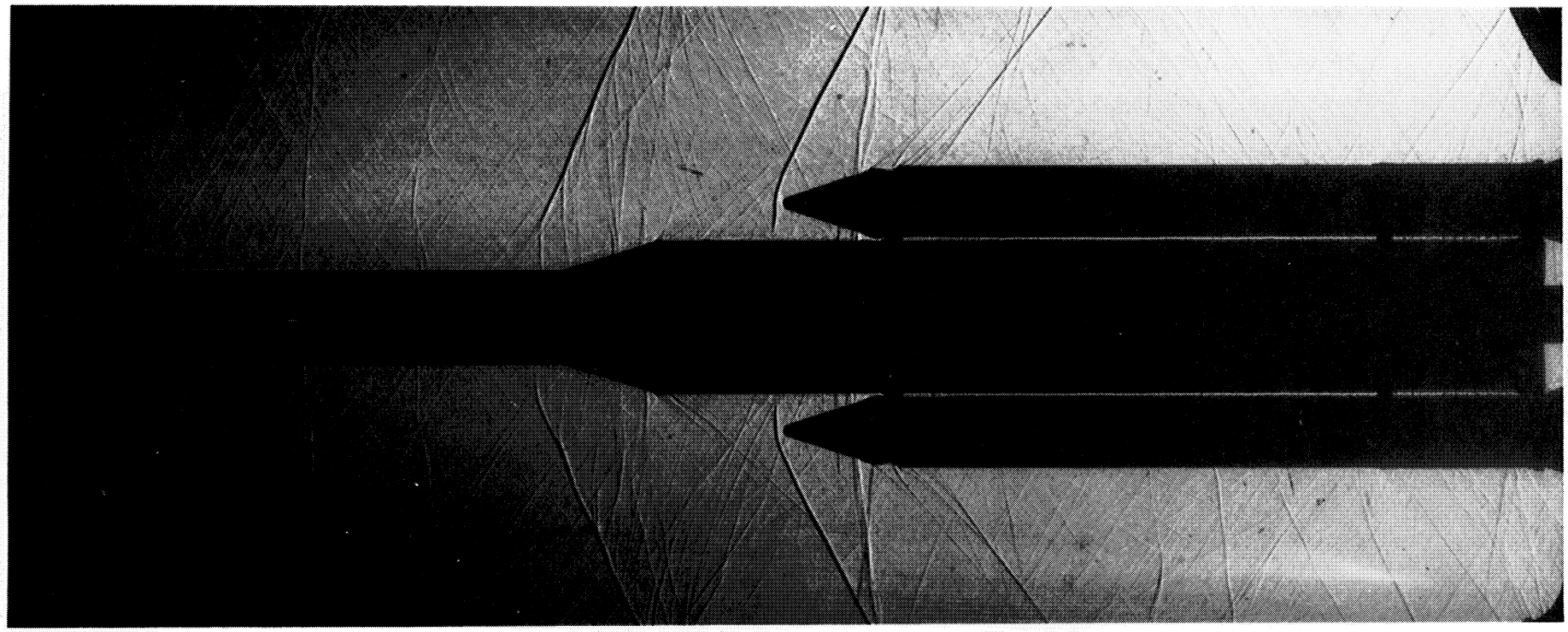

Figure 67. HLLV Mach 1.25, roll = 90°, alpha = 0°, and beta = 0°.

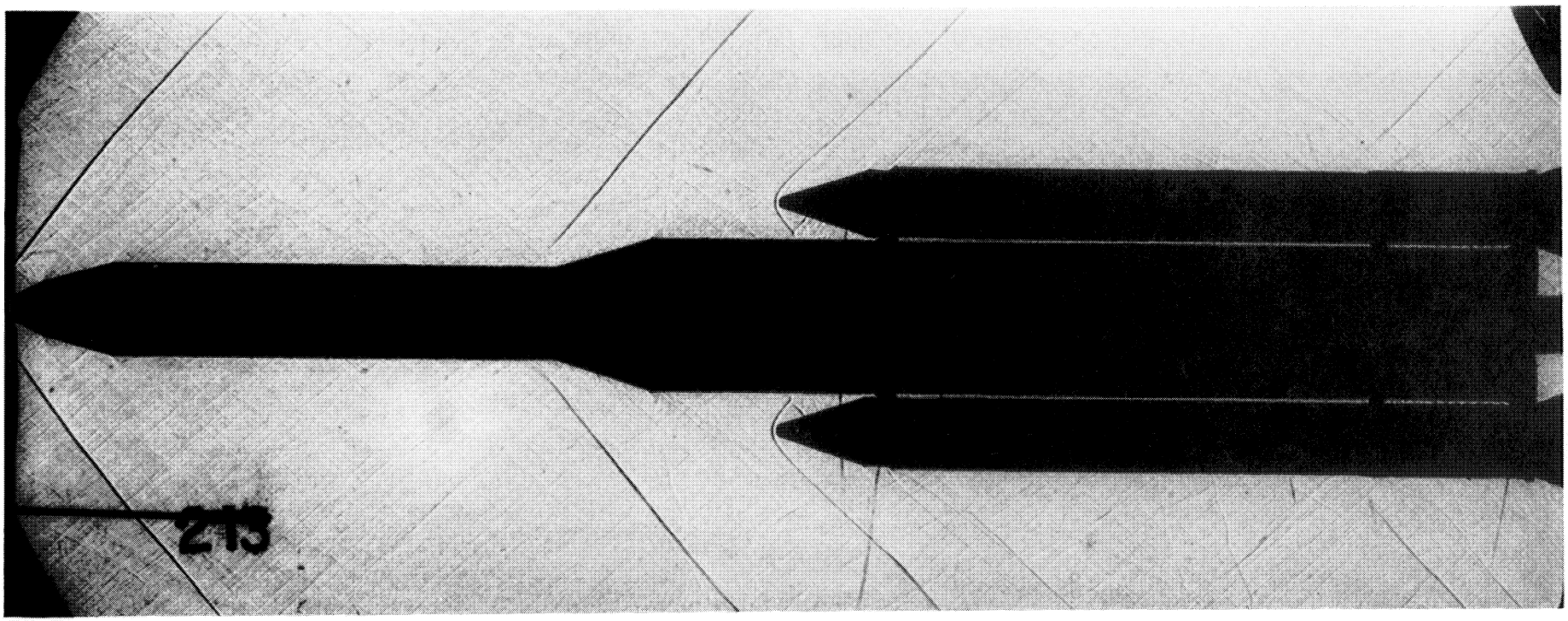

Figure 68. HLLV Mach 1.46, roll = 90°, alpha = 0°, and beta = 0°.

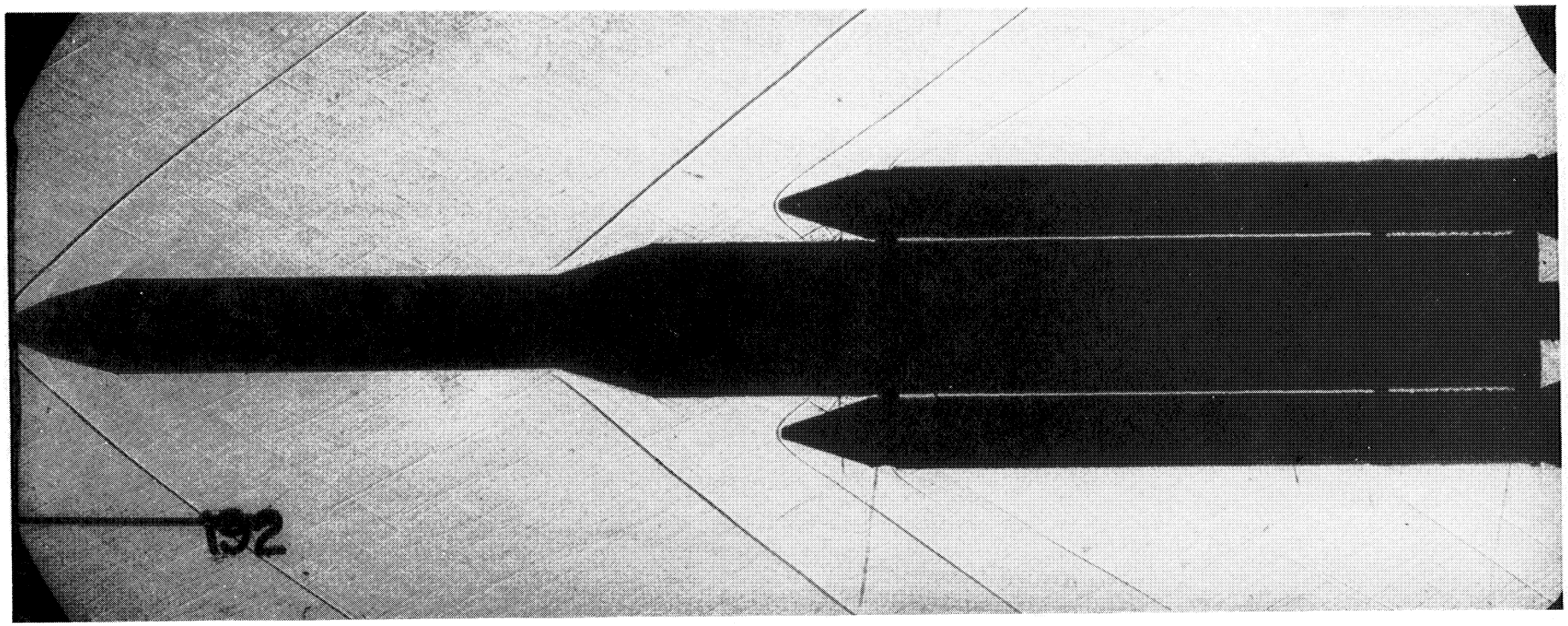

Figure 69. HLLV Mach 1.96, roll = 90°, alpha = 0°, and beta = 0°.

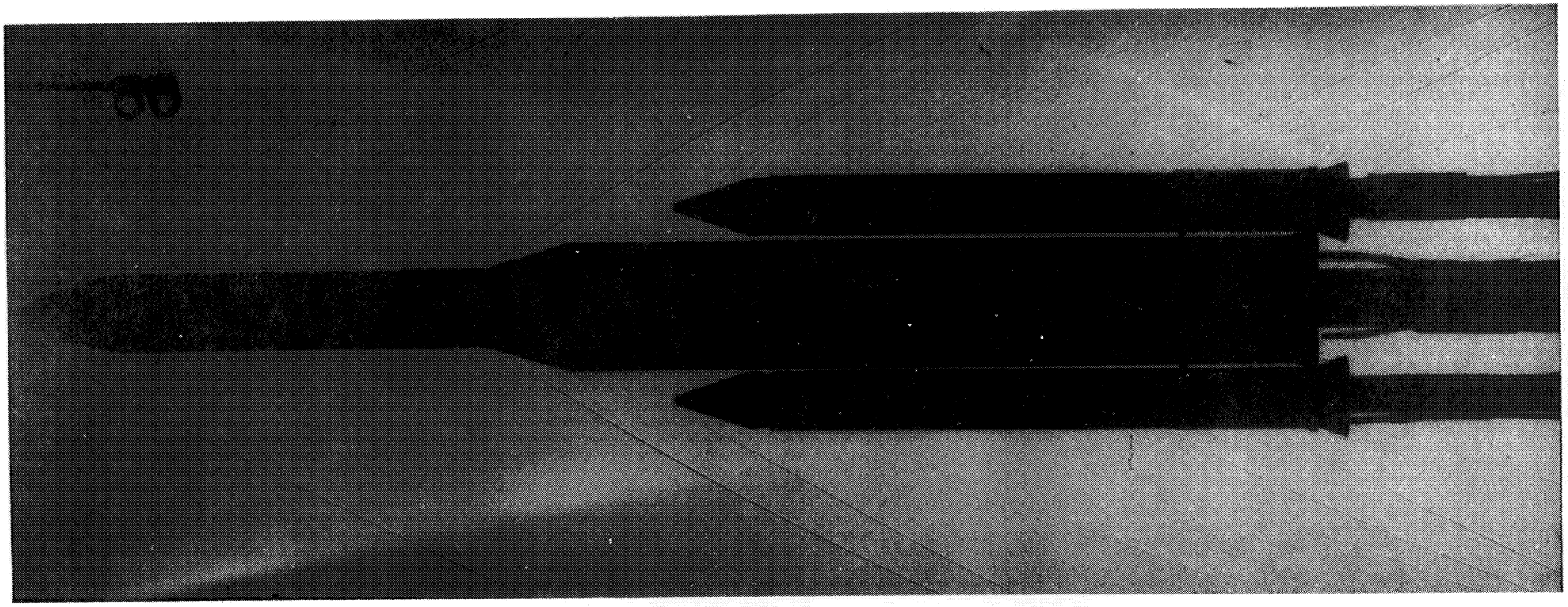

Figure 70. HLLV Mach 2.74, roll = 90°, alpha = 0°, and beta = 0°.

Figure 71. HLLV Mach 3.48, roll = 90°, alpha = 0°, and beta = 0°.

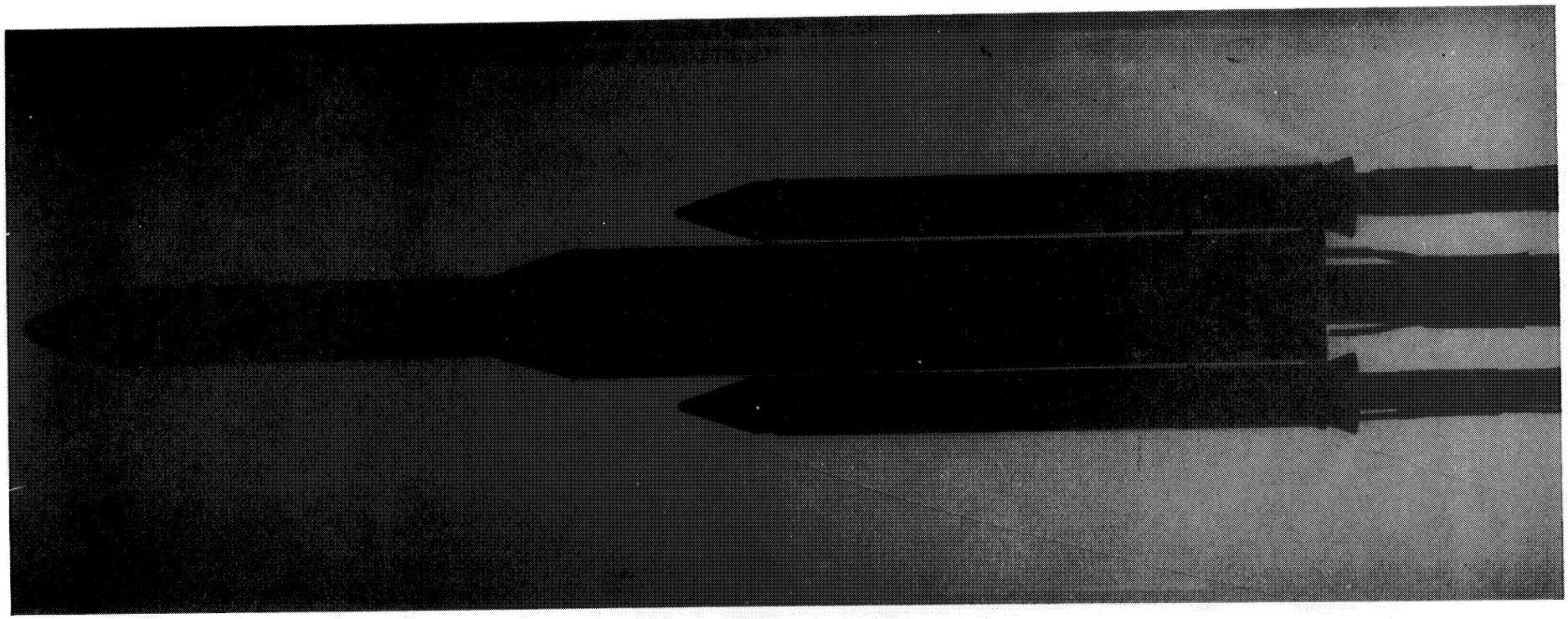

Figure 72. HLLV Mach 4.96, roll = 90°, alpha = 0°, and beta = 0°.

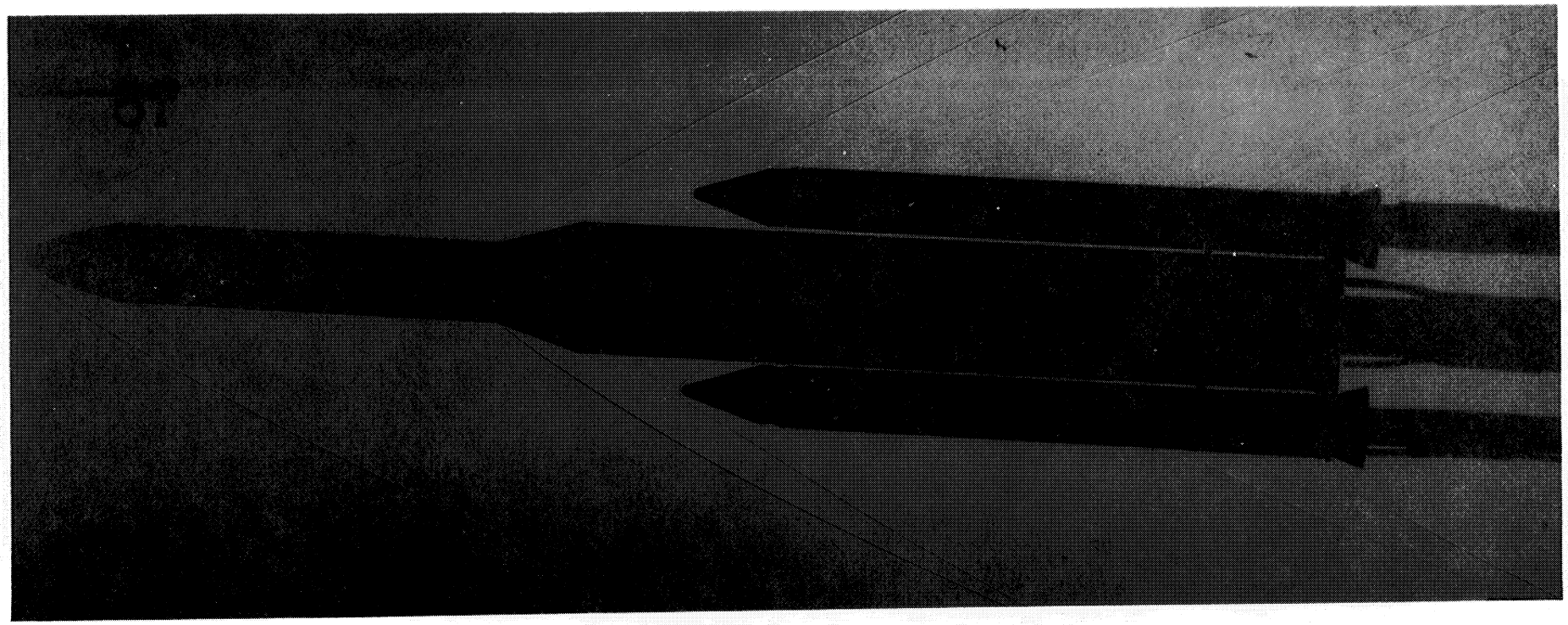

Figure 73. HLLV Mach 2.74, roll = 90°, alpha = 4°, and beta = 0°.

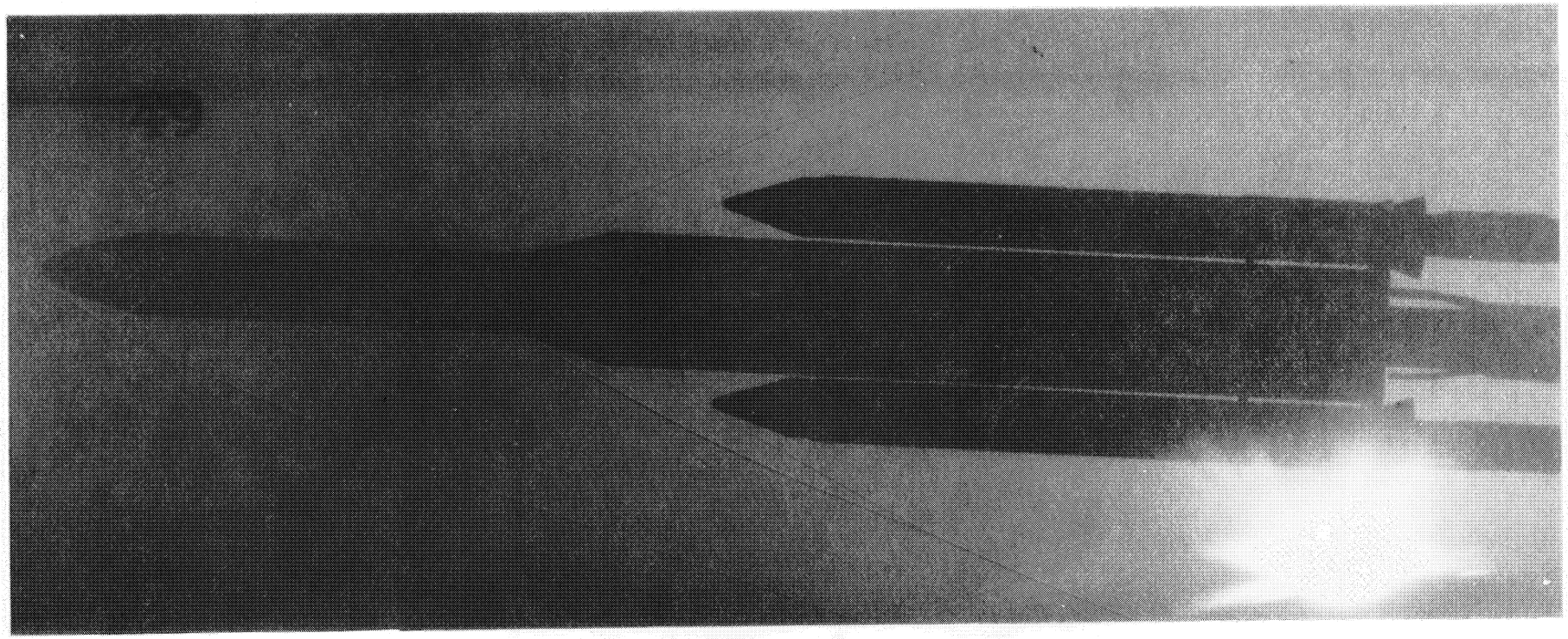

Figure 74. HLLV Mach 3.48, roll = 90°, alpha = 4°, and beta = 0°.

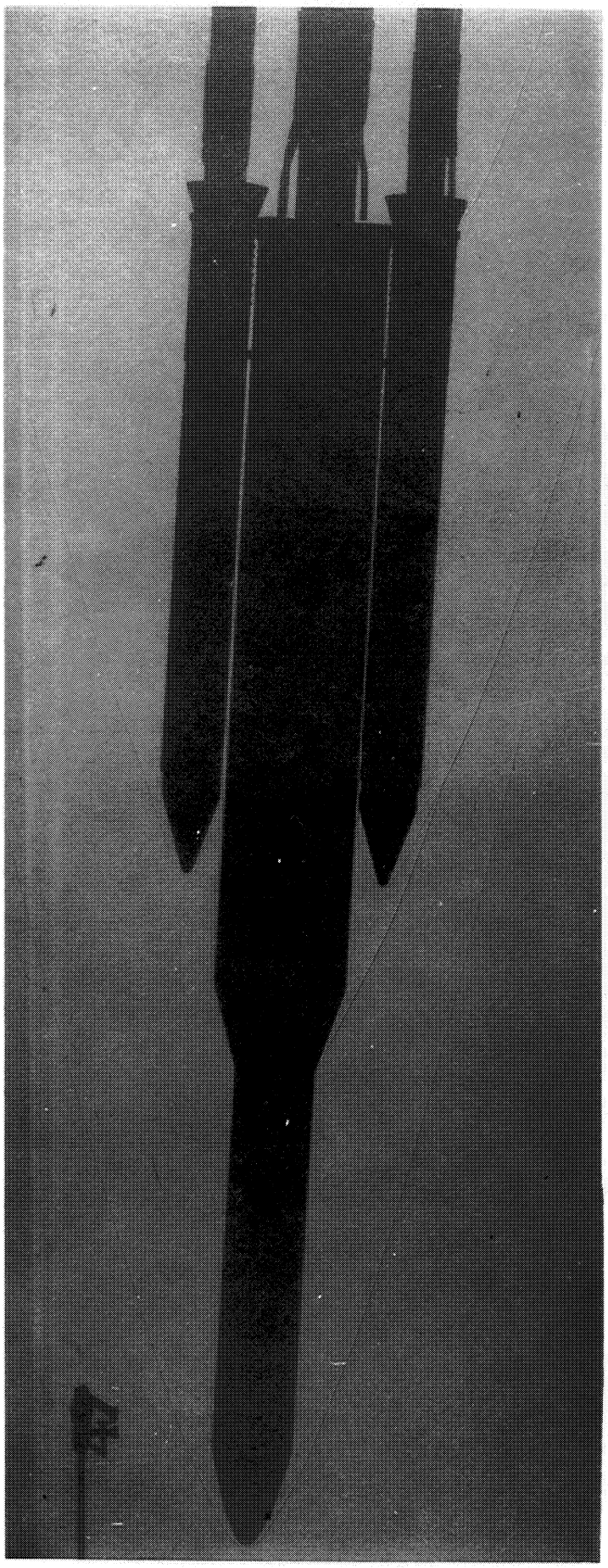

Figure 75. HLLV Mach 4.96, roll = 90°, alpha = 4°, and beta = 0°.

☆ U.S. GOVERNMENT PRINTING OFFICE 1994—533-108/00102

REPORT DOCUMENTATION PAGE

Form Approved
OMB No. 0704-0188

1. AGENCY USE ONLY *(Leave blank)*	2. REPORT DATE	3. REPORT TYPE AND DATES COVERED
	August 1994	Reference Publication

4. TITLE AND SUBTITLE

A Shadowgraph Study of the National Launch System's 1 1/2 Stage Vehicle Configuration and Heavy Lift Launch Vehicle Configuration

5. FUNDING NUMBERS

6. AUTHOR(S)

Darlene C. Pokora and Anthony M. Springer

7. PERFORMING ORGANIZATION NAME(S) AND ADDRESS(ES)

George C. Marshall Space Flight Center
Marshall Space Flight Center, Alabama 35812

8. PERFORMING ORGANIZATION REPORT NUMBER

M-755

9. SPONSORING/MONITORING AGENCY NAME(S) AND ADDRESS(ES)

National Aeronautics and Space Administration
Washington, DC 20546

10. SPONSORING/MONITORING AGENCY REPORT NUMBER

NASA RP - 1347

11. SUPPLEMENTARY NOTES

Prepared by Structures and Dynamics Laboratory, Science and Engineering Directorate.

12a. DISTRIBUTION/AVAILABILITY STATEMENT

Unclassified—Unlimited
Subject Category: 02

12b. DISTRIBUTION CODE

13. ABSTRACT *(Maximum 200 words)*

A shadowgraph study of the National Launch System's (NLS's) 1 1/2 stage and heavy lift launch vehicle (HLLV) configurations is presented. Shadowgraphs are shown for the range of Mach numbers from Mach 0.6 to 5.0 at various angles-of-attack and roll angles. Since the 1 1/2 stage configuration is generally symmetric, no shadowgraphs of any roll angle are shown for this configuration. The major flow field phenomena over the NLS 1 1/2 stage and HLLV configurations are shown in these shadowgraphs. These shadowgraphs are used in the aerothermodynamic analysis of the external flow conditions the launch vehicle would encounter during the ascent stage of flight. The shadowgraphs presented in this study were obtained from configurations tested in the Marshall Space Flight Center's 14-Inch Trisonic Wind Tunnel during 1992.

14. SUBJECT TERMS

shadowgraph, National Launch System, heavy lift launch vehicle, launch vehicle, 1 1/2 stage launch vehicle, wind tunnel testing, flow visualization

15. NUMBER OF PAGES

88

16. PRICE CODE

A05

17. SECURITY CLASSIFICATION OF REPORT	18. SECURITY CLASSIFICATION OF THIS PAGE	19. SECURITY CLASSIFICATION OF ABSTRACT	20. LIMITATION OF ABSTRACT
Unclassified	Unclassified	Unclassified	Unlimited